Performance Modelling and Analysis of Olympic Class Sailing Boats

by

Alexander S. Reid

A thesis submitted for the degree of Doctor of Philosophy

School of Marine Science and Technology

The University of Newcastle upon Tyne

2011

Acknowledgements

I would like to thank the following people who helped me during this project and made it possible.

Professor Martin Downie of the School of Marine Science and Technology, University of Newcastle upon Tyne for being my main supervisor and helping me develop various ideas and providing continuous invaluable guidance.

Dr. Peter Wright also of the School of Marine Science and Technology, University of Newcastle upon Tyne for being my second supervisor. With his input it was possible to develop multiple forward thinking methods for solving the myriad of problems experienced.

I would like also to thank Peter Bentley from the RYA for being my industrial supervisor. Peter was the main driving force behind the project and through his enthusiasm and expertise a successful project was produced. His attitude of 'getting the job done whatever the cost' was also a great inspiration.

Many thanks to Scott Drawer and Naomi Siddall from UK Sport for providing the funding and also the various UK Sport training programs that proved invaluable. I would also like to thank them for various pieces of equipment provided including multiple laptops.

An important part of the project was made possible by Dr Martin Smith and his assistant Ahmad Taha from the Institute of Engineering Surveying and Space Geodesy at Nottingham University who provided valuable knowledge in more than one area.

A special thanks to Dr. Martyn Prince of the Wolfson Unit at Southampton University whose expertise enabled a significant section of the project to become a success.

I would also like to thank all my family and friends who have supported me for the past three years as well as the many I have made through working with the RYA.

Authors Declaration

I declare that all the work in this project is that of the author. Where information has been taken from other sources it has been referenced appropriately.

Alexander Stanley Reid

Preface

The work in this thesis is preceded by a Master of Research in Marine Technology project between September 2004 and October 2005. The project was supervised by Professor Martin Downie and was carried out with significant time present in the field, working closely with Olympic sailors from multiple different classes. This project was funded by UK Sport and considered a pilot project to investigate the feasibility of using data logging equipment with GPS in the marine Olympic environment.

A series of prototype systems were engineered to meet the requirements specified by the Royal Yachting Association. The engineering and validation of the software and hardware formed a key part of the project to ensure that the results obtained were accurate and repeatable. This included software design within two different software platforms as well as embedded hardware developments. Significant testing and development were implemented in the laboratory as well as on the water during the beginning of the project and as a continuous background task throughout the project. Over eighty days were spent in the field developing and testing hardware and software as well as determining the optimum performance analysis methods.

Data loggers were fitted to several Olympic class boats during the evaluation process to ascertain the performance of the data logging system as well as the performance of the boat and crew. Data was logged from the onboard GPS and accelerometers and analysed post training. Later in the project, wind information was also collected and fused together with the onboard data post training. The hypothesis was to demonstrate performance gains in the participating classes through the means of quantitative analysis. Prior to the project the performance analysis had been almost entirely qualitative. Through the course of the project various techniques were developed allowing quantitative performance analysis to supplement the efforts of the training group and coach.

Key performance factors were determined by data analysis techniques developed during the project. One of the significant tools developed was a tacking performance analysis routine which analysed multiple different styles of tacks, calculating the distance lost with respect to wind strength and course length resulting in an important strategic tool. Other tools relating to starting performance and straight line speed were also developed in custom software allowing rapid analysis of the data to feed back to the teams in the debrief.

At the close of the project, when wind measurement was used for the first time with data collected from the target boats, the truly dynamic problem of modelling high performance dinghies was apparent. This resulted in a search for a method that would be able to cope with the highly dynamic environment with temporal datasets. An extensive search in future methods was conducted primarily focussing on creating a VPP for dinghies, or using Neural Networks to model the performance of the boat.

After the pilot project was concluded, sufficient evidence had been demonstrated to UK Sport to ensure that further research could improve the performance of the Olympic classes, leading on to a deeper investigation and a PhD in Marine Technology at the University of Newcastle upon Tyne.

Table of Contents

Contents

List of Figures

List of Tables

Abstract

Throughout the years ever more sophisticated modelling techniques have been developed in order to improve the sailing performance of yachts. These have been almost exclusively in the higher echelons of yacht racing, most notably the Americas Cup (AC). The performance of these large displacement yachts is viewed as almost steady state due to their large momentum. This view is adopted in more than one modelling technique, most notably the Velocity Prediction Program (VPP). Through these techniques the performance of these large displacement yachts is very well understood from years of research and racing.

There is, however, one area of sailing where it is very difficult to measure the performance of yachts accurately. This is in the light and ultra light displacement yachts, and constitutes the scope of this project - the sailing dinghy classes of the 2008 Olympic Games. It is very difficult to model accurately most of the Olympic classes with traditional methods as it is not valid to use the quasi static approach due to the dynamic environment. This is due to the boats possessing a highly dynamic performance due to low momentum and the constant changes to the settings of the boat by the crew.

This project focuses on creating a modelling technique which is able to analyse accurately the performance of the various Olympic classes. This is achieved through the use of Neural Networks which learn the performance of the yacht and the crew together in relation to the environmental factors influencing the boat. This novel approach creates a powerful new tool which enables direct comparison of performance between boats and crews. This is accomplished by inserting the collected raw environmental data experienced by the yacht into a trained Neural Network which effectively sails another boat in exactly the same conditions. This eliminates the randomness caused by the differences in conditions as the wind is never consistent.

This technique also allows the creation of other tools by including well known methods of predicting performance such as a velocity prediction programme (VPPs). With these two modelling techniques included, accurate polars may be created by correcting VPPs at relevant points of sailing. With these techniques employed improvements in boat performance were achieved in a number of classes for the 2008 Olympic Games, most notably the Finn and the Star which both won gold medals.

Nomenclature

Symbol	Definition
α_M	Momentum
α	Leeway
AIC	Akaike's Information Criterion
ANN	Artificial Neural Network
AR	Aspect ratio
AWA	Apparent wind angle
BAD	Boom above deck measurement
β	The gain factor
β_t	TWA with respect to the course of the yacht
B_{wl}	Beam of the yacht at the waterline
C_d	Coefficient of drag for the sail combination
C_f	Coefficient of frictional resistance (ANN VPP)
C_l	Coefficient of lift for the sail combination
C_m	Midship coefficient
CoE	Centre of Effort
C_p	Prismatic coefficient
$CRARM$	Distance from amidships of crew
CV	Cross validation
C_w	Average crew weight
D	Drag
Δ	Displacement of yacht
$\nabla J(k)$	The gradient
DOP	Dilution of position, can be in horizontal and vertical formats
$\Delta R_{fh\varphi}$	Change of frictional resistance of the hull due to heel
$\Delta R_{rh\varphi}$	Change of residual resistance of the hull due to heel
$\Delta R_{rk\varphi}$	Change of residual resistance of the keel due to heel
$\Delta R_{r\varphi\beta}$	Induced resistance of the hull and keel

$\Delta Rrh\theta$	Change of residual resistance due to trim
E	Foot of the mainsail length measurement
EGNOS	European Geostationary Navigation Overlay Service
EHM	Height of the mast above the deck
EMDC	Average diameter of the mast section
F_{avg}	Average freeboard of the yacht
F_H	Heeling force of the sails
Fn	Froude number
η	The descent controller
GA	Genetic Algorithm
GFF	Generalized Feed Forward network
I	Maximum hoist of the genoa.
J	Distance between the bow and the mast
JEN	Jordan/Elman network
L	Lift
L	Length
LPG	Shortest distance between the clew of the jib and the forestay
L_{wl}	Waterline length
MDL	Rissanen's minimum Description Length
MLP	Multilayer Perceptron
MNN	Modular Network
M_r	Righting moment
MSE	Mean Square Error
$MVBLCR$	Number of moveable crew
ϕ	Angle of heel
P	Maximum hoist of the mainsail above the BAD measurement
r	Correlation coefficient
R_h	Resistance due to heel (ANN VPP)
R_f	Total resistance on hull and appendages (ANN VPP)
R_{fh}	Frictional resistance of hull

R_i	Induced resistance (ANN VPP)
Rn	Reynolds number (ANN VPP)
R_{others}	Resistance of other components (ANN VPP)
R_r	Residual resistance on canoe body (ANN VPP)
R_{rh}	Residual resistance of hull
R_{rk}	Residual resistance of keel
$R_{t\varphi\beta\theta}$	Total resistance of hull with appendages and leeway
R_{vkr}	Viscous resistance of keel and rudder
ρ_a	The density of air
PCA	Principal Component Analysis network
PE	Processing Element
ρ_w	Density of water
RBF	Radial Basis Function network
S_c	Wetted surface area of the hull
TWA	True wind angle
TWD	True wind direction
TWS	True wind speed
T	Total draft
T_c	Draft of hull
Ua	Apparent wind speed at the centre of effort of the sails
υ	Kinematic viscosity
V_b	Hull velocity
∇_c	Volume of displacement of the hull
VMG	Velocity made good
$V_i(10)$	TWS at 10 metres above the water
WAAS	Wide area augmentation system
w_i	Weighting
XOR	Exclusive or truth table
z_0	The height of 0 metres

Chapter 1

Introduction

1.1 Context

The propulsion of boats and ships by wind power has been exploited since ancient times and has continued to be developed for, predominantly, sailing leisure craft and the auxiliary assistance of larger ships. Historically, evolution in the design of sailing vessels to improve performance was mainly based on experience to achieve a small progression from a previous successful design. This process can be viewed as almost 'Darwinian' as hull and rig designs evolved highly suited to their intended purpose. Due to this evolutionary development, the design of sailing craft was traditionally viewed as more of an art based craft than a science. Over the last three centuries a more scientific approach to naval architecture has developed. However, the field of yacht design has largely remained craft based and has lagged behind shipbuilding in the adoption of more scientific methods of assessing performance. This is particularly true in yacht racing, where the majority of the performance assessment methods are still mostly based on human interpretation in an otherwise highly technical and competitive arena. This approach nevertheless has provided very good quantitative results despite the qualitative nature of the human input.

Although sailing yacht design has lagged behind the other fields of naval architecture it has certainly developed significantly with the increasing adoption of rigorous scientific methods of assessing performance. One of the major driving forces behind this progress is the Americas Cup (AC) which, with large budgets, enables teams to refine designs and produce measureable incremental differences in performance. This is also the case for other yacht high level racing where significant resources are expended on the design of more competitive boats, including the Volvo Ocean Race and the Olympic Games.

Some of the advanced techniques in performance prediction that have become well established and have facilitated such further refinements in performance include Velocity

Prediction Programs and extensive tank testing closely coupled with high level Computational Fluid Dynamics simulations (CFD).

It is of particular note that none of these tools include the dynamic input from the crew and they are largely based on steady state modelling assumptions. Such assumptions are more valid for large displacement yachts with significant momentum but in small and ultra light displacement yachts they are no longer applicable due to the highly dynamic nature of the yachts and the influence of the crew.

1.2 Aims and Objectives

In addition to its academic objectives, this study had clearly defined aims and objectives set by the sponsors of the project, UK Sport and the RYA. The principal aim in this respect was to produce a method capable of correctly modelling and assessing the performance of Olympic sailing classes and their crews. The key objectives to meet this aim were:

- The collection of data using innovative equipment and procedures that continued from the MRes project.
- To develop and enhance the procedures and techniques for the collection of data using novel equipment.
- To use the data to develop hardware and software tools for performance prediction and the assessment of discrete skills for multiple Olympic sailing classes.
- To verify and validate the performance models developed in the work..
- To apply the approaches developed to support the sailing programme and enhance the competitiveness of boats and crews for future Olympic sailing events.

In addition to the research implicit in realising the above objectives, the academic objectives of this study included the development of a novel approach to performance assessment based on neural networks; the development of a methodology allowing the separate objective assessment of the different components making up ‘performance’; and, an understanding of the effective use of this approach to the practical enhancement of the performance of realistic competing systems.

It is recognised that there have been various attempts in the past to model small high performance boats through various approaches with varying success. The aim of this project

was to build upon these methods and attempt to develop a novel and more accurate modelling technique for small boat performance assessment than is currently available.

The principal challenge of this project was that the steady state assumptions of existing tools are not appropriate for representing the more chaotic time series data associated with small high performance sailing boats. An associated, not insignificant, challenge was the collection of the necessary data on such boats where weight and space limitations make it difficult to instrument the boat due to the weight and bulk of the equipment required to collect accurate data.

The problem of producing a better modelling technique for small boat performance is an open ended one which has multiple solutions. In the scope of this project, only one of many potential paths to solving the problem was pursued to the full extent due to time restrictions, hardware development and the time consuming process of instrumenting boats and collecting data in the field.

1.3 Chapter Outline

The chapters in this thesis follow in a logical progression starting with an investigation into the existing techniques that are used to model the performance of yachts. After a review of this area in Chapter 2 the main topic of the thesis, Neural Networks are introduced in Chapter 3. . It starts by assembling the components that form an Artificial Neural Network (ANN), before reviewing the different designs and techniques used to produce effective ANNs as well as the known pitfalls

Chapter 4 examines existing performance analysis techniques. These methods fall under the umbrella of optimising the design of experiments based on the findings of chapter 2. Various pieces of equipment are analysed as well as different aspects of the data collection procedures.

Chapter 5 integrates the material in the previous three chapters by building upon their strengths and ideas, and demonstrates the processing of data through the two main methods of ANNs. In this chapter the key work and development carried out by the author in this area is illustrated, and several new concepts and modelling techniques are introduced before presenting the final results with the analysis at the end.

Chapter 6 builds upon the ANN methods that were used in the previous chapter and develops an accurate diagram of polar performance for all of the Olympic classes. This is achieved through correcting two different VPPs. To complete this chapter, the polar performances are then used in a performance analysis format which is compared to the methods developed in Chapter 5.

Chapter 7, in essence, sums up the new ideas and results that have been formed from this project. The first half, however focuses on the outline development of an image recognition technique that was proposed in this project as a further refinement to the performance modelling. This is carried out by extending some of the more advanced concepts that were explored in Chapter 2, which were cut short in the project due to funding and time restrictions. In the final section further aspects of performance analysis and modelling are discussed, and the potential for the results from this project to be developed further with more modelling considered.

The Appendices contain a variety of extra images and tables that were too numerous to fit into the main body of text. Appendix 4, however, is different from the other appendices as it contains the methods that the author used for building the original VPP. This differs to the last section of Chapter 6 as it is presented without the correction techniques discussed in the main body of this thesis.

Chapter 2

Methods of Yacht Performance Analysis

2.1 Introduction

In this section, the current methods of predicting and measuring performance in the sailing environment shall be explored. This exploration shall begin by investigating the Velocity Prediction Program (VPP), before moving on to looking at current data collection methods and performance analysis techniques. The calculation methods of the traditional VPP shall also be examined. The final part of this chapter shall investigate another method of performance analysis on yachts which is the analysis of sail shape through different available methods. During the early stages of the project, it was clear that there was a considerable lack of ANN based research that had been carried out in the area of performance analysis in sailing.

2.2 Velocity Prediction Programs

2.2.1 VPP Background

The fundamental theories of sailing are well established and have been known for a considerable amount of time (Philpott et al, 1991). With this understanding of the basic principles of boat performance it was a natural progression that yacht performance would be represented as some sort of algorithm. This algorithm is commonly referred to as a VPP, which calculates the performance of a yacht through balancing all of the forces that the sailing yacht experiences in all wind conditions through an iterative process (Fassardi, 2002). These forces and moments are made up of several components:

- The heeling moment and righting moment that are equal and opposite as the boat is assumed to be in equilibrium;

- The driving force generated from the sails is counteracted by the total resistance of the boat due to aerodynamic and hydrodynamic drag;
- The buoyancy of the boat is equal to the weight, due to gravity;
- The side force is counteracted by the side force which holds the boat in a steady horizontal plane;
- The pitching moment is counteracted by the restoration moment provided by reserve buoyancy;

As mentioned earlier there are multiple forces and moments that require balancing in order to solve the VPP, by optimisations with respect to maximising boat speed, and therefore the yacht performance can be determined for a given condition. There are several different types of VPPs that can be used; the most well known one uses the Delft Systematic Yacht Hull Series (DSHYS) for the simplest and quickest solution. The DSHYS is a collection of different yacht design models now totalling 50, which are varied in multiple parameters. There has been extensive testing on this series and more designs have been added over the years (Gerritsma et al, 1991). VPPs can also work in conjunction with Computational Fluid Dynamics (CFD), which have greatly improved over recent years with better simulations (Scarponi, 2007). These function by replacing the empirical aerodynamic corrections with Reynolds-Averaged Navier-Stokes (RANS) simulations (Korpus, 2007). Towing tank data can also be used in a VPP as it can provide more accurate hydrodynamic data than the DSHYS (Graf, 2005).

This knowledge and understanding led to the foundations of the VPP being laid in the 1970s with one of the most noted applications being the development of the handicapping system (Kerwin, Newmann, 1978). Before the Kerwin paper, handicaps had been relatively crude and determined by a mainly empirical method, and race results, with handicaps such as the Thames Measurement having multiple loop holes. A deeper history of the yacht handicapping history is described by Strohmeier, (1975).

As yacht racing evolved and different designs of boats were racing against each other some designs and sizes were faster than others. In order to create a fair method of racing against each other a time correction factor was created dependent on aspects such as water line length. This process is known as a handicap and is known in several different formats today. VPPs became the backbone of more than one handicapping system, the first of which rule was the Measurement Handicap System (MHS) which developed into the International Offshore Rule (IOR) in 1970 (Pedrick, 1979). There were several different versions of IOR which each in turn tried to close loopholes exploited in previous versions. Unfortunately the

IOR rule encouraged a higher centre of gravity (CoG), by favouring strong hulls and rigs which had a higher CoG and penalising boats with a lower CoG. This actually encouraged light racing yachts to have little or no lead in the keel, which would lead to spectacular broaches in downwind breezy conditions (Strohmeier, 1979). This combination of unseaworthy boats can be considered to have contributed in part, to the infamous Fastnet disaster in the summer of 1979 (Fisher, 1980). The IOR rule developed into the International Measurement System (IMS) rule which is still active today, but no longer as popular. With the introduction of IMS, more and more sophisticated VPPs were produced by designers and the Offshore Racing Council (ORC) who managed the IMS rule. With this increase in sophistication also came an increase in the complexity of the IMS rule, which started using changes in wind shifts and strengths to handicap boats more accurately (Cane, 1994). This complexity eventually led to the virtual downfall of the IMS rule.

VPPs have historically have always been applied to displacement yachts. In the scope of this project, the boats that will be featured differ greatly from the types of yachts which have traditionally used VPPs. The Olympic classes, most notably boats such the 49er and Tornado, are by no means displacement boats. Even the heavier boats such as the Star and Yngling will plane and surf downwind in sufficient breeze. Another factor which would differ from the traditional VPP is that most Olympic classes are sailed with the boat flat, whereas in VPPs the yacht is generally allowed to heel. Traditionally, the VPPs are also a static solution to a static problem, whereas the Olympic classes are very dynamic in the way which they respond and are sailed. With these smaller boats, there is significantly more rudder movement coupled with the dynamic movement of the crew to also factor into a VPP. This leads to a complex model being required in order to simulate the crew's response to environmental conditions.

There are, however, two notable VPPs that are able to predict the performance of small planing dinghies. Carrico, (2005) produced a Laser VPP written in Visual Basic and Excel, with the hydrodynamic data collected in a full scale test. The other notable VPP is that of the Wolfson Unit which has relatively recently added a dinghy and Olympic class package into their program. The latter package is viewed as one of the best in the assessment of sailing yacht performance.

The Carrico VPP assumes a similar strategy to the previous VPPs that we examined, by assuming that the boat is in equilibrium and also governed by iteratively balancing the six equations of motion. The area where the paper differs is in the hydrodynamic data which is neither derived from the Delft series nor collected from the tow tank. In this case the Laser dinghy is towed alongside a motorboat with a load cell attached to the end of a pole which is

then attached with a rope around the mast of the Laser. The data collection was conducted in a canal with no tide or wind affecting the results. Once the hydrodynamic data was collected the rest of the VPP process was fairly similar to a conventional VPP. In order to get the correct sail coefficients the data was borrowed from the Finn dinghy. The results of the VPP for the Laser can be seen in Figure 1 below, with TWA on the Y-axis and boat speed on the X-axis. There do seem to be some irregularities with the finished polar plot, as the boat speed does not drop below the optimum TWA speed even when sailing downwind. Carrico also mentions in his conclusion that the VPP is producing some strange results in the higher wind speeds which could be to do with maintaining the equilibrium.

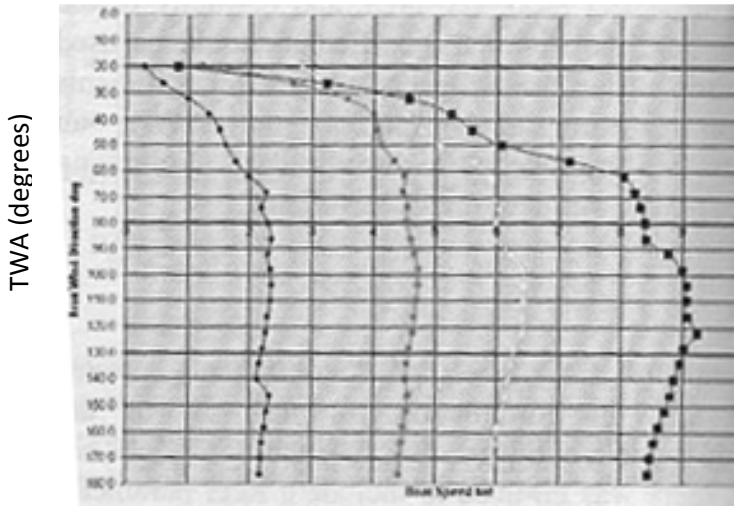

Figure 1 – Laser VPP Output, (Carrico, 2005)

The Wolfson Unit VPP shall be examined later in the project.

2.2.2 VPP Methods

There are several methods used to create a VPP, with varying degrees of complexity. This investigation into VPPs will be based on one of the less sophisticated methods. Here the emphasis is on the simpler methods as this was found to be most appropriate for the given time scale and project aims. VPPs have until recently been generally viewed as expensive and relatively unreachable for the average yacht designer (Martin, 2001) explained in greater detail than before the methods that are used to produce a VPP.

The VPP requires various hydrodynamic and aerodynamic forces requiring balancing. In terms of the resistance components that require balancing, they can be summed up by the

Equation (1) below (Keuning et al, 1998). In this section a few of the basic methods and equations shall be examined from previous VPPs and methods. The calculation of resistance shall be looked at first before moving onto the stability and sail forces calculations.

$$Rt\varphi\beta\theta = Rfh + Rrh + Rvkr + Rrk + \Delta Rfh\varphi + \Delta Rrh\varphi + \Delta Rrk\varphi + \Delta Rr\varphi\beta + \Delta Rrh\theta \quad (1)$$

Where $Rt\varphi\beta\theta$ is the total resistance of hull with appendages and leeway, Rfh represents the frictional resistance of hull, Rrh is the residual resistance of hull, $Rvkr$ corresponds to viscous resistance of keel and rudder and Rrk is the residual resistance of keel. The changes in resistance can be summed by $\Delta Rfh\varphi$ which is the change of frictional resistance of the hull due to heel, $\Delta Rrh\varphi$ symbolising the change of residual resistance of the hull due to heel, $\Delta Rrk\varphi$ which stands for the change of residual resistance of the keel due to heel, $\Delta Rr\varphi\beta$ is the induced resistance of the hull and keel and finally $\Delta Rrh\theta$ stands for the change of residual resistance due to trim.

Equation (1) is reduced to Equation (2) as seen below (Martin, 2001) and in the next section each of the components of total resistance shall be examined and the various methods used to determine the total hydrodynamic resistance of the yacht.

$$R_{total} = R_f + R_r + R_i + R_h + R_{others} \quad (2)$$

Where the R_f represents total frictional resistance on hull and appendages, R_r is the residual resistance on canoe body, R_i corresponds to the induced resistance, R_h is the resistance due to heel and the final component is R_{others} which covers the resistance of other components. The next five sections shall examine methods for calculating each of the components that produce R_{total}.

2.2.2.1 Frictional Resistance

A known method for calculating frictional resistance is with the 1957 ITTC extrapolator which can be seen below, Equation (3). With this equation it is possible to calculate the

coefficient of frictional resistance (C_f) to be used in Equation (5) which calculates the total frictional resistance.

$$C_f = \frac{0.075}{(\log(Rn)-2)^2} \tag{3}$$

Where Reynolds number (Rn) is calculated from Equation (4).

$$Rn = \frac{V \cdot L}{\upsilon} \tag{4}$$

Where L is the length, υ the kinematic viscosity and V, which is the velocity of the yacht. This then allows the frictional resistance to be calculated.

$$R_f = {}^1\!/_2\, \rho_w \cdot V^2 \cdot S_c \cdot C_f \tag{5}$$

Where S_c is the wetted surface area.

The surface areas and frictional coefficients of the keel, rudder and hull can be substituted into the equation in turn and the total resistance can be calculated.

Another aspect to consider is the need for form factor k. Its value for a keel can be calculated by (Keuning and Sonnenberg):

$$(1+k) = \left(1 + 2\left(\frac{t}{c}\right) + 60\left(\frac{t}{c}\right)^4\right) \tag{6}$$

If there is a bulb on the underneath of the keel this can be calculated by the following equation as suggested (Keuning and Binkhorst, 1997).

$$R_{fb} = q \cdot S_b \cdot C_{fb}\left(1 + 1.5\left(\frac{d}{l}\right)^{\frac{2}{3}} + 7\left(\frac{d}{l}\right)^3\right) \tag{7}$$

2.2.2.2 Residuary Resistance

The other major component of the resistance of a yacht hull is residuary resistance; it is produced by the wave making effect of the yacht. There is a simplification in this process as it does not include all the appendages. To calculate the residual resistance a table produced by Gerritsma et al, (1991), provides values of residual resistance for different Froude

numbers. The range of the table is between 0.125 and 0.45 and from 0.475 to 0.75 and can be seen in full in Appendix 4. There is some dispute on the size of the residuary resistance on the appendages when the hull is upright and can sometimes be ignored. However, it was shown by Keuning (1998) that this was not always the case, especially when there is a large sweep back of the keel.

The residual resistance formula that uses the table discussed on the previous page is described by the polynomial given by (Gerritsma, 1991).

$$\frac{R_r}{\Delta_c} \times 10^3 = A_0 + A_1 C_p + A_2 C_p^2 + A_3 LCB + A_4 (LCB)^2 + \frac{A_5 B_{WL}}{T_c} + \frac{A_6 L_{wl}}{\nabla^{\frac{1}{3}}} \quad (8)$$

2.2.2.3 Induced Resistance

When a yacht is moving through the water, especially at higher speeds, the hull produces lift which has the effect of partially counteracting the heeling force experienced by the yacht. The induced resistance is proportional to the square of the side force or leeway and can be shown by the following equation (Gerritsma et al, 1993), (Helvacioglu, 1995).

$$R_i = \frac{1}{\pi \cdot AR_E} \frac{F_H^2}{q \cdot S_c} \quad (9)$$

Where AR_E is the effective aspect ratio of the combined sail plan, F_H stands for the heeling force of the sails, q = $^1/_2 \rho V^2$ and S_c corresponds to the calculated wetted surface area of the hull.

2.2.2.4 Added Resistance due to Heel

As most yachts heel the wetted surface area increases and hence resistance. For the types of boat considered here, heel may not be a major factor as the majority of classes are sailed upright apart from the displacement classes. There are a couple notable exceptions to this rule in the form of the Tornado and Star classes. The Tornado experiences a drop in resistance when there is sufficient heel to lift the windward hull just out of the water. The Star has a prominent chine which acts efficiently to reduce the wetted surface area at certain angles of heel. A VPP which uses the DSHYS will not recognise the chine and hence the reduction in wetted surface area. A more advanced VPP with a Lines Processing Plan (LPP) is able to recognise the chine and calculate the correct resistance due to heel. The equation

for added resistance due to heel which was derived by Gerritsma et al in 1993 can be seen below in Equation (10).

$$R_H = q \cdot S_c \cdot C_H \cdot Fn^2 \cdot \phi^2 \tag{10}$$

Where the coefficient of heel is determined in Equation 11 below

$$C_H \times 10^3 = 6.747\left(\frac{T_c}{T}\right) + 2.517\left(\frac{B_{wl}}{T_c}\right) + 3.71\left(\frac{B_{wl}}{T_c}\right) \cdot \left(\frac{T_c}{T}\right) \tag{11}$$

The resistance of heel is dependent on the heel angle (ϕ), Froude number (Fn) and the resistance coefficient of heel (C_H) as stated by Gerritsma et al, (1993).

2.2.2.5 Other Resistance Components

There are several additional resistance components that affect the performance of a yacht; these are regarded as minor but need to be considered for completeness These include a change of frictional resistance due to heel, this considered only minor as the wetted surface increase is only minor. The same conclusion was also drawn by the DSYHS (Gerritsma, 1991). Other minor increases in resistance include the increased resistance due to trim, however for this project it is safe to assume that this would be maintained close to the optimum setting by the crews sailing the boat. All the components of resistance that have been investigated so far have assumed that the yacht has been sailing in flat water. Including waves into the VPP would produce a more accurate assessment of the performance of the yacht in real conditions. Flat water assumptions are considered valid for the approach adopted here. In the next section the stability forces shall be examined before concluding with the sail forces.

2.2.2.6 Righting Forces

Stability of a yacht falls into two different regimes: the static and dynamic stability, including the addition of the crew weight. This can be summarised by Equation (12).

$$M_r = \Delta(GN + MN) \cdot sin\phi + M_{rc} \tag{12}$$

Where M_{rc} is calculated in Equation (13).

$$M_{rc} = C_w \cdot MVBLCR \cdot cos\phi \cdot CRARM \tag{13}$$

Where M_r is shown as the righting moment of the yacht, Δ in the displacement, C_w is the average weight of the individual crew, $MVBLCR$ is the number of crew that are able to move in the tacks and provide ballast and $CRARM$ is the distance from amidships to the hiking position of the crew.

Gerritsma shows in Figure 2 how the righting moment equation is calculated.

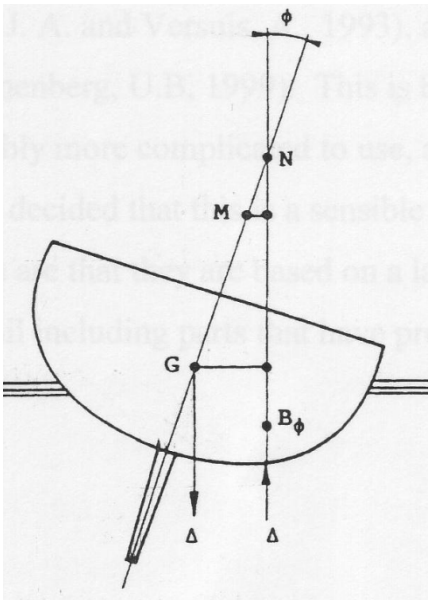

Figure 2 - Righting moment derivation (Gerritsma et al, 1992)

MN is calculated with Equation (14) below.

$$MN \cdot sin\phi = (D_2 \cdot \phi \cdot Fn + D_3 \cdot \phi^2) \tag{14}$$

Where the dynamic increment coefficients D_2 and D_3 substitute into Equation 14.

$$D_2 = -0.0406 + 0.0109\frac{B_{wl}}{T_c} - 0.00105\left(\frac{B_{wl}}{T_c}\right)^2 \tag{15}$$

$$D_3 = 0.0636 - 0.0196\frac{B_{wl}}{T_c} \tag{16}$$

2.2.2.7 Side Forces

There are several different methods for calculating the side forces affecting the yacht which produce leeway. The simplest method and one of the most robust is approach of Gerritsma et al, (1993) given in Equation (17).

$$F_{side} = \frac{\alpha \cdot q \cdot S_c}{cos\phi}\left[b_1\left(\frac{T^2}{S_c}\right) + b_2\left(\frac{T^2}{S_c}\right)^2 + b_3\left(\frac{T_c}{T}\right) + b_4\left(\frac{T_c}{T}\right)\left(\frac{T^2}{S_c}\right)\right] \quad (17)$$

Where α is the yacht's leeway in radians, T is the total draft of the yacht including hull and keel, T_c is the draft of just the hull, and S_c symbolises the surface area of hull and finally $b_1 - b_4$ which are the lift slope coefficients for different angles of heel.

Gerritsma's equations have had more focus rather than the more recent work by Keuning et al due to reduction of complication. In the next section the hydrodynamic forces acting on the yacht shall be examined. This includes the windage on the hull and the rig.

2.2.2.8 Lift and drag of Sail Forces

There are several different methods which can be used to determine the sail forces, we shall examine the method first suggested by Larsson and Eliasson which is based on the Hazen method (Hazen, 1980) for initial sail force calculations. The lift and drag forces can be calculated with Equations (18 and 19) below (Hansen et al, 2002).

$$L = C_l \, {}^1\!/_2 \, \rho_\alpha U a^2 A_n \quad (18)$$

$$D = C_d \, {}^1\!/_2 \, \rho_\alpha U a^2 A_n \quad (19)$$

Where C_l is the coefficient of lift for the sail combination based on A_n, C_d stands for the coefficient of drag for the sail combination based on A_n, Ua is the apparent wind speed at the centre of effort of the sails, A_n is the sum of A_f and A_m, the A_f is the area of fore triangle calculated by 0.5 JI, and finally the area of the mainsail is represented by A_m and calculated by 0.5 PE.

Two of the most difficult variables to obtain correctly are sail coefficients for lift and drag. They can be collected experimentally as demonstrated by Marchaj (2003) with wind tunnel measurements at different TWS and TWA. In the Marchaj method the following formula is used:

$$C_L = \frac{L}{S_A \times 0.00119 V_a^2} \quad (20)$$

$$C_D = \frac{D}{S_A \times 0.00119 V_a^2} \quad (21)$$

The output from this experiment is a polar diagram which represents lift and drag values for different angles of incidence. The two curves show the lift and drag coefficients as experienced by the sail. The diagram clearly shows that the driving force on a yacht changes from relying on lift upwind to drag downwind to maximise performance, in Figure 3 (Marchaj, 2003).

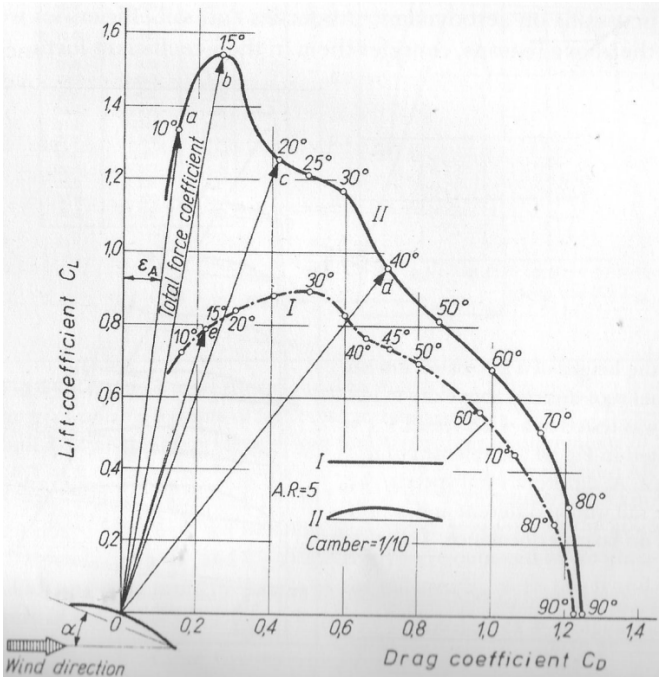

Figure 3 - Lift and Drag w.r.t. change of angle of attack (Marchaj, 2003)

The coefficients are provided by Claughton, for the main, jib and spinnaker at several different TWAs. Larsson also provides similar coefficients, both tables can be found in Appendix 4. These cover the polar angles sufficiently and are regarded as an approximation. For TWAs in between Larsson's points an interpolation is used. There are other factors included in the sail coefficients including reefing in the higher wind speeds. In terms of correcting the polar with the ANN the usual correctional method is to modify the sail coefficients in order to match the desired point.

2.2.2.9 Hull and Rig Drag

In order to calculate the windage of the hull and the rig a windage drag coefficient is used which is shown by Equation (22) below.

$$C_{do} = 1.13\left(\left(BF_{avg}Q_{rat}\right) + (EHM\,.\,EMDC)\right)/A_n \tag{22}$$

Where EMDC is the average mast diameter, $Q_{rat} = U_h^2/U_a^2$, U_h is the TWS relative to the hull, U_h at z = $F_{avg}/2$ and U_a at z calculates the CE. Q_{rat} was proposed by Claughton (1999), where the above equation for the treatment of windage drag is derived. It was recognised that the dynamic pressure at the centre of effort of the sails is higher than the height of the hull. With this last segment now complete the total drag can be shown as Equation (23).

$$C_d = C_{dp} + C_{di} + C_{do} \tag{23}$$

2.3 Performance Data Collection

In this section the data collection methods of large displacement yachts shall be investigated initially. In the next section two examples of data collection and processing methods for dinghies shall be explored, finishing off with some ANN analysis.

2.3.1 Yacht Data Collection Methods

There are other alternatives to modelling performance than by VPPs which have also evolved from displacement yachts. Collecting data and analysing it by comparisons to previous data or predictions has been used for almost thirty years in the world of performance yacht sailing. Onboard computers first came into favour in the late 70s after Lawson's publication in 1978. An example of one of the early onboard computers can be found in *"A Microcomputer Beats to Windward",* (Clauser, 1979)

The computer, as described by Clauser, used four different sensors; an anemometer; a wind vane; a water turbine for measuring boat speed; and an accelerometer for measuring leeway. With these inputs, other values were able to be derived such as Velocity Made Good (VMG) which can be calculated from Equation (24) (Clauser, 1979).

$$VMG = V_a \cos(\beta + \lambda) \tag{24}$$

Where V_b is the boat speed, V_a stands for the apparent wind (AWS), V_t corresponds to the true wind speed (TWS), β is the apparent wind angle (AWA) and the leeway is represented by the symbol of λ.

The system was crude compared to today's standards but an important step forward as it was able to monitor these inputs and also record the performance of the yacht, which could be used for performance analysis.

One of the most famous uses of onboard computers, and post processing of collected data, was from the famous victory of Australia II in the 1983 Americas Cup. The main driving force for using the computer system aboard the Australia II was that the tune up boat had been sold to the British so there was no direct benchmark (Oossanen, 1985). The computer system allowed the track of the boat to be plotted, and also for data to be compared against previously saved data which was stored in a polar format and used as performance targets for the crew. An example of the data is shown in Figure 4 (Oossanen, 1985).

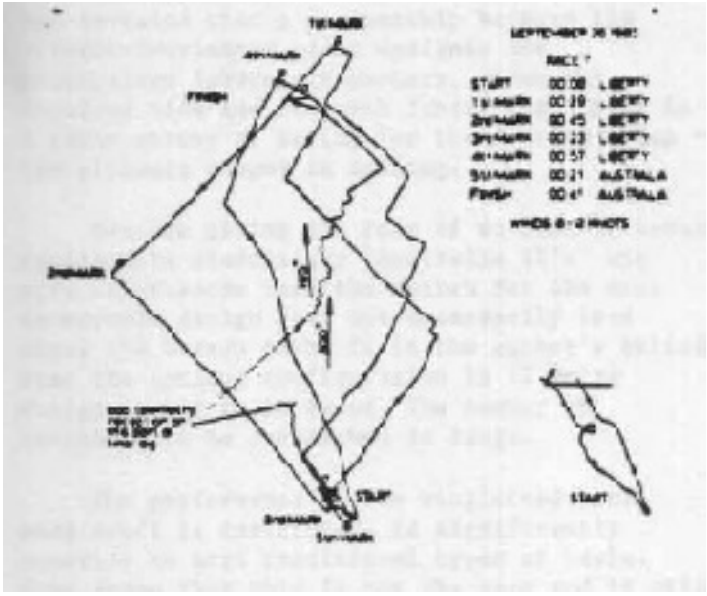

Figure 4 - Performance analysis as used by Australia II, (Oossanen, 1985)

The plots shown in Figure 4 are more sophisticated than Clauser's plots and, as well as plotting the position traces, they included the lap times of each leg and were able to evaluate the strategy and tactics that they had employed. In the following text, newer methods are employed in the performance analysis with an examination of the 1987 Stars and Stripes Americas Cup campaign.

The main difference between the 1983 Australia II and the 1987 Stars and Stripes campaign was that the latter was able to use two boat testing from the beginning. A great deal of the collected data was able to be validated with this method even though the two boats were sailing in slightly different conditions (Letcher, 1987). Letcher also states that there was also the use of a telemetry system which transferred the collected data from both yachts back to a following tender. Once the tender had received the data, it saved the data onto a hard

disk and also processed both sets of data to produce a summary of performance analysis. There were two main problems that had to be overcome in the data collection and testing process. The instrumentation that was used was not accurate enough to measure small differences, the TWD was only accurate to the level of integers and the V_b measurement was accurate to plus or minus 0.1 knots. Letcher also chooses to ignore the dynamic affects that are present and decides to use only quasi-steady analysis. Letcher is able to ignore the dynamic affects as the dynamic affects of the 12 metre AC yacht are small compared to the overall steady-states forces. For the scope of this project, that assumption could not be applied for the Olympic classes apart from the heavier displacement boats. This is due to the highly dynamic behaviour of the boats as the TWS, TWD and V_b are never stable enough to use a static model. The end result of the data process not only allowed detailed analysis but also the production of useful target polars to be produced, as shown in Figure 5 below (Letcher, 1987).

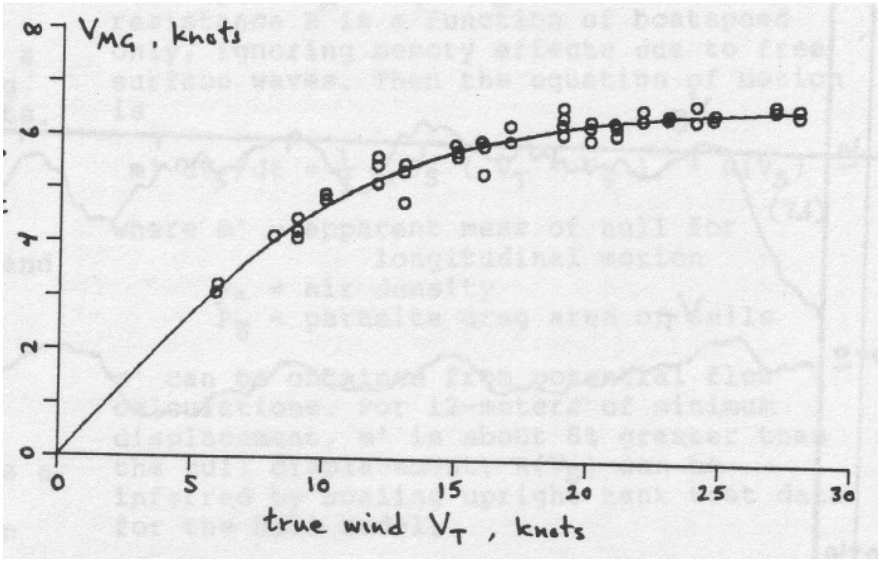

Figure 5 - Early performance analysis (Letcher, 1987)

The data collection and analysis process was once again improved in the third to last Stars and Stripes campaign in the 1992 AC. This process used the combined input of Computational Fluid Dynamics (CFD), Finite Element Analysis (FEA) and towing tank data as well as the full sized data performance analysis (Todter et al, 1992). With these processes, superior equipment, and data analysis techniques a comparison of the VPP polar and the filtered collected data was able to be compared in a real time format. A polar diagram displays the performance of the boat through a range of wind speeds and true wind angles. Head to wind is aligned to the top of the page and dead downwind at 180 degrees pointing towards to the bottom of the page. Each curve signifies a different wind speed and the further the curve is from the centre of the plot the higher the speed of the yacht.

Maximum VMG can also be found via using a polar diagram with respect to the highest point on each individual curve having the highest maximum VMG. At this point the true wind angle and boat speed can be found. The opposite is true for sailing downwind with the lowest points having the best VMG. An example of this can be seen in Figure 6 below (Todter et al, 1992). From Figure 6 it can be seen that there is quite a lot of scatter in the polar plot data; this could be due to the assumption of the static model approximation as mentioned in Letcher's paper earlier.

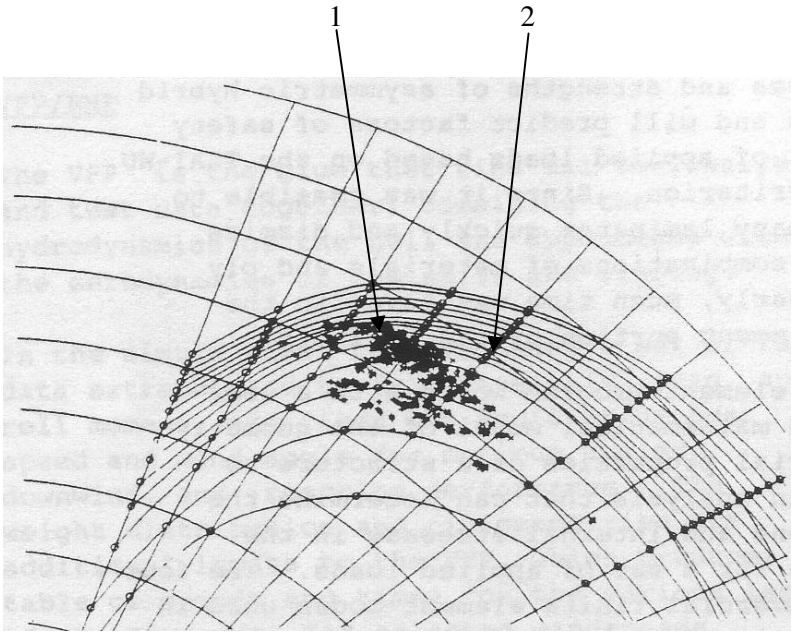

Figure 6 - Stars and Stripes polar data, (Todter, 1992)

Another observation of the data which links into the measurement error of the equipment is that in some cases the data plotted in the scatter is at a higher VMG than the data plotted in at the theoretical optimum point. This is highlighted by point number one. The error could be due to the delay or difference of measuring the wind data at the top of the mast to the course that the helm is steering from following the telltales lower down. This is also true of the data plotted at point two which also highlights similar errors in the data.

Modern data analysis tools are similar to the 1992 AC Stars and Stripes campaign except again with better instrumentation and superior software. Below is a screenshot from a program used by the 2003 British AC challenge in Figure 7 (Elliot,2004). The similarities between the previous performance analysis techniques can be readily seen. However, the software uses a commercial navigational tool known as Deckman (Elliot,2004). Images of the sails are also added into the software package which allows the crew to relate different performances to sail settings. The software also includes a data replay control which allows the crew to assess their performance during or after training sessions. Similar to Letcher's

paper, the performance analysis also relies on a static model. It is interesting to note that when comparing the Polar Window of Figure 7 to the same plot in Figure 5 the scatter and therefore the accuracy of the points are very similar. This could be due to the shortcomings of the static model assumption as some of the data could have been collected in gustier conditions which could have produced a slower performance. This, however, is not quantified.

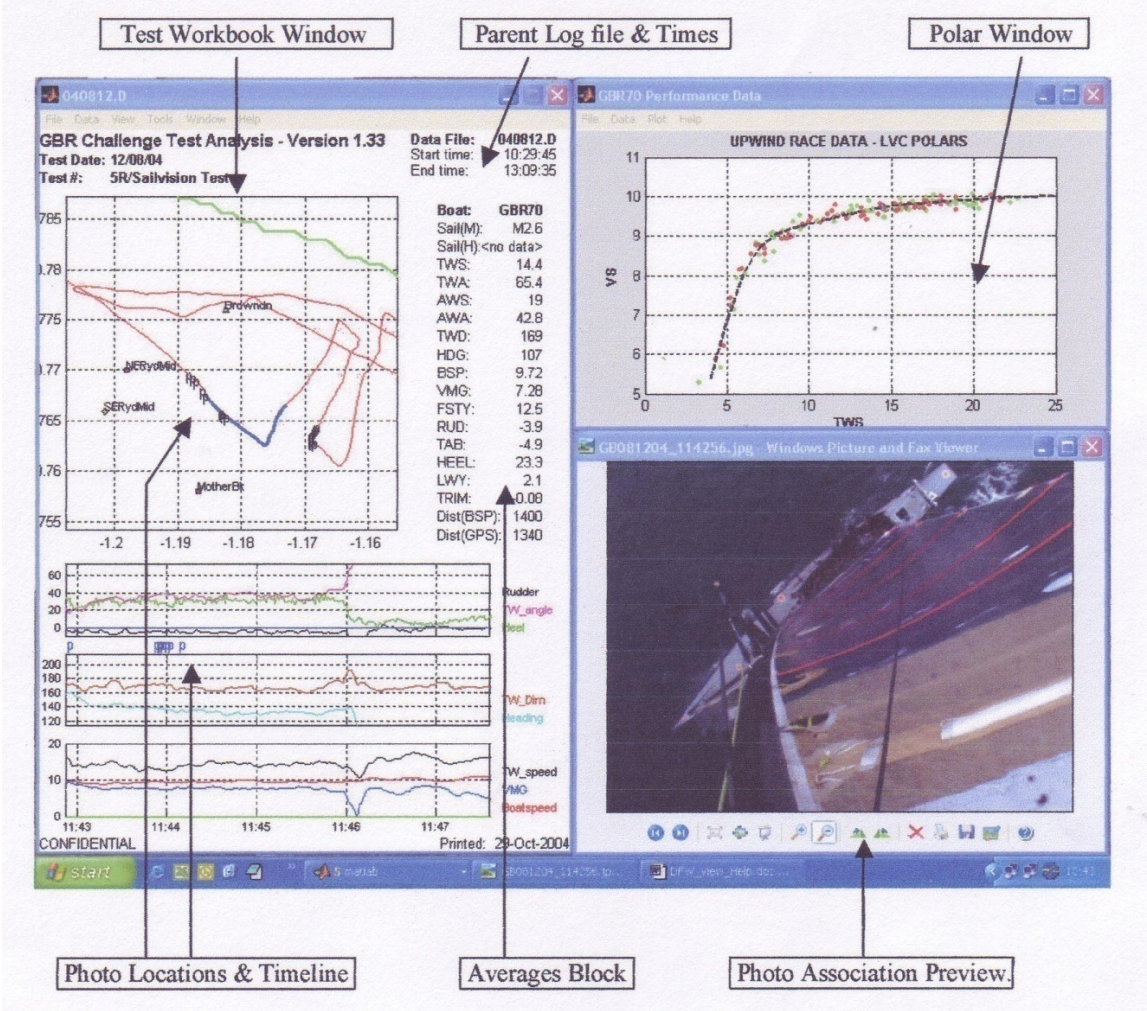

Figure 7 - Screenshot from the previous British AC challenge

2.3.2 Dinghy Performance Analysis

2.3.2.1 49er Methods

The final and most recent work to be examined is that of Julian Bethwaite, with his research into designing a new rig for the 49er class. The work of Bethwaite is particularly relevant as

it was written in early 2008 and uses the 49er, one of the Olympic class boats. Bethwaite's aim is to produce a polar performance for a 49er with three different rigs, the first is the current rig and the other two are potential rigs. With a polar performance for each combination, Bethwaite aims to select the fastest rig through a quantitative decision. The experimental set up uses a ½ Hz GPS unit which was accurate to 0.2 knots, a 49er, a compass for measuring the TWD and an anemometer for measuring TWS. There was also a meteorological station a mile from where the testing was carried out which was used for wind information. During the data collection the wind was also measured every two minutes and within 200 metres of the 49er (Bethwaite, 2008). Some of the data collected can be seen below on the left of Figure 8 in its raw format (Bethwaite, 2008). There is a great deal of scatter in the data but it was processed by averaging the V_b for every TWA for each TWS. This filtered polar can be seen in the right of Figure 8.

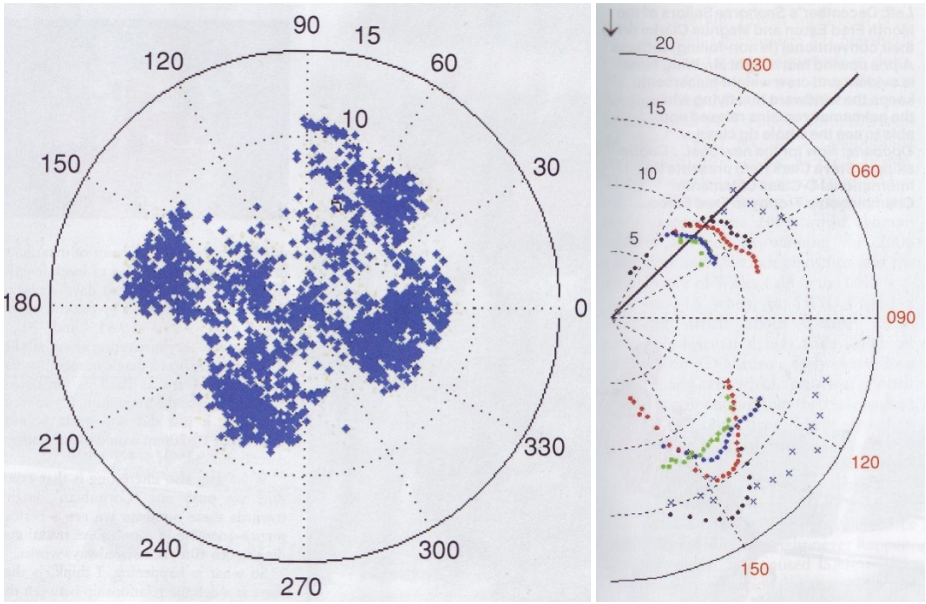

Figure 8 - Bethwaite's polar performance plot of the 49er (Seahorse, 2008)

Comparing Figure 7 to Figure 8, the scatter of the data is vast; this could be due to several reasons. Firstly the 49er is very dynamic compared to an America's Cup boat which results in rapid fluctuations in V_b and TWA, possibly explaining some of the scatter. This was also found in Tatano's Flying 15 paper (1978), however the scatter was less than experienced by Bethwaite due to poor experimental design. However a Flying 15 is less dynamic than a 49er due to significantly more displacement. One of the other factors is that the TWS and TWD were not continuously logged which would add some smearing of the data. There would also have been some significant errors in using the data from a meteorological station a mile away. The sampling rate of the GPS was also lower and the accuracy was less than the previous examples that we have studied so far. The data from Bethwaite was also

collected on tidal water which could explain why the raw data plot in Figure 8 is slightly skewed showing the port tack slower upwind and faster downwind. The main reason why the data quality is not as good as the AC collected data is due to the fact that the 49er is a very light displacement boat and significantly restricting the amount of equipment that can be carried on the boat due to weight considerations. All of the issues need to be considered carefully in order to avoid infringing on the performance of the boat.

2.3.2.2 Masayuma Methods

The last part of the collected data section shall be an examination into alternative existing performance analysis techniques that have been used. In these techniques two different dynamic models are used to measure the performance of a yacht. In this section we shall first examine the paper by Masayuma, written in 1993, which uses conventional naval architectural methods to model dynamic performance with a static polar. As mentioned previously the lack of literature containing Artificial Neural Networks (ANNs) was stated in terms of performance analysis Masayuma, (1995) also investigates modelling tacking with the aid of ANNs. Although tacking is only a small part of racing around a course, an investigation into the methods that Masayuma used is critical for the scope of this project.

The experimentation that Masayuma carried out in 1993 consisted of a 10.6 metre yacht with the various usual instrumentation described in the previous AC projects. However, Masayuma used a wave rider buoy in order to measure the waves that the yacht would be experiencing. The dynamic measured data was compared to VPP predictions that had been carried out previously and the two matched relatively well. There were some problems with the experimentation as the testing had to take place in close proximity to the wave rider buoy. However, as the experiment included modelling the performance of the boat in waves in various wind speeds there was significant scatter in the data collected, as can be seen on Figure 9 below. Masayuma also states that there was lack of data in the 10 knot wind which reduces the accuracy of the data.

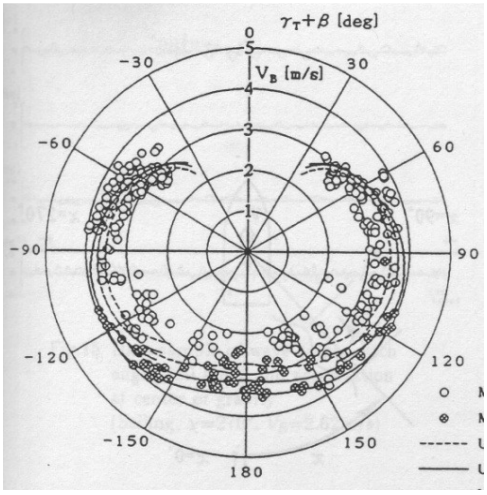

Figure 9 - Masayuma's Flying 15 polar plot

In the subsequent paper (Masayuma, 1995) it focuses on an investigation into tacking with mathematical modelling and also an ANN, he is able to train an ANN without giving it the equations of motion and instead feeding the following channels of data into the ANN. They are fed in as individual channels and also as the derivatives of each of the data channel for the time step. Channels that are logged are the rudder angle, heading angle, roll angle, V_b and V_b in sway.

During the training process there are two different styles of tacking that are carried out. These are a small and a large rate of turn for which the ANN is fed both. The ANN is of the Multi Layer Perceptron (MLP) variety and has two hidden layers. Masayuma's ANN, however does not have a Genetic Algorithms (GA) optimising the ANN structure of Cross Validation (CV) checking the training procedures. The ANN produces a very low MSE of less than 3×10^{-5} after over 30,000 iterations which is an acceptable level of error. The output of the ANN is compared to the output of the yacht's motions during the tacking procedure. This can be seen in Figure 10, Figure 11 and Figure 12; however the correlation seems better in Figure 10 than the other two figures. The output of the yacht's motions are from newly acquired data, the ANN does show some relatively large differences to the output data from the yacht in the top trace which is the heading 'ψ' comparisons. However, the second trace roll 'φ' and the trace at the bottom, velocity 'V_b' outputs are not too different from the output of the ANN. This could be due to the V_b being at a largely constant speed which could be helped by filtering.

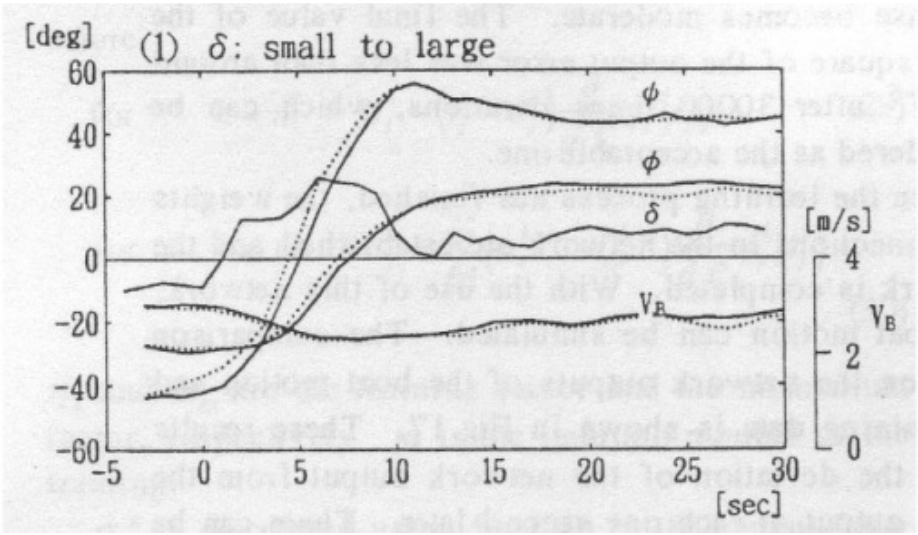

Figure 10 - ANN Tacking (Masayuma, 1995)

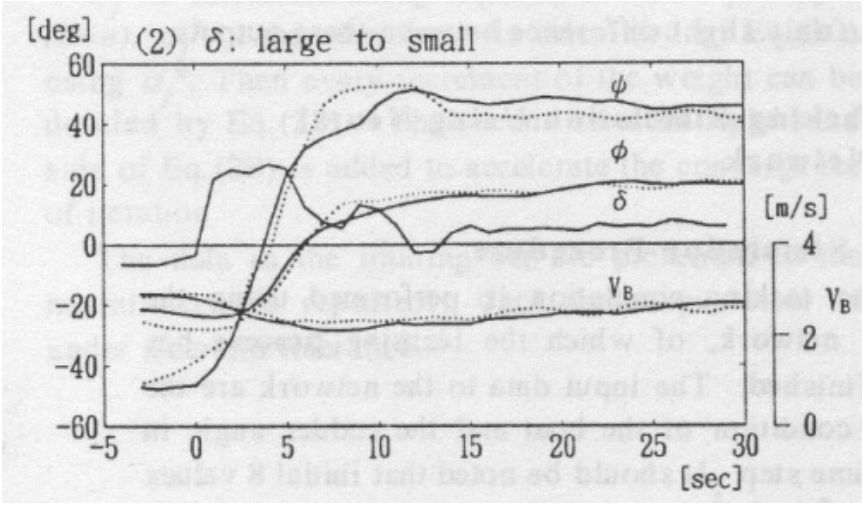

Figure 11 - ANN Tacking (Masayuma, 1995)

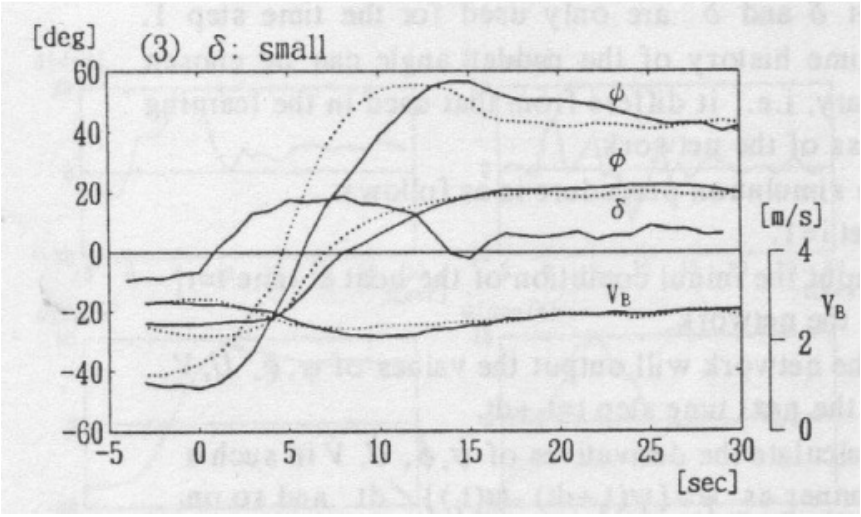

Figure 12 - ANN Tacking (Masayuma, 1995)

It is also interesting to note that the heading ANN output for Figure 11 and Figure 12 is very similar even though the turning rates are different. This could suggest a possibility of overtraining the ANN (Tzafestas, 1996). The two hidden layer MLP is prone to overtraining with such a large number of iterations, which is perhaps why there is a large difference in ψ. The presence of Cross Validation would have stopped the overtraining from happening as discussed later in this document. Masayuma, states that there is a lack of data which was used for the training of the ANN. Another inherent weakness of the MLP compared to other ANNs as discussed later is that they do require a lot of training data to produce an accurate answer. The variety of inputs does show the flexibility of ANNs to cope with very varied problems as demonstrated by Masayuma.

Chapter 3

Artificial Neural Networks

3.1 Introduction

During the early stages of the project it was decided that one of the routes to explore was that of the Neural Network as it was anticipated it would be able to understand the complex relationships between performance and the marine environment. An extensive literature search was conducted by the author. During this literature search and early testing it became apparent that this was the most promising route for the project to take as initial data was encouraging. The Neural Network subject area therefore is the core focus of this project and begins with the history of Neural Networks, before delving deeper into the various design and structural aspects of the network and finishing with the conclusion.

3.2 The Development of Artificial Neural Networks

There are two types of Neural Networks, Biological Neural Networks (BNN) and Artificial Neural Networks (ANN). Neural Networks consist of assemblies of simple processors or neurons (Siegelmann, 1999), which are commonly found in both biological and artificial networks. In this project the focus has been on ANNs but it is instructive to consider Biological Networks initially as they were the forbears of the ANN.

The Biological Neural Network has existed for thousands of years and consists of real neurons that are connected in a network to form the nervous system of higher life forms. In the human brain there are billions of cells called neurons and they are formed into a complex Neural Network. An example of a biological neuron is illustrated in Figure 13 below (Petriu, 2004).

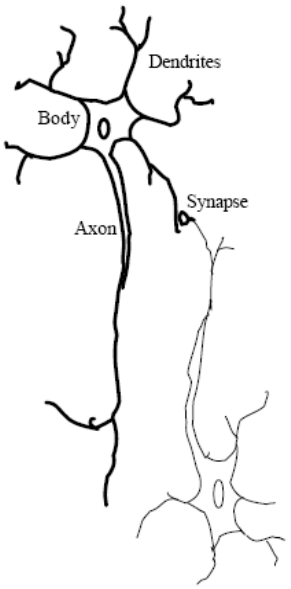

Figure 13 - A biological neuron (Petriu, 2004)

It is clear from the figure that a neuron is composed of multiple parts which each play an important role in the function of the neuron. The dendrites carry electrical signals into the neuron body and the axon is a single long nerve fibre that carries the signal from the neuron body to the other neurons (Petriu, 2004). The purpose of the synapse is to connect the dendrites to other dendrites in the system. Communication by biological neurons is significantly slower than in computers but the parallel arrangement of the human brain allows it to process more efficiently than have so far been achieved by computers (Rumelhart, 1986).

The concept of neural computing has appeared in the literature for approximately 60 years, since McCulloch and Pitts (1943) first published their paper entitled A Logical Calculus of the Ideas Immanent in Nervous Activity (1943). In their paper they list five assumptions governing the operations of a class of neurons that have since become known as the McCulloch-Pitts neuron, and which are familiar to computer scientists working in the field (Anderson and Rosenfeld, 1988). The concept of Neural Networks spread increasingly through the late forties and fifties until Rosenblatt produced the first ANN that was practical and effectively functioned as a perceptron. However, after Rosenblatt's paper (1958), the subject of ANNs was relatively neglected due to other Artificial Intelligence (AI) advances. During the 60's the research dwindled on the subject of ANNs further due to limitations of perceptron networks which was discussed by Minsky and Papert (1969) in their book entitled Perceptrons (1969). There were several issues raised by Minsky and Papert over the real-world usefulness of Neural Networks. In particular they presented the example of a

perceptron with linear threshold functions which was shown to fail the XOR problem classification problem as will be examined further in the next section.

There were other factors that slowed down the development of ANNs such as the widespread resistance to the whole idea of actually building an artificial "chunk of brain" (Widrow, 1987). The media were also partially responsible, with brain models lending themselves well to dramatic, almost science-fiction like news stories, and reporters for daily newspapers in the 1960s that were not noted for their scientific understanding (Anderson & Rosenfield, 1988). It was not until the 80's that the area of Neural Networks saw a revival after an influential book was published by Rumelhart and McClelland (1986). In 1987 the revival was such that the International Neural Network Society was formed, and today it has over 2000 members. During the late 80's and 90's computer hardware and software became more powerful enabling more users to adopt ANNs. From then on the general usage of ANNs increased significantly and today they are used in a wide variety of applications in areas such as speech, image recognition and financial predictions, where the mechanism of the problem is difficult to model (Huang, 1997). Since ANNs are used as solutions in multiple application styles they are therefore available in several different designs. Each of these designs have various strengths and weakness and are mostly suited to a narrow band of applications. These changes in design and style shall be looked at later on in the chapter.

3.3 Implementation of Artificial Neural Networks

An example of a simple ANN, otherwise referred to as a perceptron, is illustrated below in Figure 13Figure 14.

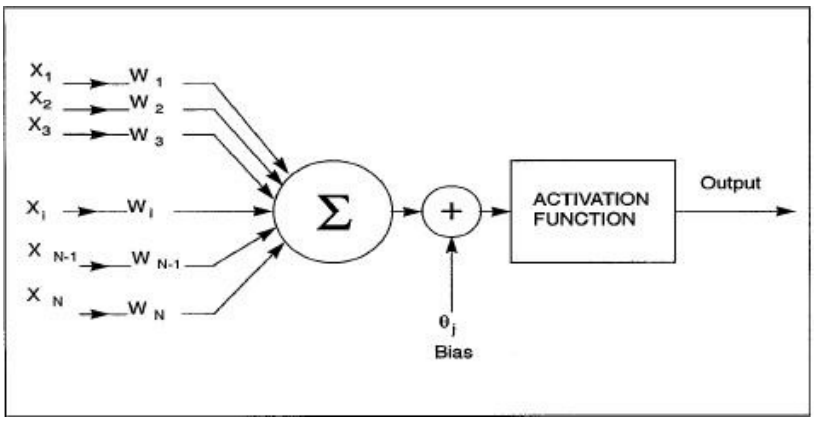

Figure 14 - Neuron as described by Minsky

In the figure, X_N, which could be in a variety of formats or types, are the inputs to neurons used in an application such as function approximation or a classification problem. Each input is assigned a weighting, W_i which is used to form a weighted sum and the result is passed though through a nonlinearity to produce an output of the desired form (Sanchez et al, 1992). In this example, a bias is added before passing the result through the activation function. The final step of the process is producing the output. In an ANN that has been trained, the final values of *Wi* are such that known input data produces an accurate estimate of known corresponding outputs.

The key components of a network are known as Processing Elements (PEs), which in mathematical terms may be thought of as linear regressors. Their basic form is illustrated with just one PE in Figure 15.

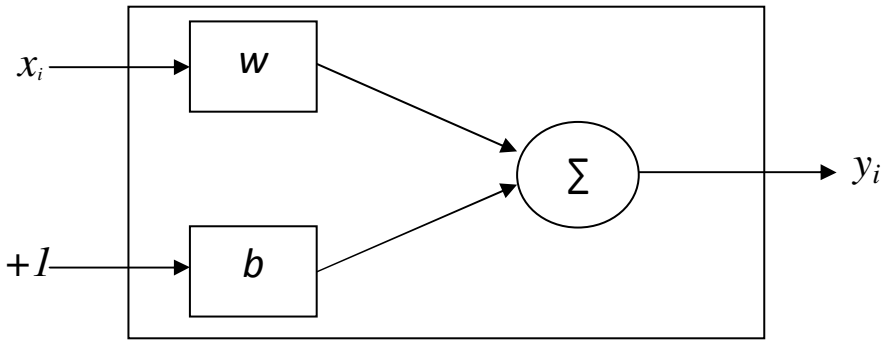

Figure 15 - A simplified Neuron with one PE

where x_i and $+1$ are inputs, w is the scales input, b stands for the multiplier bias, y_i is represented by the output as a linear value and $\sum$ symbolises the PE.

The ANN used in the present study is one of the most commonly used ANNs, referred to as a Multilayer Perceptron (MLP) ANN. It is instructive to consider error minimisation in ANNs before discussing the wider issues in their training and testing.

3.4 Assessing ANN Performance

3.4.1 Measuring Error

ANNs may be optimised with respect to a measure of the error between the desired response and the actual output from the ANN, such as their mean square error (MSE). The MSE can

be calculated from the estimated data on the basis of an L2 criterion, an efficiency measure, (Cassella et al, 1999) as in equation (22).

$$MSE = \frac{1}{2N}\sum_{i=1}^{N} \varepsilon_i^2 \tag{22}$$

Where N stands for the number of observations and ε is the instantaneous error. The MSE in this form gives a definitive measure of the performance of the ANN as it is independent of factors such as the structure of the ANN or the number of PEs in the network unlike some of the other methods of measuring performance. The calculation of the MSE can also be viewed as twice the average cost.

Equation (22) can be expanded for a larger network to use other components including the number of exemplars in the data set and the number of PEs as shown in Equation (23) below:

$$MSE = \frac{\sum_{i=0}^{P}\sum_{i=0}^{N}(d_{ij}-y_{ij})^2}{N\ P} \tag{23}$$

Where P is the number of PEs, y_{ij} is the actual output for exemplar i at PE j and d_{ij} is the desired output for exemplar i at PE j.

It is worth noting that the MSE can also be normalised, which is useful for comparing the size of the error to the data that is used for training the network. The final major measure of error is the percentage error between the desired and actual output. This is calculated by using Equation (24) below.

$$\%Error = \frac{100}{NP}\sum_{j=0}^{P}\sum_{i=0}^{N}\frac{|dy_{ij}-dd_{ij}|}{dd_{ij}} \tag{24}$$

Where P stands for the number of output processing elements, N is the number of exemplars in the data set, dy_{ij} is the denormalised network output for the i exemplar at processing element j and dd_{ij} is the corresponding denormalised desired output. The percentage error is a useful measure of the error but it can also be misleading in some cases. This can happen when there is a large numerical range of data and when the desired and actual outputs are close together and small compared to the size of the numerical range.

There are other performance measuring parameters for ANNs such as Akaike's Information Criterion (AIC) and the Rissanen's Minimum Description Length (MDL), which shows the relationship between the training performance and the size and the number of degrees of freedom compared to the error respectively (Murata, 1994). The AIC can be written as:

$$AIC(k) = Nln(MSE) + 2k \tag{25}$$

The MDL can be written as:

$$MDL(k) = Nln(MSE) + 0.5kln(N) \tag{26}$$

where *k* is the number of network weights and *N* the number of exemplars.

These equations can be useful when considering the effectiveness of network size such as the number of hidden layers and the affect of the data set used for training the ANN. Larger datasets and more hidden layers increase the training times for only marginal improvements in performance of the ANN.

3.4.1 Goodness of Fit

A measure of how well the regression equation represented by the PE fits the data is given by the correlation coefficient, as expressed by Equation (27). The value of the correlation coefficient approaches unity as the PE tends towards a perfect fit to the data. It is not to be confused with fitness which the MSE provides as the correlation coefficient represents the outputs moving in the same direction.

$$r = \frac{\frac{\sum_i (x_i - \bar{x})(d_i - \bar{d})}{N}}{\sqrt{\frac{\sum_i (d_i - \bar{d})^2}{N}} \sqrt{\frac{\sum_i (x_i - \bar{x})^2}{N}}} \tag{27}$$

Where r is known as the correlation coefficient. The output and desired output in the equation are designated as *x* and *d*. The range of the correlation coefficient is between -1 and 1. A higher number suggests a better correlation of the data whereas number closer to -1 would suggest a negative correlation. A correlation that results in a value that is close to 0 suggests that there is little or no correlation.

3.5 Training Neural Networks

3.5.1 Error Minimisation

The ANNs are 'trained' by adjusting the weights in the performance surface, as shown by Figure 16, so that the differences between the predicted and the measured results are minimised. One approach to this is to use a gradient descent optimisation method. The gradient descent method effectively allows the ANN to become "aware" of its performance and modify its parameters in such a way as to determine the optimum solution (Principe et al, 2000). The gradient descent method is applied to a performance surface based on a MSE equation. Firstly the boundaries of the system are changed, which are *w* and *b*. These two parameters are important as they are used in the least squares method to reduce the difference in desired and actual output. Then *b* is set to zero which reduces the MSE equation to a function of *w* as seen below in Equation (28) (Principe et al, 2000):

$$J = \frac{1}{2N}\sum_i (d_i - wx_i)^2 = \frac{1}{2N}\sum_i (x_i^2 w^2 - 2d_i x_i w + d_i^2) \tag{28}$$

With *w* as a variable and the other parameters set at constant, *J* can be seen to be a positive quadratic. This quadratic forms the major component of the gradient descent method and is known as the performance surface. The performance surface can be plotted for ANNs during training on computers and is usually represented by a scatter plot of an L2 Criterion. The L2 Criterion represents the quadratic cost between the output and desired responses. This shows the plot of the performance surface, which is effectively plotting weightings (w) on the x axis and cost (*J*) on the y axis. We are then able to use the performance surface to understand how the MSE is affected by the weights. The minimisation of the performance curve by the gradient descent method has been represented graphically by Principe et a al. (2000) as shown in Figure 16.

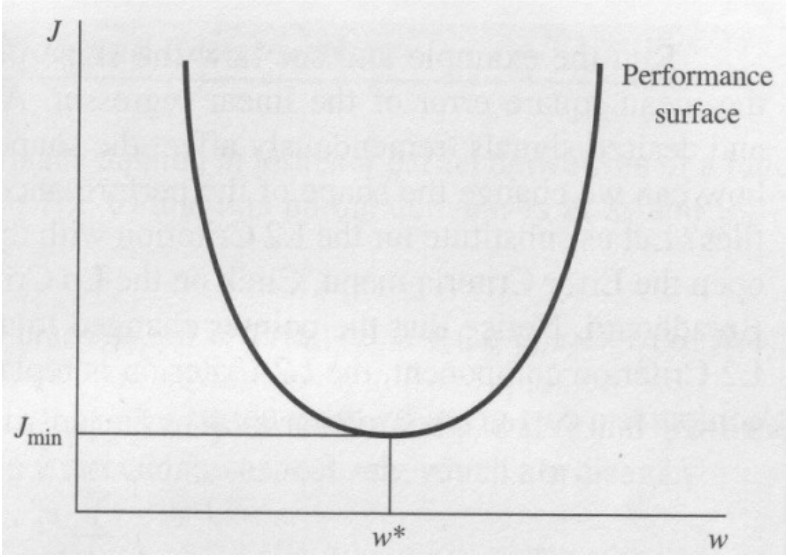

Figure 16 - Showing the performance surface

The aim of the procedure is to find the minimum point on the performance surface, w,* by conducting a series of univariate searches in the direction of steepest descent defined as the opposite direction to that of the local gradient, and as represented by equation (29) (Shu-Heng Chen, 2006).

$$w(k+1) = w(k) - \eta \nabla J(k) \tag{29}$$

Where the descent controller, η, determines the step length adopted during the search and $\nabla J(k)$ is the gradient. The step size can be determined manually or can be automatically adjusted during the training.

An example of the gradient descent method can be seen in Figure 17 (Principe et al, 2000) below, as it searches for the minimum point. The curve that the gradient descent method is searching is known as the performance surface and can also be seen on the figure below.

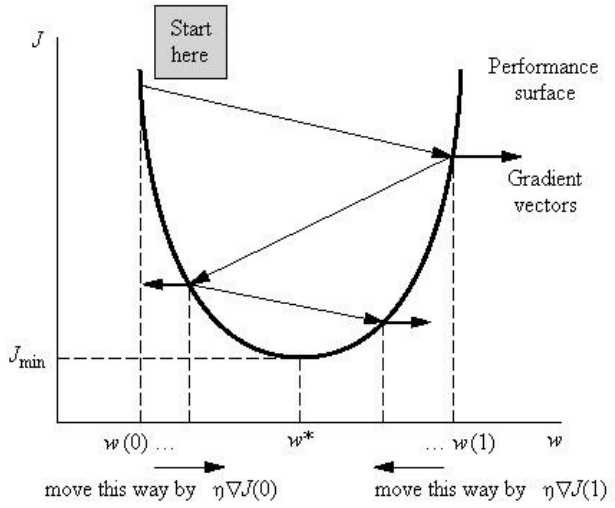

Figure 17 - Gradient descent method on the performance surface

3.5.2 Rattling and Step Size

In the previous section the parameter, η, which controls the descent rate in the gradient descent method, was introduced. If the step size in the search procedure is chosen inappropriately the phenomenon known as Rattling may occur. Rattling can sometimes be seen during the training process in network output plot. The problem of Rattling appears when the gradient descent method is close to w^* and the gradient of the curve is very similar to that obtained for the previous w. The larger the step size the greater the risk and the increased severity of Rattling that appears. When Rattling occurs, larger values appear in the MSE due to the gradient descent method finishing a distance from w^*, commonly known as the misadjustment (M), as can be seen in Equation (30).

$$M = \frac{J_{final} - J_{min}}{J_{min}} \tag{30}$$

In order to avoid Rattling the obvious choice is to decrease the step size in the search for w^*. This however means that the search time for w^* will be longer as more iterations are required. The appropriate magnitude of the step size is a trade off between the importance of a low MSE is compared to obtaining a quicker training time and solution. A limited number of iterations (epochs) could also prevent the solution being found.

There is a technique which uses a variable step length and is known as scheduling. This method starts off with a large step size in order to get near w^* quickly. As it gets closer and

closer to w^* the step size is gradually reduced in linear format for each iteration by β. This can be seen in Equation (31).

$$\eta(k+1) = \eta(k) - \beta \tag{31}$$

The size of the constant β is determined by trial and error. If β is too large there is a risk of stalling, conversely if β is too small the calculation time tends to take a lot longer.

3.5.3 Momentum

The gradient descent method with linear changing step size is almost one of the most robust search methods, especially compared to Newton's which has a higher performance but a much lower robustness (Moller, 1990). Its performance can be further improved using the concept of momentum. Adding momentum to the gradient descent method effectively speeds up the convergence and also stops the search from identifying a local minimum as the global minimum (see Figure 27) through Equation (32).

$$w_{ij}(n+1) = w_{ij}(n) + \eta\delta_i(n)x_j(n) + \alpha_M(w_{ij}(n) - w_{ij}(n-1)) \tag{32}$$

Where α_M is the momentum and usually is between the following range (0.5-0.9).

The difference between a gradient descent search method with or without momentum can be seen in Figure 18 below. Without momentum the gradient descent can mistake w^L as the global minimum whereas with momentum it can find w^*, which is the actual global minimum. The concept of momentum can be viewed as a ball rolling down a slope similar to Figure 18 from right to left. The ball starts at the start of the curve and rolls down the first hill. If the ball does not have momentum it will stop at the local minimum w^L. However if the ball has a greater momentum it will roll past w_i^2 and find the global minimum at w^*. Adopting the momentum approach in the optimisation procedure leads to an improved estimate of the minimum, and hence a lower MSE and leading to a better solution (Gautama, et al, 2003; Sontag 1988).

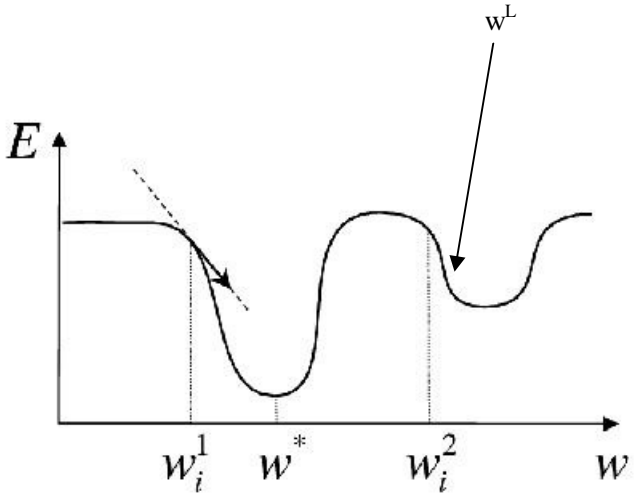

Figure 18 - Local versus global minimum solutions

3.6 Neural Network Designs

In the previous section the mathematical techniques behind ANNs were explored in some detail. This section will consider the many different types of ANNs that could be used in this project as well as such core concepts such as backpropagation and cross validation. The discussion, which could be more wide ranging, will be limited to the software resources available for use in the project. The following types of ANNs will be reviewed:

- Multilayer Perceptron (MLP)
- Generalized Feed Forward (GFF)
- Modular Neural Network (MNN)
- Jordan/Elman Network (JEN)
- Principal Component Analysis (PCA)
- Radial Basis Functions (RBF)

3.6.1 Multilayer Perceptron (MLP)

The MLP ANN is probably one of the most common ANNs. Several other ANNs are derived from the basic structure of an MLP ANN including all of the ANNs in the list above. The standard MLP is a good starting point for early initial research into new data and has

proved useful in the current project. During the review of the MLP we shall also cover some of the other core topics mentioned in the introduction.

The MLPs that shall be examined are all feed forward networks with multiple hidden layers. Usually only one hidden layer is used initially but additional hidden layers can be added if the learning power of the ANN is not sufficient. Additional hidden layers add more PEs to the ANN and therefore more power to solve the problem. It might appear to be a good strategy to add several hidden layers in the ANN but adding more layers increases the training time and also the danger of over training the data (Principe, et al, 1999). Over training occurs when generalization performance begins to reduce as the network includes the noise in the model. When it is tested on new data the result will be inferior to that of a network with guards against over training. Hidden layers allow the use of back propagation, this method increases the learning power of the network through supervised learning which informs the network which neuron is producing errors (Rumelhart, et al, 1986). MLPs also have the problem of requiring a lot of data to train the ANN successfully which means spending longer on collecting good data compared to other network designs. An example of an MLP can be seen on the following page in Figure 19 (Kong, 1998).

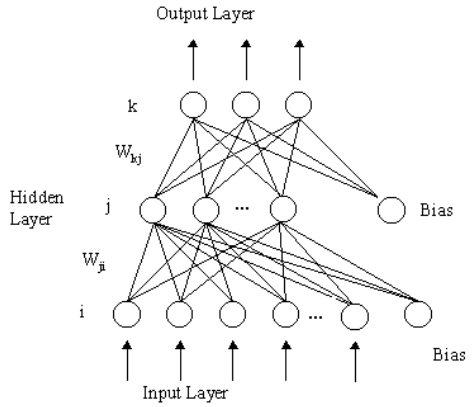

Figure 19 - An MLP with one hidden layer

This example of an MLP shows the structure very well with one hidden layer (*j*). The inputs (*i*) can be seen at the bottom of the figure with the outputs (*k*) at the top. The two bias axons are also featured to the right of the main ANN. Axons are paths between the hidden layers. A bias Axon is used for non linear solutions or as an output (Principe et al 1999). The weightings (W_{kj}) and (W_{ji}) are featured on the left hand side.

This MLP features backpropagation which enables the network to measure the progress of training (Kong, 1998). Werbos was the first to describe backpropagation in 1974 but it was not until 1986 that it was a recognised feature (Rumelhart et al, 1986). Backpropagation functions by sending the calculated errors further back into the ANN. This uses the method

of gradient descent which allows the weights with the smallest error to be found (Werbos, 1994; Ballard 1987).

Below in Figure 20 is an example from the NeuroSolutions software of an MLP that the author designed and built for early data testing.

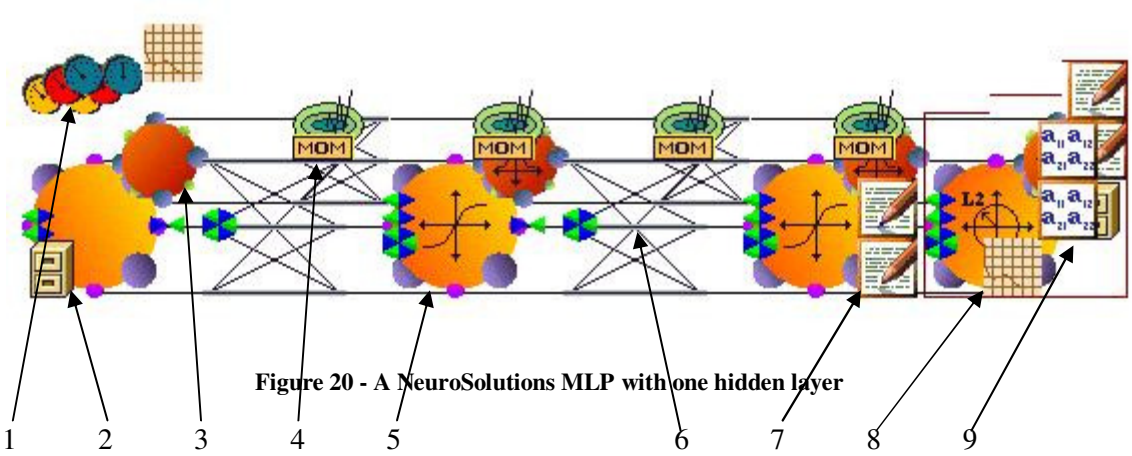

Figure 20 - A NeuroSolutions MLP with one hidden layer

The format of the MLP in Figure 20 enables the user to gather more information from the MLP than the ANN in Figure 19. The features of interest of this typical MLP shall be include:

1. Back, Genetic and Static Control Inspectors which control a multitude of settings for the ANN. The Back Inspector enables the ANN to use batch or online backpropagation and which search method to use, in this case gradient descent is chosen (Han, 1996). The Genetic Inspector controls the Genetic Algorithm (GA) which controls the number of generations, population size, progression and the cost to minimise. The cost to minimise is cross validation (CV) in this scenario. The final part is the Static Inspector which controls the number of epochs and data set.
2. This is the File Input Axon which controls which data sets are imported into the ANN from various file locations.
3. This is an Input Axon which forms part of the backpropagation feature.
4. Momentum Inspector for implementing the gradient descent function which is normally hidden.
5. This is the first hidden layer which in this case is a Tanh Axon Inspector.
6. This is the synapse that connects the layers together.
7. Another Tanh Axon Inspector, however this one is not hidden and has two data writing functions for the outputs.
8. Data graph feature which enables the user to view the progress of the training for the ANN. This is both in the training and CV function.

9. Implementation of L2 Criterion as described in section 3.4.1 as various forms of error measurement. The icon with blue writing features the output matrix that shows the performance of the ANN during training, testing and production.

An important feature of the ANN that was briefly mentioned in point one above is the GA function. This feature allows the optimisation of the ANN through GAs which changes the inputs, number of hidden PEs as well as the learning rates of the ANN (Plumer, 1996). GAs are usually used for optimisation problems which are loosely based on an evolutionary process. There are several different procedures for finding the optimal solution. The most common procedure used in this project consists of a stochastic method of selecting the chromosomes with the best fitness for each generation. There are multiple chromosomes per generation and several generations in the evolutionary process. The GA fine tunes the design of the ANN through several generations, each of which consists of several chromosomes where a new ANN is trained for each of them (Ignizio, Soltys, 1996). When GA is enabled for the ANN, this process takes considerably longer than the standard ANN training, however, the final result is more accurate.

Cross Validation was also mentioned in point one; this is an important feature in testing and training of the ANN. A good example is an MLP with two hidden layers that has a longer than usual training schedule, these are sometimes associated with overtraining. Overtraining occurs when the ANN starts to match the output data too closely to the desired data and begins to be unable to recognise unknown data (Tzafestas, 1996). An example of overtraining can be seen below in Figure 21 (Tzafestas, 1996).

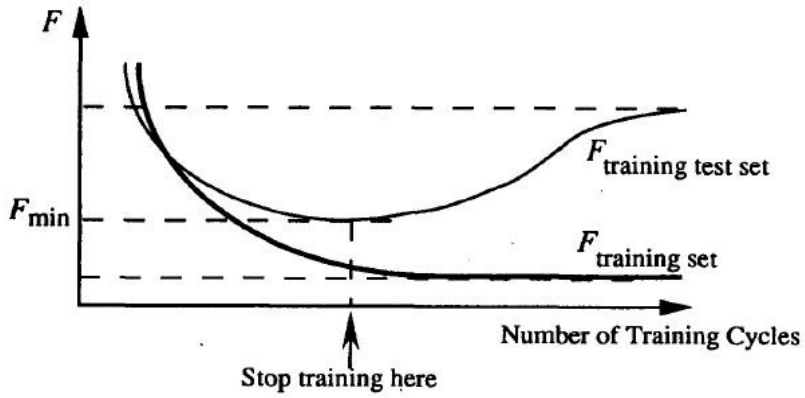

Figure 21 - An example of ANN overtraining

Looking at Figure 21, the training curve that we would ideally see is the lower one called $F_{training\ set}$. If we were training an ANN with no CV this would be the only curve visible and the assumption would be that the network has trained well. However with CV we are able to see the performance on the test set which is not used in training represented by the upper

curve called $F_{training\ test\ set}$. With the ability to see the training test set it is clear that training should have been terminated at the point where the arrow is as the $F_{training\ test\ set}$ begins to increase suggesting overtraining. It is worth noting that termination can be adjusted through other methods such as detecting a rise in the MSE after a certain number of Epochs (Srivaree, et al, 2000). When training and testing an MLP ANN on the computer it is possible to cut out a percentage of the input data to be used for CV and testing. On the previous page in point number 8, the data graph feature was mentioned. In this feature, during training and testing, it is possible to watch the ANN terminate overtraining from the CV plots and the testing data.

The fifth item in the list of ANN features presented above relates to ANNs with hidden layers. As mentioned earlier in this section of the literature review the addition of hidden layers enables the use of backpropagation which compares the ANNs output with the desired output and calculates the errors. It then adjusts the weights of the individual neurons to reduce the output errors. Backpropogation was not used or recognised until the late eighties after the work by Rumelhart et al. With hidden layers and backpropagation the XOR problem described by Minsky in his 1969 paper can be solved as follows.

Below in Table 1 is the well known XOR truth table used for the inputs and expected outputs of the ANN.

Table 1 – XOR Truth Table

IN1	IN2	Expected Output
0	0	0
0	1	1
1	0	1
1	1	0

The aim is to teach the perceptron to output the Boolean value of 1 when the inputs are different and zero if the inputs are the same as can be seen in Table 1. The perceptron is faced with three different types of combinations of inputs. When the inputs are both zero this is well below the threshold of 0.5 and 0 is the output which is correct. When one input is 0 and the other 1 this raises the net input above 1 so the output is therefore one. The third and final combination of having both inputs as 1 is where the perceptron fails. This is due to the lack of a hidden layer, with no hidden layer there can be no backpropagation. With no

hidden layer the network can be considered only first order, the hidden layer increases the power of the network to second order status which has no problem in solving the XOR problem (Sejnowski, et al, 1986). With backpropagation however the third combination would initially fail as the difference between the desired and actual output is very large. Once the ANN has found such a large delta it corrects the weights of the neurons and enters another iterative cycle until the error measure such as MSE is under the acceptable level. The actual outputs would be within a couple of percent of the desired.

3.6.2 Generalized Feed Forward (GFF)

As mentioned earlier, the GFF ANN is a well known modification of the MLP. In structural terms it is very similar but it has the ability to jump over multiple layers of the network. GFFs can therefore solve some problems much more efficiently than MLPs as they require less significantly less epochs (Han, 1995). There is one famous example of this known as the double spiral problem (Singh, 1997). The double spiral problem is often used as a benchmarking test as shown by Singh in his 1997 paper, where he compared Parametric Feed Forward (PFF) ANNs with different backpropagation settings. The double spiral can be below in Figure 22 (Singh, 1997). Other testing has been conducted on the double spiral problem which is regarded generally as a challenging problem to solve (Hwang et al, 1993). To solve the network needs to be capable of using temporal data and also reduced back propagation (Han et al, 1996).

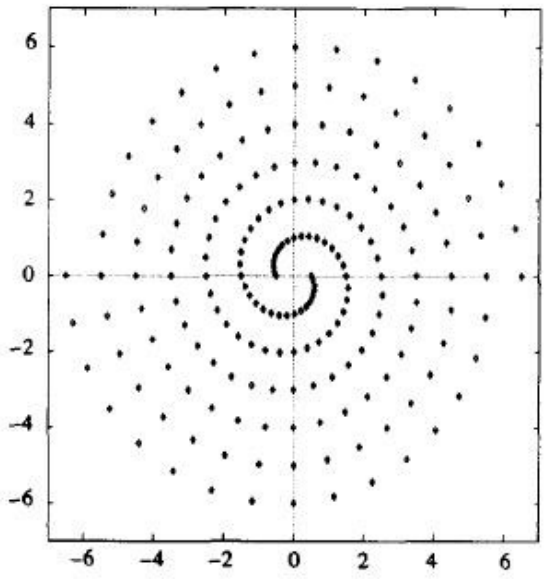

Figure 22 - The classic spiral problem

The GFF ANN is able to solve this problem more efficiently due to a number of factors such as the design and weights being fully optimised, "*the training results are robust against changes of these parameters"* and there are no random numbers that are being used (Tomandl, 2001). There are a few disadvantages, such as slow training with a high number in the dataset and the lack of ability to ignore bad data as inputs. The lack of ability to ignore bad or noisy data which is inputted could have some negative effects on performance. As mentioned before, the data gathered in the sailing environment will be noisy as it is a naturally noisy environment and the boats are also very dynamic (Holley, 2007). In the next section we will look at another major type of network the MNN ANN.

3.6.3 Modular Neural Network (MNN)

Similar to the GFF ANN, the MNN is a special development of the MLP. MNNs consist of several MLPs working in parallel in a variety of structures (Guler, 2005). They have several layers that are arranged in a modular format; in the NeuroSolutions software package there are four different modular layouts that are available. Compared to the MLP, the GFF has a smaller number of weights and PEs which increases the training speed without compromising on accuracy. The MNN consists of more than one network, normally of the expert and gating variety (Hodge et al, 1999). There is competition between the expert networks which are being trained, and the gating networks control this competition between the expert networks (Sharma et al, 2003). MNNs are also able to function with GAs which optimise the structure and weightings. There are some difficulties with the design of MNNs due to the fact that there are several ways to structure an MLP into each of the modules and there is no real link between the topology and the data. The optimum structure of the MNN would have to be determined by some experimentation with early datasets. An example of an MNN network can be seen below in Figure 23.

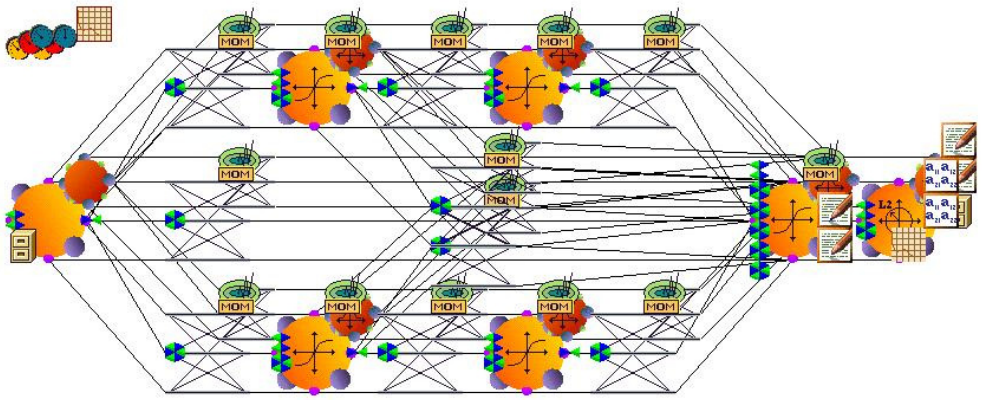

Figure 23 - A MNN developed in NeuroSolutions

Figure 23 shows that the MLP modules are situated in the top and the bottom of the ANN and that they are using backpropagation. The gradient descent with momentum is being used and that GA's are also optimising the ANN. The ANN in Figure 24 is also of the fully feed forward design, similar to design 3 in Figure 24 below, but with the first layer also fed to the last layer. Other popular modular designs can be seen below in Figure 24.

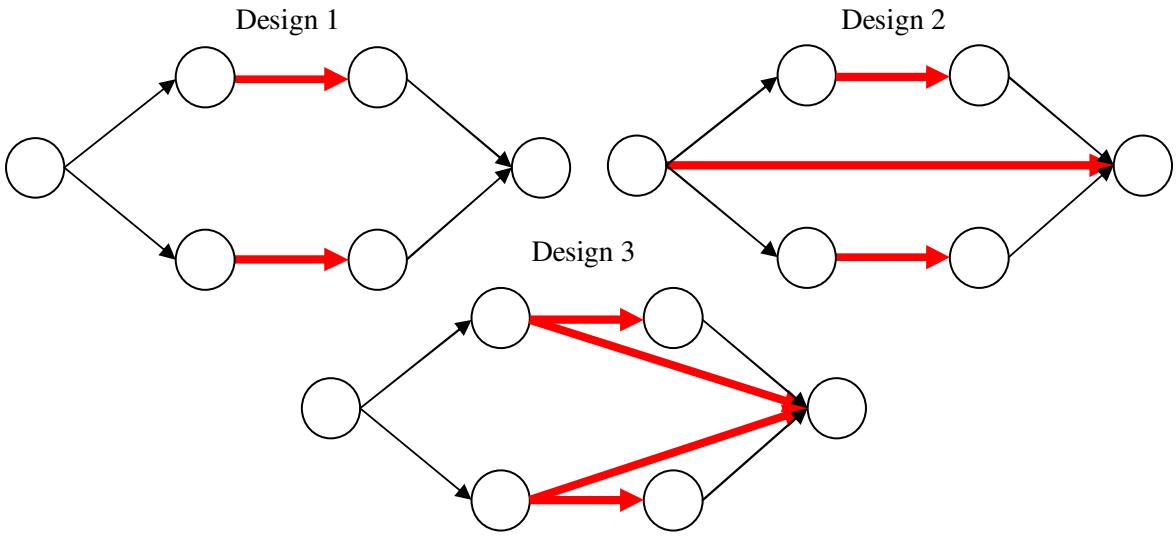

Figure 24 - Different configurations of the MNN ANN

3.6.4 Jordan/Elman Network (JEN)

The JEN is yet again an extension of the MLP, however the main difference is that they have a component called a context unit, giving them an important advantage over the other models. The previous models are static in terms of temporal data whereas the JENs are able to solve dynamic problems with a time base. The Context PE unit gives the JENs a memory

capacity for storing previous data and they are known as recurrent networks (Pham, 1998). Recurrent networks are also better able to deal with noise. As mentioned previously the environment that the data is being collected in is very noisy, so the dynamic JEN could be better suited for the problem than static ANNs (Holley, 2007).

The main difference between the Jordan and the Elman networks is that in the Elman network the results from the PEs, which are hidden, are fed directly into the context unit. However, in the Jordan network the output of the total network is fed into the context units. A Jordan ANN can be seen in Figure 25, with the outputs being fed back into the context unit to the right of the diagram (Jordan, 1986). In comparison, Figure 26 is an Elman ANN which shows again the hidden layer feeding back into the hidden context units.

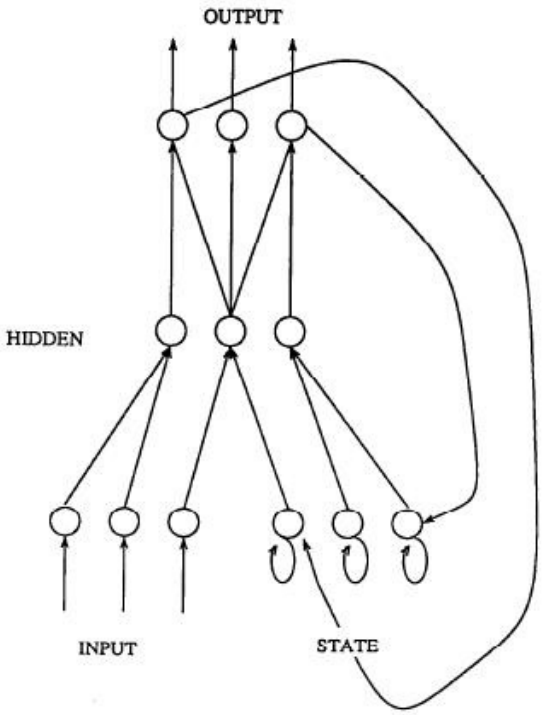

Figure 25 - Jordan ANN

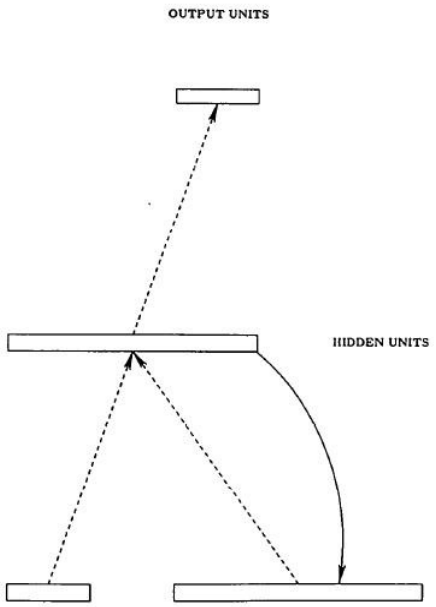

Figure 26 - Elman ANN

As mentioned previously the JENs are able to cope with time due to having a context unit, which gives them a dynamic feature. This should not be confused with Time Lagged Recurrent Networks (TLRN) which have a smaller network size than MLPs for solving time series based problems. The problem with these networks is that they require considerable processing power, they have a habit of getting stuck in a local minima, the time constant is also difficult to tune correctly. The JENs are less versatile dynamically as the time constant is normally fixed and the past is "*exponentially attenuated" (Principe et al, 2000).*

There is a possibility that the JENs could have an advantage over the static models as the data that is fed into the ANN will be of a time series format (Elman, 1990). This was investigated with an extensive testing process as discussed in a later section. In the next two sections, the PCA and RBF ANNs shall be examined in detail before looking at relevant literature in the scope of this project and finishing with conclusions drawn.

3.6.5 Principal Component Analysis (PCA)

The PCA networks have a fundamental difference from the static and dynamic networks that have been described so far in this chapter. The main difference is that PCAs use supervised and unsupervised learning and are well known for being used for image analysis and enhancement applications (Bao et al, 1999). During the training process, the PCA is

performed before the MLP in order to make the computational processes more efficient. Figure 27 below shows an example of a typical PCA ANN.

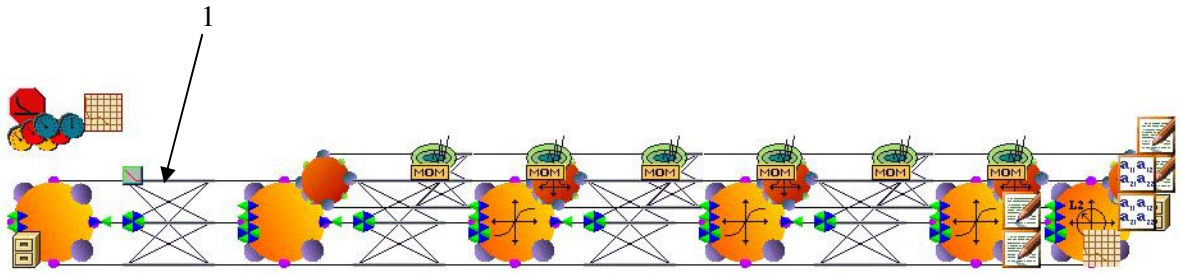

Figure 27 - A PCA ANN with two hidden layers

Looking at Figure 27 at a first glance the structure appears very similar to that shown in Figure 20. However there is an additional important component known as the SangersFull Inspector (SI) as shown by point 1. This part of the ANN is the unsupervised Hebbian learning procedure which is the key component of the PCA ANN (Sanger, 1989). PCAs are very powerful and often converge very quickly with the PCA able to reduce the amount of data. The performance of this network will be examined later in this project during the ANN testing procedure.

3.6.6 Radial Basis Functions (RBF)

RBFs are similar to PCAs in the sense that they both use supervised and unsupervised training procedures. They differ in that their sole hidden layer uses a Gaussian transfer as opposed to a sigmoidal transfer, as used by the other ANNs that have been considered so far. Compared to the MLP the RBF requires significantly fewer PEs to train effectively (Selmic, 2000). RBFs are also better at coping with noise than MLPs and also generate a better estimate of pure error (Tsai, 2004). An RBF can be seen below in Figure 28.

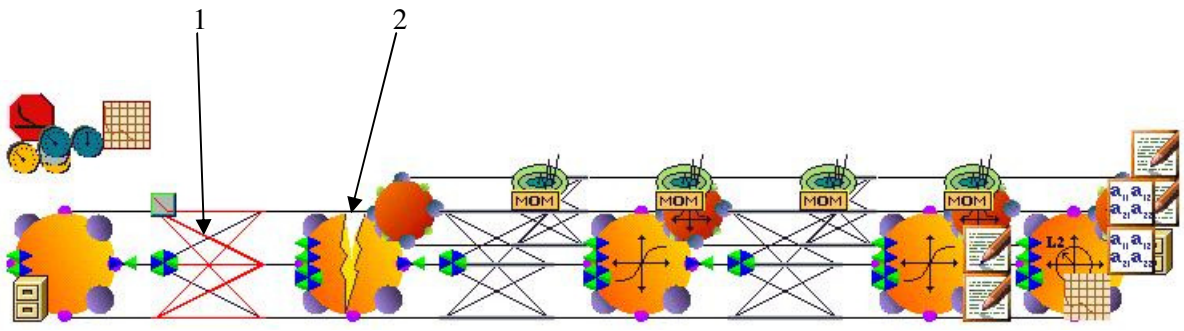

Figure 28 - RBF ANN with a conscience for competitive learning.

Similar to Figure 27, the PCA ANN structure of the MLP is still visible in the three inspectors on the right hand side. The interesting aspect of this type of ANN is called a ConscienceFull (point 1) component which allows the competitive learning to take place. The learning is unsupervised and normally of a low number of Epochs, and as for the PCA ANN, occurs before the supervised learning takes place. The second aspect of interest is known as a GaussionAxon component (point 2). In Figure 28 there is a 'crack' in this component which means that the supervised segment of the ANN is not active. However once the training has been completed in the unsupervised section (1) the GaussionAxon (2) becomes active once again and the rest of the network is able to run. The MLP is able to solve the same problems that a RBF can, however the advantage that the RBF offers over the MLP is that the latter requires more weights and training which produces a slower convergence than the RBF.

3.7 Conclusion

The review of the RBF concludes this part of the literature review, now that a thorough examination of the inner workings and the different types of ANNs has been studied. It was mentioned earlier in this project that ANNs are sometimes regarded as black box applications which has been shown as untrue in this chapter, due to the wide variety of designs. In the next chapter the material that has been reviewed in this section shall be used in various different formats and designs to maximise the performance of various types of boats and crews. Building on this chapter various internal parameters of the ANNs shall be optimised for each problem.

Chapter 4

Instrumentation and Data Collection

4.1 Introduction

Having established in chapter two that an ANN based approach as shown by Masayuma can provide valuable information, the next important consideration was concerned with the instrumentation of the boats when sailing to allow collection of the necessary data. During the early stages of the project there was a lot of development on the hardware and software platforms. This was implemented in order to ensure repeatable and good quality data was being recorded. The hardware and software packages were supplied by a company called Pi Research, a motor sport based company which was making the transition into the performance sailing market. During the final quarter of 2006 the development process for the equipment was complete and encouraging data was being produced by the ANNs. Several different ANNs were being tested with the final choice being the NeuroSolutions software due to the configurability of the Networks and the superior stability when running simulations.

It is also worth noting that there were several other small projects taking place at the same time, such as the optimisation of GPS settings with the help of (Gilbert 2006)from Dettica. Roger and the author also were testing and developing the telemetry system for the GPS units. There was also significant training required for the author and the rest of the RYA technical team in areas such as presenting complex technical data into a simple format for the sailors in order for the sailors to fully understand and interpret the results and also optimising the location of the GPS units on the boat to minimise multipaths. In a couple of the situations, brackets had to be designed and built in order to improve the quality of the data.

The data collected was logged on an embedded system with a 5 Hz GPS. Figure 29 shows the unit on a Yngling boat. The aerial is for the telemetry system and the GPS unit was sufficiently sensitive that it was able to function below deck.

Figure 29 – Pi Research data logger secured onboard a Yngling boat.

4.2 Summary of Data Collected

Throughout the project mainly four Olympic sailing classes were focused on, normally following requests from the coaches for problem solving or optimisation. There was work carried out in the majority of other classes, bar the windsurfers, but the amount of data was never sufficient in these to train an ANN to an acceptable error level with a minimum collection selected dataset of approximately an hour. These classes chronological order were the Star, Tornado, 49er and Finn.

The Star (method 1) ANN work was carried out near the end of 2006 with data collected remotely from Miami. The use of the NeuroSolutions software was for the first task able to

significantly reduce the raw data scatter with the ANN and aided presentation in a useful polar format. With this ANN produced polar the sailor and sail designer were able to improve the performance of the Star as the performance of the boat was more accurately known which enabled new sails to be designed more accurately from the ANN polar which had a positive impact.

During early 2007 the author worked with the Tornado (method 2) squad producing upwind polars for the class. During the early data collection and analysis there were significant problems with training the ANN effectively as the Tornado was significantly more dynamic in terms of boat-crew interaction than the Star. This started off an extensive program of ANN design and testing, using several different inputs and types of ANNs. After a few months the error was reduced to an acceptable level and the virtual tuning tool was created. The virtual tuning process trained the ANN by teaching it the performance of a boat and crew through a range of different wind conditions. Then the wind conditions of the target boat were inserted into the ANN and the response compared to the raw data produced from the target boat. This tool was applied in assessing quality of kit and changes of ability between different time periods. During the middle of 2007 the idea was formed to produce an image recognition program for analysing the sail stripes and feeding the data into the ANN. This led to the development of a Matlab based tool.

Near the end of 2007, an opportunity arrived to work with the 49ers (method 3) in optimising rig settings with the ANN. Data was collected in Weymouth with the rig settings recorded and fed in as inputs allowing various models to be designed and built. This was then tested in early 2008 in Palma in theory and practice.

This chapter focuses on the methodology, analysis and discussion of the ANN virtual tuning tool that was developed during this period of learning and improvement and builds upon the data collection and instrumentation.

4.3 GPS

Throughout the project the Global Positioning System (GPS) is one of the primary measurement tools in all the data collection and a thorough understanding of the GPS unit and system as a whole is critical to ensure that valid data is collected as this ensures the validity of the proposed approach. The chapter will start by looking at the development of the system and then move on to investigate all the relevant concepts of the GPS system and then lead to the applications of GPS for this project.

4.3.1 Historical

The GPS is a satellite based radio navigation system used to compute precise time and three dimensional positions anywhere on the Earth (Kaplan, 1996). The GPS system has been around for several decades but it is only since 1986 that it has been made available for civilian use. During the early days of GPS the only user was exclusively the United States military and the system was then known as the TRANSIT system (Navstar GPS, 1996). Development of the system began in 1958, and a prototype satellite was launched in September 1959 (Guier, Weiffenbach, 1997). Its main purpose was to provide position fixes for the Fleet Ballistic Missile Weapon System Submarines (Danchik, 1984). This system calculated the position through measuring the Doppler Shift from the orbiting satellite. Compared to the GPS as we know today the performance of the system was significantly less accurate with a positional accuracy of approximately 200 metres (Kaplan, 1996). The other problem with the TRANSIT system is that there was a lack of constant availability mainly due to there being only six satellites. The TRANSIT service was terminated in 1996 however the satellites were then adapted into the Navy Ionospheric Monitoring System (NIMS) (Lunt, 1999).

The TRANSIT system was replaced by the NAVSTAR system, which is the system that is widely used today. The NAVSTAR system consists of 24 satellites in six planes with four satellites in each (Dana et al., 1996). As of September 2007 there have been seven additional satellites added to the constellation. The additional satellites improve the precision of GPS receiver calculations by providing redundant measurements. With the increased number of satellites, the constellation was changed to a non uniform arrangement. Such an arrangement was shown to improve reliability and availability of the system, relative to a uniform system, when multiple satellites fail (Massatt, Wayne, 2002). The orbits are arranged so that at least six satellites are continuously within the line of sight from almost anywhere on the Earth's surface (US Department of Homeland Security Navigation Centre). The NAVSTAR system was initially only available to the US military but in 1983, President Ronald Reagan issued a directive in making the system available free for civilian use as a common good (History of GPS, 2006). Initially the units were of low volume production and very expensive for the average user compared to today. The GPS also had inaccuracies built into it on purpose called Selective Availability (SA), which represented the dominant error source for stand-alone users of the Global Positioning System (Braasch et al., 1992).

With SA included all civilian GPS units experienced a spoofing problem which reduced the accuracy of the position to approximately 100 metres (U-Blox Reference Dictionary, 2001). However on the 1st of March 2000 SA was turned off and the positional accuracy was greatly improved to approximately 15 metres (Zogg, 2002). With the accuracy of the GPS improved by approximately an order of magnitude it was the start of the higher number of GPS units being owned commercially.

There are several methods to obtain a more accurate position than 15 metres, one of these is to use a Wide Area Augmentation System (WAAS) GPS. There are several advantages to using WAAS GPS systems compared to the ordinary single phase GPS. The advantages are from correcting the GPS satellites instantaneous positions and clock errors as a fast correction and also the WAAS uses ground stations at known locations to receive GPS satellite signals and calculate corrections for atmospheric errors (Adams et al., 1996). The typical improvement in horizontal position is under three metres as long as the GPS unit can receive the WAAS correctional signal. Currently the WAAS signal is only available in North America, however several other augmentation systems are either in test phase or close to being developed. The other most notable system is the European Geostationary Navigation Overlay Service (EGNOS) which has suffered from multiple delays but has a theoretical accuracy of less than two metres. EGNOS was supposed to become operational from 2006/2008 onwards (Gauthier, 2001) however a recent update predicts the date of full certification some time in 2009 (GPS World, May 2008). During publication the system has still not been certified. The coverage and accuracy can be seen in Figure 30 below.

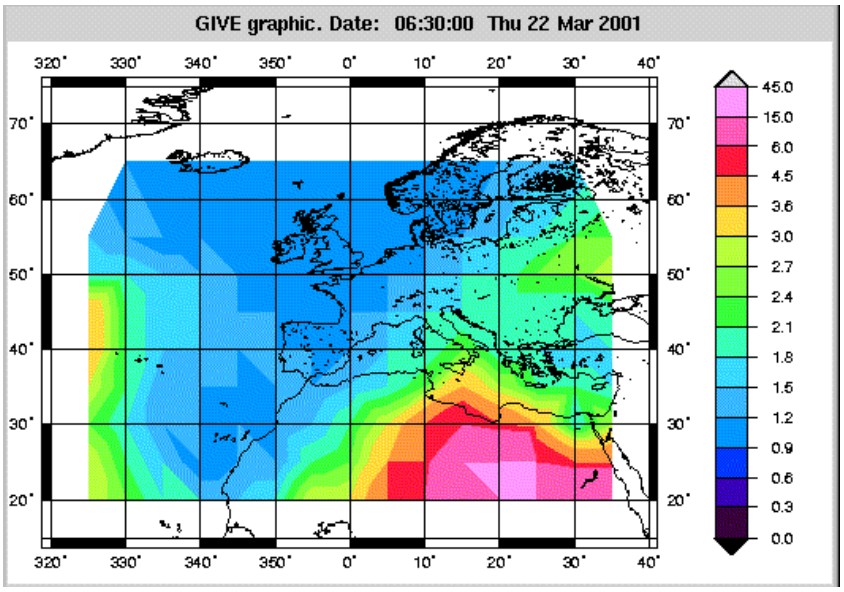

Figure 30 - Showing EGNOS coverage and availability (GPS World, 2008)

There are other signal correctional GPS methods, the most notable is Differential GPS where the position is corrected by reference to a known position station that broadcasts the observed error, however this system is being replaced by the WAAS system which does not require the extra complexity of an additional correction being broadcast. Differential GPS provided very beneficial improvements in accuracy when SA was enabled as it effectively provided a means of correcting for the effect of SA.

Several other GPS methods are also available with much higher accuracy. Of particular note is the Real Time Kinematic (RTK) navigation technique that has typical low latency horizontal position accuracies of typically 1 to 3 cm (Neumann, 1996). However these systems are not suitable for the application considered here as they are typically too bulky and heavy to mount on any of the Olympic class boats and they are also are significantly more expensive than a WAAS enabled GPS unit.

4.3.2 A Summary of the GPS Functional Requirements

There is a considerable amount of literature readily accessible in this area. The GPS system is a complex structure that is compromised if three distinct components or segments; namely the space; control and user segments. Consideration of each of these provides understanding of how the GPS system functions and allows position data to be determined.

The space segment consists of 31 satellites, which transmit signals on two phase modulated frequencies, P(Y)-codes and C/A codes (Leick, 1995). Even though the signal is travelling at the speed of light it takes time to reach the GPS unit on the ground. This delay in the signal being sent and received allows the unit to calculate the distance to the satellite. If the GPS unit is locked onto four or more satellites then it is able to calculate its precise latitude and longitude. This process can be seen below in Figure 31.

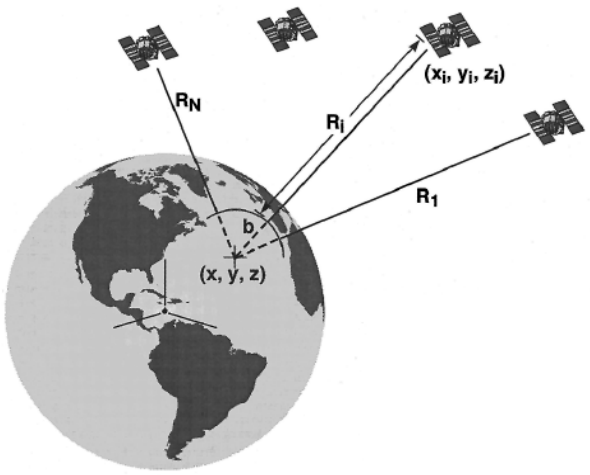

Figure 31 - Calculation of position (Kaplan, 1996)

The satellites orbit the earth at approximately 20,200 kilometres (Featherstone, 2003), each satellite makes two complete orbits each sidereal day (Agnew, Larson, 2007). In each of the satellites is an atomic clock which were initially yielding an uncertainty of a few parts in 10^{13}. The reason why such an accurate clock is needed is due to such a short time between the satellite transmitting the signal and the user on the ground receiving it which is known as the pseudorange. Any small error in the timing makes a large difference in the positional calculations. In the cluster of satellites there are five different types of satellites: Block I, II, IIA, IIR and IIF. Each newer version of the satellites are more sophisticated than the previous with the IIA version able to function up to 180 days without interaction from the ground control segment through momentum management capability. Whereas the Block IIR satellites have a crosslink feature for inter-satellite communication which enables autonav capabilities allowing graceful degradation (16m SEP) of navigation accuracy up to 180 days without ground contact (Aparicio et al., 1996).

The control segment is responsible for operating the GPS system (Leick, 1995). The master control system is based in Colorado Springs in the USA. The control segment maintains and corrects clock and orbit corrections. There are four other control segments which are based around the world on US and UK soil, the locations of all the stations can be seen in Figure 32. These stations monitor the condition of the satellite and are responsible for all operational control functions, such as navigational information processing, satellite data upload, vehicle command control and overall system management (Francisco, 1996).

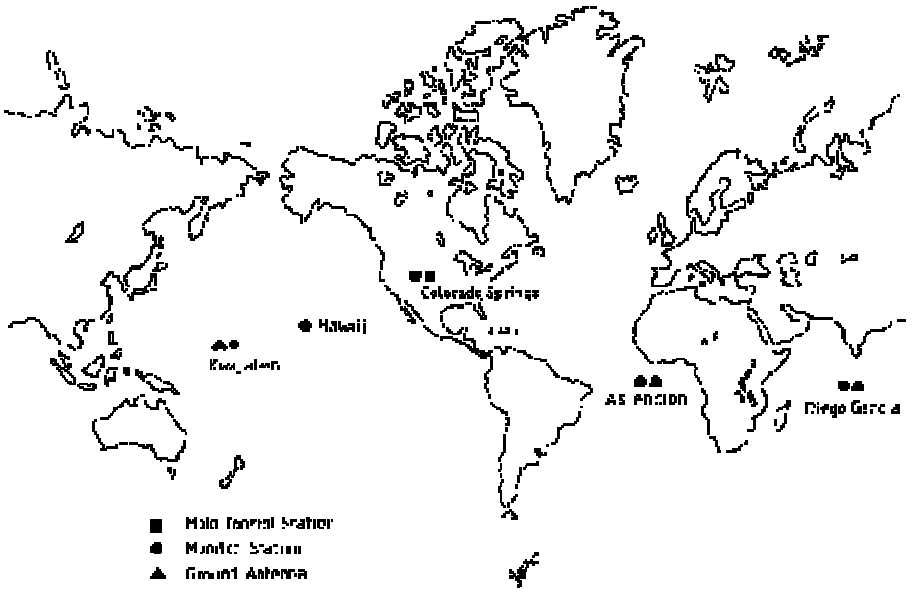

Figure 32 - Location of the GPS control centres (Francisco, 1996)

The user segment is, as its name suggests, controlled by the user of the GPS system. With this GPS unit users are able to determine position, time, speed and bearing with also a variety of specific data including the accuracy and number of satellites that the unit is locked onto. As mentioned in the space segment the units are able to determine their position from calculating the pseudoranges. The pseudorange is calculated by the GPS receiver for each satellite of which it needs four to solve the four unknowns which can be linked to the non linear equation found below in Equation 21.

$$R_i = \sqrt{((x_i - x)^2 + (y_i - y)^2 + (z_i - z)^2} - cb) \quad (21)$$

Where 'i' is the satellite index , R stands for pseudorange, x_i, y_i, z_i are the coordinates, x, y, z are the coordinates of the user, c represents the speed of light and b is the bias of the clock.

The GPS unit that was used in this project is a development of a system with which experience was gained in a previous study. (Reid, 2005). This unit is a 4 Hz rate Satellite-Based Augmented System (SBAS) enabled GPS which can be considered as a relatively high quality unit at the time of manufacture. Understanding the previous GPS segments allows for some appreciation of the problems that could be encountered in using such a system to collect position and speed data. A thorough understanding of what can cause there

errors and how they can be avoided is crucial for the collection of data of sufficient quality for the intended purpose.

4.3.3 Sources of GPS Errors

The reliability of the GPS is affected by the possibility of errors in all three segments of the GPS system. In the next section the source and effects of the principal errors shall be examined. The errors that shall be investigated are satellite orbit prediction, satellite orbit drift, Ionospheric dealt, Tropospheric delay, receiver clock offset and signal multipath (Townsend et al, 1994).

4.3.3.1 Satellite Error Due to Orbit Prediction and Drift

The orbit error is one of the smallest producers of errors in the GPS system and is the responsibility of the monitoring process of the control segment. It has improved over the previous decade in terms of accuracy. This is demonstrated by Lachapelle (1997) noting errors of between 5 and 10 metres. Comparatively, recently the orbit accuracy of GPS-based Precise Orbit Determination (POD) has been improved to 1 cm in radial direction due to various improvements in data, GPS orbit quality, mean gravity and other force models (Haines et al., 2003, Kang et al.,2007).

4.3.3.2 Ionospheric Delay

The Ionospheric delay is potentially one of the greater error sources for the GPS system with a range of errors between two and fifty metres (Aparicio, 1996). GPS signals must travel through the ionosphere in order to arrive at a receiver located on the Earth's surface or at a low height, as is the case of the ML1 station. In doing this they suffer from refraction by the Ionosphere (Meza et al, 2002). The Ionosphere is also greatly affected by the Sun. This is due to solar flares that produce intense X-rays that attack the Ionosphere and produce Sudden Ionospheric Disturbances (SID) (Mitra, 1974). This area is out of control of the equipment that will be used and the only defence against it is the monitoring of the GPS quality through the analysis program produced by the board manufacturer ublox.

4.3.3.3 Tropospheric Delay

The word troposphere derives from the Greek tropos for turning or mixing, reflecting the fact that turbulent mixing plays an important role in the troposphere's structure and behaviour. Most of the phenomena associated with day to day weather occurs in the troposphere (Danielson et al, 2003). It has been shown that azimuthal asymmetries in the Tropospheric path lead to errors of the estimated horizontal and vertical station coordinates (MacMillan, 1995). The magnitude of the errors according to Lachapelle in 1997 is between two and thirty metres. This is dependent on the amount of water vapour in the atmosphere. Similar to the approach for assessing the Ionospheric interference the solution is to monitor the GPS quality with ublox before a data collection session.

4.3.3.4 Receiver Clock Offset

The major source of clock error used to be SA when it was engaged, now without SA the clock errors are significantly smaller. As previously discussed, the clocks on each of the satellites are extremely accurate so there is very little drift in the time. This drift is continuously monitored by the control segment and the master control station is able to estimate the drift and transmits clock correction parameters to each of the satellites. This correction in time is also altered in the navigation data broadcasted to the GPS units. The clock offset errors are significantly smaller than the Ionospheric and Tropospheric delays (Lanyi, 1984). Similar to other errors, the best method of discovering they are present is by monitoring the GPS data with u-blox during data collection.

4.3.3.5 Signal Multipath

Townsend (1994) states that the term multipath is derived from the fact that a signal transmitted from a GPS satellite can follow a 'multiple' number of propagation 'paths' to the receiving antenna. Figure 33 (Rama et al, 2006) provides a good description of the multipath problem.

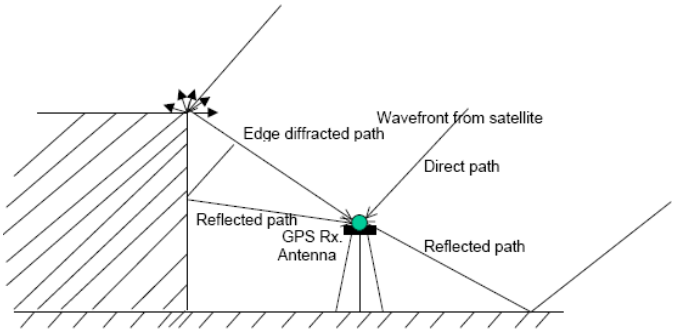

Figure 33 - Typical multipath situation (Rama et al, 2006)

With a GPS system mounted onboard a sailing boat, the multipath issues will be limited to the influence of the sails and the rig, producing a multipath off the target boat and other boats if they are in close proximity. The reflective nature of the water surface environment normally causes a high potential multipath effect which could contribute to an error of up to a few metres (Zhang, 2005). However, if the unit is situated below deck level there could be several opportunities for multipaths to form and produce invalid data. With all the possibilities of introducing multipath errors into the data there are means of preventing this phenomenon from being used by the GPS receiver. For this project a ublox SAM-LS GPS Smart Antenna Module was being used to gather the data. This module has an active multipath detection and removal feature built into it which helps in collecting valid data. The GPS also has a large array of programmable features that allow the user to customise the settings, such as altering the Dynamic Platform Model and the ability to use different NMEA sentences.

During the data collection process a unit was left onshore monitoring the GPS coverage to ensure that the coverage was sufficient. Also during the placement of the data logger on the boat, the signal strength and number of satellites was monitored to ensure that the GPS positioning, speed and course over ground were accurate.

More information on the feature is presented in Appendix 1.

4.4 Instrumentation Set Up

4.4.1 Introduction

In this section the equipment that was used in the data gathering process is described. The design of experiment shall also be discussed which includes the methods used in order to collect higher quality data. The equipment selected reflected the aims of the project with enabling the appropriate inputs into the model to be logged.

During the final data collection it was necessary to use an extensive range of equipment in order to collect the necessary level of data collection required. This data collection initially took place in Weymouth before the final collection and testing in Palma, Spain. The equipment used is as follows:

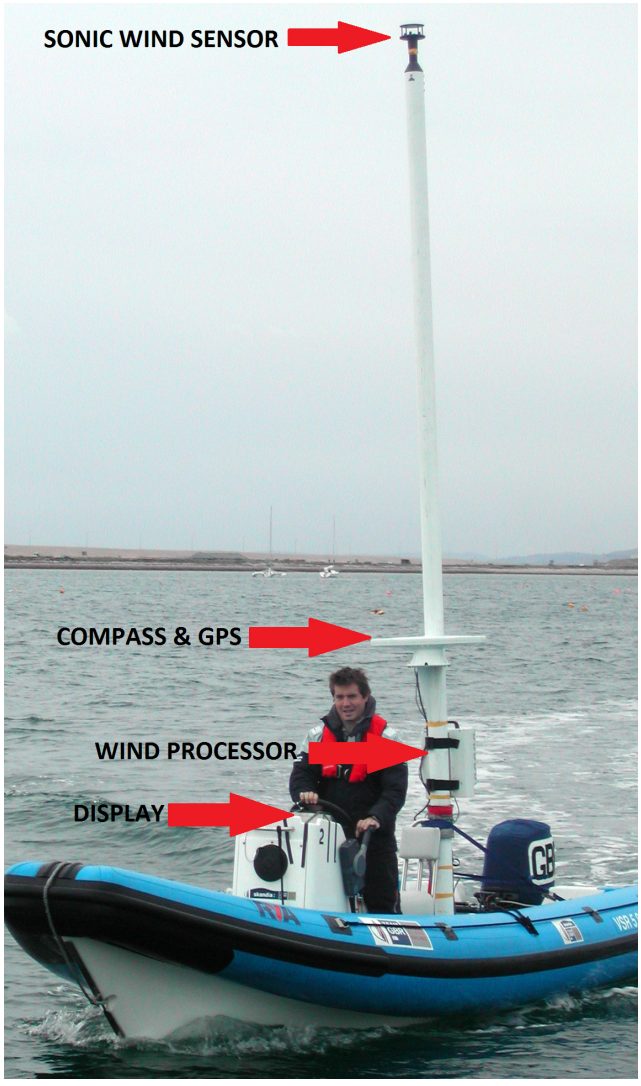

Figure 34 – RYA weather boat with instrumentation and wind processor.

- Rigid inflatable boat (RIB) to provide a platform for the environmental measurement equipment.
- Weather Mast and wind processor with logger, display, compass and GPS.
- Two GPS and logging units.
- Three Custom Strain Gauges
- Sensor junction Box
- 49er dinghy
- Laptop and offload loom.

4.4.2 Weather Mast and Logger Box

The weather mast is one of the most important components in the experimental setup as without it there is no TWS or TWD with which to synchronise it. The anemometer used was of the sonic type that allows excellent accuracy especially at low wind speeds with a minimum sensitivity of 0.02 m/s. Figure 34 shows the anemometer onboard. It also has the benefit of not being affected by inertial effects due to pitch and roll as there are no moving parts in the sensor. The accuracy of the sensor is accurate to two percent of the wind speed and three percent of the wind direction. The validation of the equipment was carried out early on in the project with the manufacturer. The weather mast also has a processing unit, also shown in Figure 34, that removes the effect of the waves and the motions of the RIB on the wind speed and direction readings which is an important feature and means that the true wind speed and direction can be calculated while the RIB is moving as it is connected to a GPS as well. The GPS and compass are situated inside the rectangular horizontal platform seen in front of the mast in Figure 34. The processing unit is located slightly above engine height and is located aft of the mast. The display unit, a Hercules B&G 2000 unit, can be seen on the console of the ribs as well. This is a useful tool as real time readings can be noted on the water.

The masts are attached to the rib via a base plate on the floor of the RIB and three ratchet straps which hold the mast in place. The actual mast structure is made out of carbon fibre tubing and is very stiff which provides a more accurate reading as there is virtually no flex. The GPS units, as described previously; are of a custom design and manufacture in collaboration by UK Sport and Pi Research. The cases of the GPS units also contained other components a three axis accelerometer, multi channel data logger and a telemetry board. The units have a sophisticated connector which allows a large variety of components to be connected and logged, such as Inertial Measurement Units (IMU) or the strain gauges which were considered previously. The full data sheet of the GPS can be found in Appendix 1.

Another feature of the GPS unit is that it has a button that allows the user to insert a marker into the data which can be used for reference during the data analysis. This allowed the start and finish of each of the data runs to be indicated on the data collected from the GPS into the RIB that then in turn provided a reference for the GPS data collected onboard the target boat during the data fusion process. This saved time during the subsequent data analysis process. During the data collection process an additional GPS units was left on shore logging the performance of the GPS system during the training session. The variables that were being examined were different measures of accuracy such as the dilution of position (DOP) which is determined by the number of the satellites and multiple other factors that are mentioned earlier in this chapter. The logger was attached to a laptop and the dilution of precision value was found through using a program from u-blox. Other factors were also monitored such as the position of the satellites as these would have an effect on accuracy. A screen shot from this program showing the monitoring in progress can be found in Appendix 1.

4.4.3 Strain Gauges

As there were also investigations into the rig settings, custom strain gauges (Figure 35), they were designed and manufactured to fit all the Olympic classes. The gauge had three different bridges to deform the wire, this depended on the gauge of the wire and they were all pre calibrated. The gauge used a conventional bridge which was amplified into a 0-5 volt single. The 0-5 volt signal was then calibrated in the data logger against force. These were plugged into the units and logged at the same time as the other channels. A validation process was carried out beforehand in order to test the quality of the strain gauges This was carried out by hanging known and accurate weights off a wire with the gauges attached and checking the data. During this process three of the six strain gauges were found to be faulty. This unfortunately reduced the number of useable strain gauge inputs to three. This reduced the desired inputs from 6 to 3. Figure 35 illustrates the strain gauges fitted to a 49er before a data collection session.

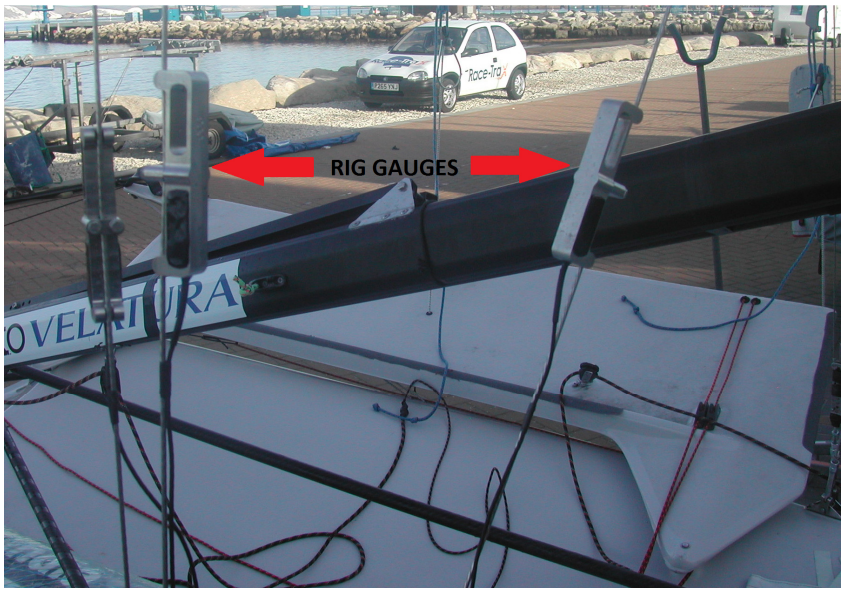

Figure 35 – Custom strain gauges fitted on a 49er

The junction box connected the wires from the strain gauges to a single loom that was fed into the GPS unit. The junction box has a capacity to receive up to six different strain gauges.

The strain gauges were mainly used with the 49er boat. Data collection in the 49er class was it was the only time that was designated to a pure data collection session, whereas during previous methods the data collection had to fit around various exercises that the coach was trying to run at the time. This limited the quality of the data and also the amount that was collected. During the first two methods a good day's data collection would produce 30 minutes of good data due to other objectives by involved with training. With method three this was extended to several hours.

4.4.4 Experimental Method

During all of the data collection methods the weather boat was required to motor along as close to the target boat as possible while not affecting it with the wake of the boat or the wind shadow. In method one the relative difference in position was much higher than method two and three due to the author not being in control of the experiment. Through analysing the effectiveness of training and testing of the ANN this distance should be no more than ten metres away. Throughout most of the collected 49er data this distance was reduced to six or seven metres. During Method 3, when strain gauges were used, the rig settings were also noted as a backup in case the strain gauges failed or were not effective

enough to train the ANN. Throughout the rig optimisation process the rig settings were adjusted incrementally from what the sailors thought was optimum to when they felt the performance dropping off significantly.

In the data collection runs of Methods 2 and 3 the crew had to sail in three different upwind modes which were pinching, normal and footing. The pinching mode is closer to the wind than optimum by a couple of degrees and footing is the opposite. This enabled more of the polar curve to be collected. In method one this was not apparent at the time and the results were initially disappointing as there was no obvious curve generated. This was due to the Star crew sailing at only one TWA which was optimum. Most of the data was collected in non tidal locations; where there was current this was measured and combined with the collected data. The measurement was relatively crude, a tide stick was dropped into the water near a known reference point such as a buoy and timed for two minutes. The distance was then measured between the start and end point. However to produce the best data non tidal locations were preferable.

As the methods progressed, more sophisticated methods of reducing the MSE were used from better ANN design and training to positioning of the weather boat with respect to the target boat. This was due to the intrinsic problem of TWS and TWA measurement which was due to the location of the weather boat. Situating the anemometer on top of the target boat's rig would have produced lower quality readings through mast twist and deflection as well as components of upwash and adding significant weight onto the target boat. Some of the classes it was also not practical to mount and anemometer on the mast such as the Laser sailing dinghy. Locating an anemometer at the top of a mast is not the optimum choice either due to the up wash effect from the sails. Thus with the external wind readings interesting situations developed where the weather boat, shown by point 3, would measure a shift or gust and the target boat, shown by point 2 would not have reached it yet and vice versa. This can be illustrated by Figure 36 and the opposite in Figure 37 below. This effect was even greater downwind when the target boat was catching up gusts shown by point 1 in front in the windier conditions that the weather boat would take time to reach.

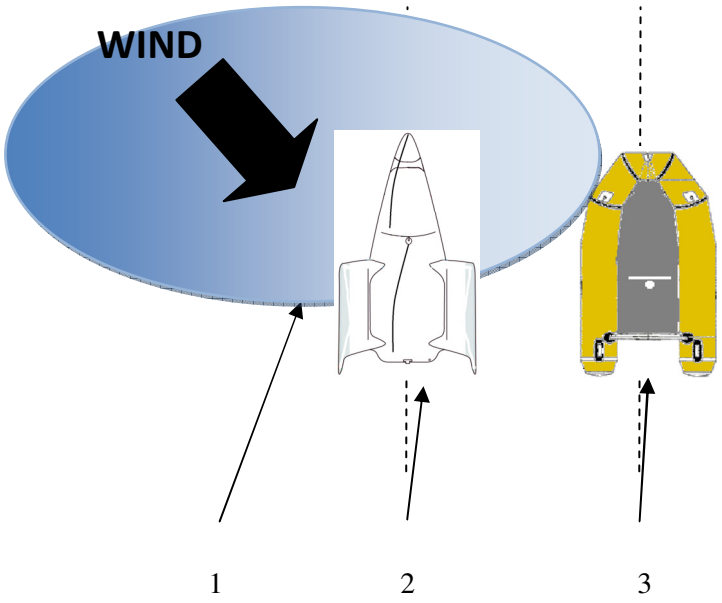

Figure 36 - The target boat is in a gust and weather boat not

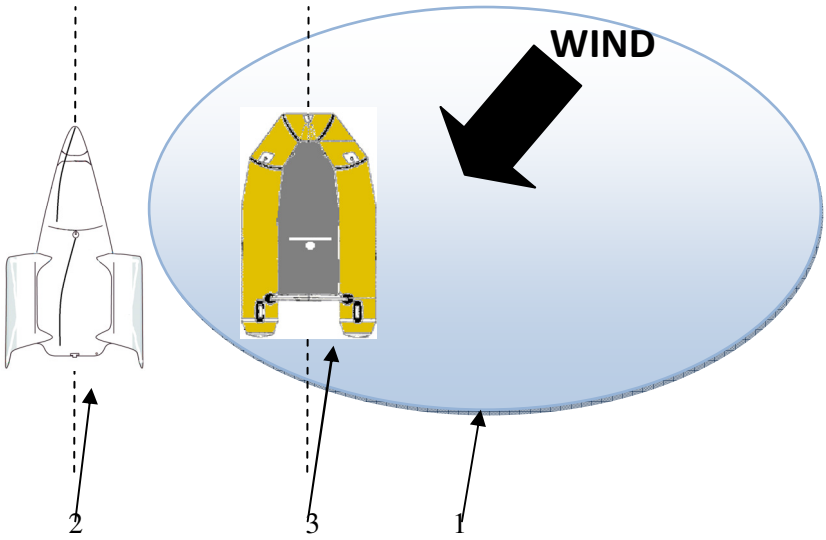

Figure 37 - The weather boat is experiencing the gust and the target boat is not

The length and duration of the shifts and gusts was variable and dependent on the conditions of the day as well as the randomness of gusts. The affect on the data would be amplified even more if the weather boat was running parallel inside a band of higher wind and the target boat was not, however this scenario did not happen often. Several of the data runs were aborted when unusual events happened such as a power boat crossing the path of the data run or any other major experimental influences. This was one of the reasons why the Star data in method 1 was not as accurate as the other methods as the author was not able to ensure correct data collection. In the next section Neural Networks shall be investigated which acts as a foundation before moving on to the chapter which uses these techniques.

4.4.5 Summary

Throughout the project the sophistication of the equipment and the data collection techniques adopted were evolutionary. This was especially true with the GPS equipment as there was a severe problem with synchronising all the data with the time stamp as well as determining the optimum location of the unit. This was due to the GPS board having synchronisation problems with the other units and switching between GPS time and GPS UTC which have a difference of 14 seconds. The methods of collecting data also improved significantly from data collected during or between training sessions which was of poor quality, to sessions specifically designed for data collection. The latter resulted in a larger quantity of data which was also of a better quality. This was particularly crucial in the more dynamic classes such as the 49er and Tornado. With the improved data collection methods more accurate analysis and conclusions could be drawn.

Chapter 5

Neural Network Data Processing and Analysis

5.1 Introduction

In this section the evolution of the data analysis techniques will be presented. To begin with, standard methods of performance analysis will be considered starting with a similar method to that which Bethwaite (Bethwaite, 2008) used in his 49er performance analysis. More sophisticated methods of data processing will be discussed, building on the ANN literature that was reviewed in the previous chapter, before producing the virtual tuning tool and the data results with it. In the next section the evolution of the modelling techniques shall be reported.

5.2 Existing Methods of Performance Analysis

At the start of the project there was already, and has been for several years, a generally accepted method for optimising boat performance. This is known as two boat testing, which is used by all of the Olympic coaches today. This testing usually involves two boats sailing upwind in close proximity to each other and used an iterative procedure to find the optimum settings, identified when one boat appears faster than the other. This procedure takes a significant number of runs and is very time consuming. The two boat testing can take several thousand hours during a campaign and also requires significant resources. There are also several pitfalls in using the two boat testing method such as sailing into a shift which resulted in a header, which always favours the boat to leeward, or sailing into a shift which resulted in a lift which has the opposite effect. This problem is sometimes hard to detect and can produce some anomalous results. In the next section the current testing methods will be considered.

5.3 Current Performance Analysis Methods

Early in the project during the final testing of the new software and hardware a standard performance analysis technique was used, plotting the unfiltered data in a polar or time/distance format. This technique is widely used and can be considered the standard method. Plotting the raw data produces the 'blob'-like effect that can be seen below in Figure 38. This technique is a valid method of analysing performance and is an improvement from two boat testing, or can be incorporated into two boat testing. However, the margins of error are very large due to the nature of the data that is collected, due to the unsteady nature of the data relating to wind measurement and boat performance, and it also requires almost as many data runs as the two boat testing in order to produce a valid quantitative answer. This method does work better on larger keelboats, as seen in the literature review, due to their greater momentum, but there is still a high standard deviation in the data due to scatter.

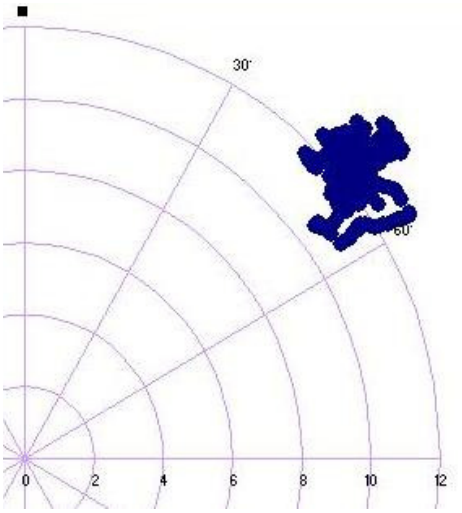

Figure 38 – Unfiltered polar data

The example shown in Figure 38 is from one of the early Tornado data collections. There is a large scatter but this is significantly less than the scatter seen by Bethwaite, (Bethwaite, 2008) in Figure 8, mainly due to the higher quality equipment used for the wind recording and onboard data logging. From a scientific perspective this blob is of little value and actually tells us very little about the performance of the boat as there is approximately a three knot deviation in V_b for a minute long data run. The plot of the data is open to qualitative analysis that could also be potentially misleading. During the data run there was a four knot difference in the TWS that would have affected the polar as well due to the unsteady conditions.

An improvement on this method, which is also adopted by Bethwaite, is to filter the data with a moving average for the TWA and TWS. In addition to filtering the data, the average V_b was calculated for each of the modes that the crew were sailing in. This can be seen in Figure 39 below.

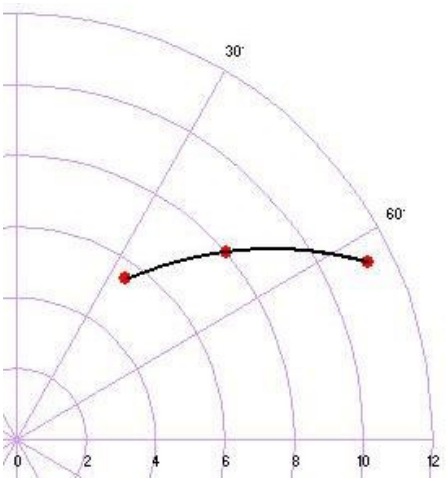

Figure 39 - A first stage improvement of the raw data plot

This polar plot is from a different data run than Figure 38 and the TWS range is binned between 7.5-8.5 knots. The three modes can be clearly seen on the plot with the sailor's opinion of optimum being the middle point. It is interesting to note that the sailor's optimum is not quite at the maximum VMG. However, the methods and reliability of the data could not fully support this as the TWS could have been on average less than the other two points. The TWD variation could also have produced harder conditions to sail in. This method of analysis also highlighted another flaw in the collected data method, namely that it is very difficult to produce a polar for exactly eight knots, as there is very little data that is close to any specific TWS. This is the reason why there was a half knot region either side of the eight knot TWS in the figure as there was only small amounts of data.

Another problem with plotting raw or filtered data is associated with the unknown dynamic affects of the environment. There are two scenarios which highlight this. The first is when the target boat is sailing in for example 8 knots of wind and sails into a gust. At the instant the gust hits, the boat is performing lower than expected as it takes time to accelerate. Using the standard method of interpolating between polars this would produce large errors in modelling the data. The same effect is also true when the boat, again sailing at a constant TWS, sails into a lull. This also produces a large error in the performance model as the boat will be over performing until its V_b is that for the given TWS.

In the next section the first usage of the ANN to model the performance of the boat effectively will be presented. First, the Star will be considered before moving onto discussing the final method that created the virtual tuning tool.

5.4 Star ANN Performance Analysis Methods

As mentioned in the introduction to this chapter the Star was the first boat that the ANN was used on. The Star was chosen as it was one of the least dynamic boats, being one of the highest displacement boats, and also having one of the best crews. The Star is a very technical boat with an open design on the sails and rig, within the class rules. This produces a multiple variables to consider in order to achieve optimum performance.

To begin with, the ANN design was only related to the TWS and time, with TWA and V_b as outputs as this combination of inputs and outputs produced the most stable ANNs with less sophisticated models. The MLP was the network which was used to produce the model. The design was as in Figure 40 with one hidden layer which can be seen below. There was also CV present using 10 percent of the data and also GA enabled to produce the best weights and design. The computation time for this model was approximately ten hours.

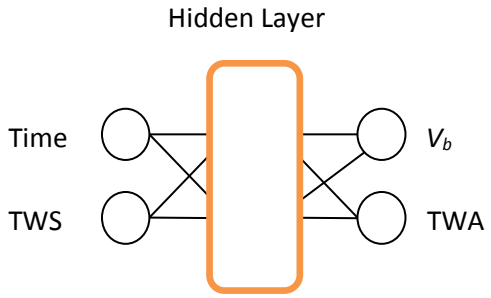

Figure 40 - Early ANN model

This process enabled a significant reduction in scatter on the polar plot and was also able to produce a response from a TWS and arbitrary point in time. This therefore enabled an array of conditions to produce a V_b and TWA response which was able to produce a polar point for a given TWS rather than a small range of TWSs. This reduced scatter polar can be seen below, alongside the raw data scatter polar in Figure 41 and post ANN processing in Figure 42 respectively. The reason for reducing the error was to produce a more repeatable and accurate model to allow real changes in boat performance to be demonstrated.

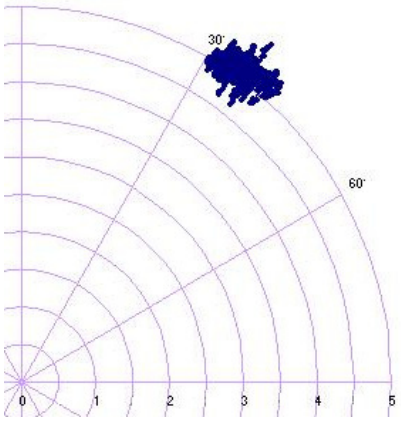

Figure 41 - Raw data example

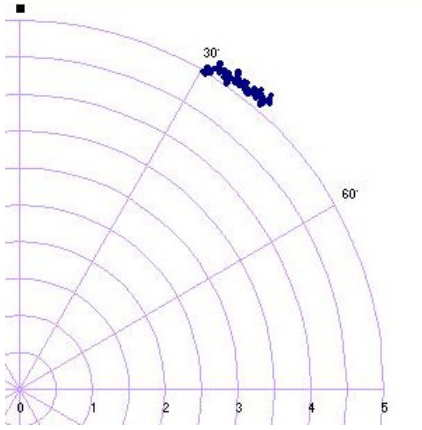

Figure 42 - Early ANN processing for the Star

It can be seen from looking at the two figures above how much of an improvement the usage of an ANN produces compared to the raw data. The reduction in standard deviation of the boat speed data is from 0.26 to 0.15 which is a significant improvement. In terms of the other technique which is the response to an array of TWS and time inputs, a single point is produced which is shown below in Figure 43.

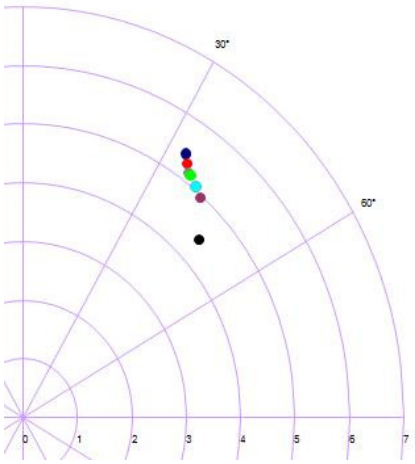

Figure 43 – ANN derived upwind targets for the Star

After producing the Star polar response it was used in the sail design process, and compared to a gold standard VPP that Juan Garay (Garay, 2008) was using, the V_bs were very similar but the TWA was always slightly less. This was because the ANN response was a dynamic model whereas the VPP is a static interpretation of the yacht's performance. It is dynamic in the sense that the crew are able to sail higher than the theoretical TWA due to the fact that when, or just before, a gust hits in hiking conditions the crew was able to anticipate it and sail slightly higher to reduce the heeling moment.

In terms of ANN performance the results were acceptable compared to the standard lookup interpolation method. The V_b prediction was quite accurate but the TWA output errors on the training and especially the CV analysis were significantly higher than the V_b prediction. This is due to position of the weather boat, sometimes the weather boat would be in the gust and the target boat not and at other times the opposite would occur. There were other factors as well, such as the corrections to the data because it was collected in a tidal area, which is never as perfect as non tidal data. As the Star is a relatively slow boat this has a larger affect compared to something like a 49er or Tornado in terms of percentage of V_b. The results of the ANN can be seen below in Table 2. In this situation the MSE and NMSE are relatively high due to the low amount of training data available and also because of its reduced quality. The percentage error is deceptively low as described in section 3.4.1 with Equation (24). The design of the ANN was also far from the optimum; later in this section improvements are shown but it is an enhancement from previous performance analysis methods.

Table 2 - Performance of the Star ANN

	Active	CV
MSE	0.161	0.131
NMSE	1.36	1.71
% Error	5.98	5.6
r	0.26	0.61

5.5 Tornado ANN Performance Analysis Methods

Although the results shown in Table 2 were deemed to be at an acceptable error level, the model is not appropriate for the Tornado. The Tornado has twice the performance of the Star and weighs significantly less due to its highly dynamic characteristics. This meant that a whole new phase of design and testing had to take place in order to reduce the error level in the ANNs when applied to Tornados. From the re-design of the ANN, several other factors also changed, such as better data collection procedures and also the amount of data collected being greater. The Tornado data collection ultimately changed the design of ANN to the configuration shown below in Figure 44. One of the interesting aspects of the study was the improved performance of the ANN when time was not used as an input. The performance was improved due to more inputs and a second hidden layer.

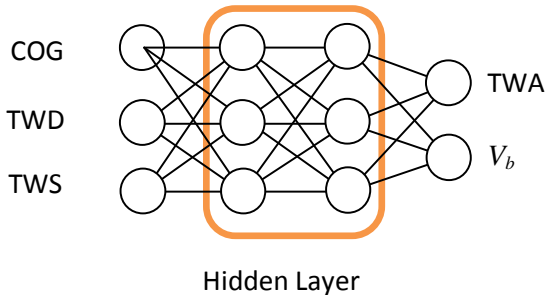

Figure 44 - ANN used for Tornado data processing

The new design of the ANN used three inputs including the wind direction as well as speed, and also the boat COG. This improved design of the ANN allowed the levels of the errors to be reduced to an acceptable level. The difference in performance of the two designs of the ANN can be seen below in Table 3. The MSE and NMSE have reduced quite considerably which produced better testing results. The correlation coefficient is also better suggesting a much better fit to the data. The value of the percentage error is misleadingly high as the

nature of the data conforms to the criteria described by equation 24. The improvement of performance can also be linked into introducing an additional hidden layer.

Table 3 - Showing the change of inputs

	MSE	NMSE	r	% Error
Old ANN	0.16	1.3	0.25	5.93
New ANN	0.12	1.1	0.56	14.05

After the initial data collecting and testing, the ANN was then set the task of predicting the boat performance in Palma before the sailors' first event of the year using the same crew but with different sails and boats. The boats which the sailors were sailing during the early data collection process in England were training boats, which were not as well maintained and had older equipment. In theory, the sailors should be able to sail faster in Palma with the better equipment and boats. This was tested by using data collected in Palma for the two Tornado crews as input to the ANN trained on data collected in Weymouth and the outcome was as expected. The detailed results can be seen below in Table 4 in which the faster data runs are highlighted by the green coloured VMG cells on the right of the table, obtained from the ANN trained on the Palma data. During the training time in Palma it was found that Rashley was quicker 80% of the time than Gimson in the moderate to heavy conditions. This trend however was reversed in the lighter conditions. The first of the comparisons in Table 4 is the data collected in the old boats in Weymouth against Rashley's data collected in Palma with a newer boat but with the same crew in both tests. This was a comparison of the raw data collected in Palma versus the response from the ANN for those conditions which was based on the Weymouth data. In all the cases the performance was better in Palma than the Weymouth benchmark due to the better equipment and perhaps some improvement in sailing ability of the crews after a whole winter's training in the UK. On average, the differences in VMG between Rashley in Palma and the ANN benchmark was about 0.1 of a knot. This increase in performance was also visible in the raw data but the environment was too noisy to produce as definitive an answer as the ANN. Other factors such as water density, temperature and viscosity were not included in the modelling.

Table 4 - Showing the Tornado Weymouth and Palma comparisons.

Rashley Palma vs Weymouth Benchmark					
		TWA	VB	TWS	VMG
Run 5	Weymouth	44.85	11.88	18.5	8.42
	Palma	44.84	12.18	18.5	8.64
Run 6	Weymouth	47.98	12.5	19.2	8.37
	Palma	46.88	12.41	19.2	8.48
Run 7	Weymouth	49.18	12.52	16.39	8.18
	Palma	50.88	12.98	16.39	8.19
Run 8	Weymouth	50.88	12.98	15.32	8.19
	Palma	50.27	12.95	15.32	8.28
Rashley Raw Palma					
Rashley	Run 7	50.88	12.98	16.39	8.19
Gimson	Run7	52.72	12.97	16.39	7.86
Rashley	Run8	50.27	12.95	15.32	8.28
Gimson	Run8	50.61	12.61	15.32	8
Rashley	Run9	44.81	11.28	12.33	8
Gimson	Run9	40.27	10.78	12.33	8.23
Gimson Palma vs Rashley Benchmark					
Run 7	Gimson Raw	52.72	12.97	16.39	7.86
	Rashley	50.52	12.66	16.39	8.05
Run 8	Gimson Raw	50.61	12.61	15.32	8
	Rashley	49.83	12.67	15.32	8.17

The second section of the table consists of raw data collected in Palma. This is due to some of the early ANN results suggesting that the sailors were not sailing at the optimum TWA upwind as suggested in Table 4. This was discovered when the sailors were asked to sail in the three different modes upwind and the ANN suggested that they were sailing slightly too high to produce the optimum VMG. This test was carried out in Palma several times between two of the Tornados lined up against each other in a two boat testing format. Every time the test was carried out the footing boat was always quicker than the boat that was sailing at the previous optimum. After a discussion with the coach it was concluded that it was faster to sail with a greater TWA but it was not always possible in a race environment due to the influence of other competitors nearby. The result of this study enabled the sailors to adjust their optimum upwind angle during training and when permitted on the race course.

The final section of the table is a comparison of Gimson against Rashley's Weymouth benchmark. In both situations, Rashley's Weymouth benchmark was faster than Gimson in Palma. This was obvious as well on the water and in the previous testing and can be mainly attributed to the short length of time that Gimson had spent in the Tornado. This can also be seen in Figure 45 which shows graphically the difference in performance between Gimson's raw data and Rashley's ANN response. The main contributing factor of the difference in performance is the better height that Rashley has than Gimson and even though Gimson has a higher V_b, Rashley's VMG is better overall. This could be due a wide variety of factors such as rig set up or choice of sails.

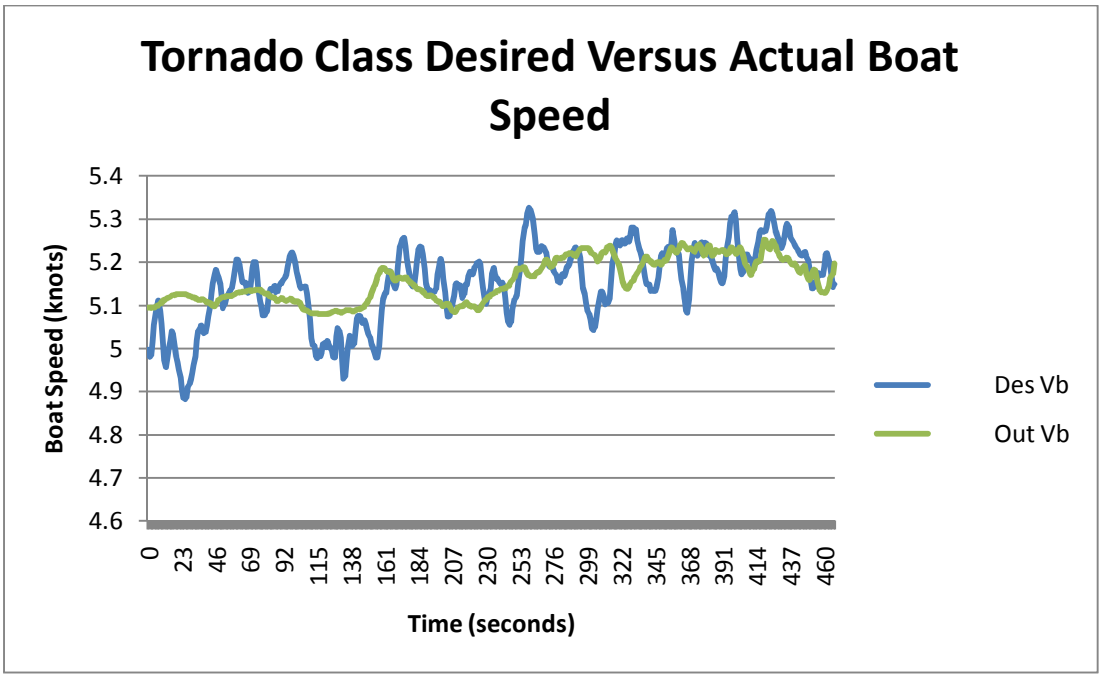

Figure 45 – Desired boat speed (Gimson) versus ANN boat speed (Rashley).

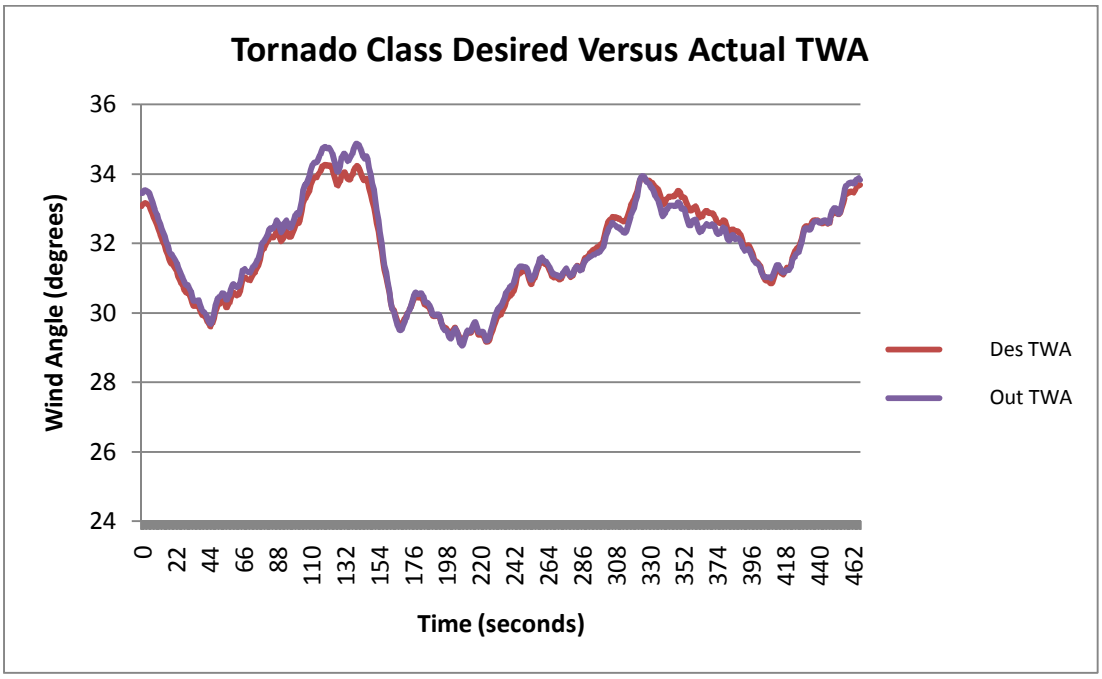

Figure 46 – Desired wind angle (Gimson) versus ANN TWA (Rashley).

In the next section, the developments of the ANN for the Tornado are taken onto the next stage of ANN performance processing with the 49er. Other aspects of performance are

investigated in this section including a rig optimisation process and also more ANN validations.

5.6 49er Performance Analysis Methods

The 49er ANN is the culmination of the ANN performance analysis method and also produces the virtual tuning tool which is validated against the Olympic squad's tuning guide. There was more data collected from the 49er than the other major data collection sessions of the Star, Tornado and Finn combined due to reduced restrictions on data collection length. At the start of the 49er data collection it was supposed that the current ANNs would be able to cope, given the highly dynamic environment which was experienced with the Tornado. However, in the event this was not the case and another ANN design and testing process had to be undertaken. The differences could be due to the Tornado being naturally form stable (being a catamaran) whereas the 49er is notorious for being very unstable in certain conditions. Some of the additional knowledge gained by the author during the early stages of the 49er ANN data collection was from collaborative work with the University of the West of England (UWE). This collaborative work was in assessing the accuracy of modelling performance and decision making through the method of data mining. The author was able to use the knowledge of Professor Bull with not only developing new ideas but validating the existing work with his design and use of ANNs (Bull, 2007).

During the early data collection, before the use of ANNs in performance analysis, the author had worked with the 49ers trying to model performance using existing performance analysis techniques. During this initial work there were several problems experienced with multipaths and loss of signal from the positioning of the GPS. To counteract this, a carbon fibre bracket was designed and built to mount the GPS units off the stern of the 49er. This improved the performance of the GPS to an acceptable level and can be seen below in Figure 47.

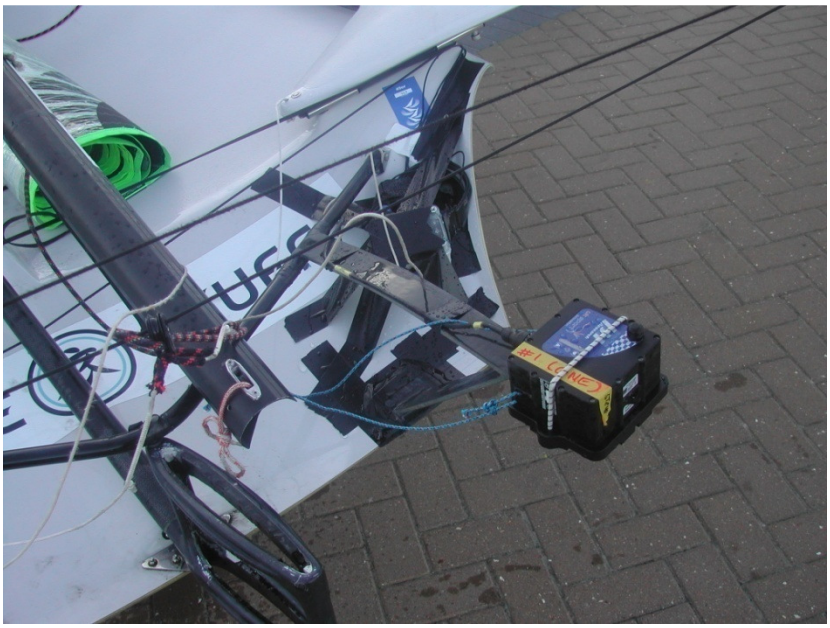

Figure 47 - Final position of the GPS unit on the 49er

It is worth noting that during the measurements, data was collected in almost all TWAs, with reaching and running sailing modes included, in order to build a full performance model. However, the errors for the down wind conditions were relatively large, mainly due to TWS and TWD measurement errors. These were due to the poor positioning of the weather boat adopted so as not to adversely affect the target boat's wind. Partly for this reason, method 3 focuses on the optimum performance upwind.

There were two different designs of ANNs that were used for method 3. The first can be seen in Figure 48, which uses the dynamic rig settings and is known as the Alpha design. The second design is an evolution of the Tornado ANN, known as the Beta design, which is a higher performance ANN and is shown in Figure 49. This ANN compares the base setting data with individual data runs that are on different settings, and attempts to optimise them by relative performances.

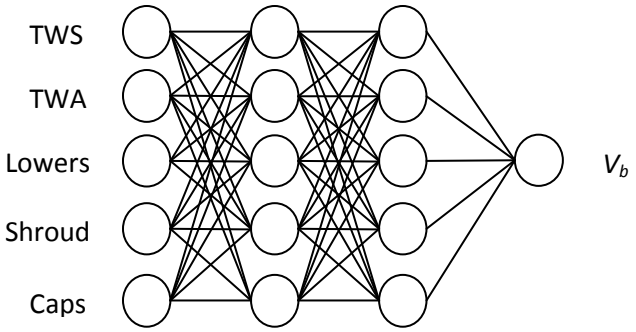

Figure 48 - Alpha Design

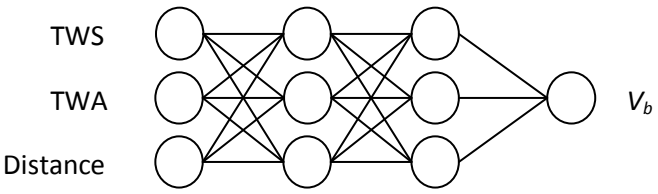

Figure 49 - Beta Design

One of the new inputs was distance; this is the distance between the weather boat and the target boat. TWA was no longer used as an output as this improved the accuracy of the modelling. This was an evolution of the ANN design which improved performance by the ANN giving more weighting to data which had a smaller distance. This meant that the closer the weather boat was to the target boat the more accurate the data. The distance was calculated by using the spherical law of cosines formula which can be seen below in Equation (33).

$$distance = \cos^{-1}(\sin(Lat_1) \times \sin(Lat_2) + \cos(Lat_1) \times \cos(Lat_2) \times \cos(Long_2 - Long1)) \times r \quad (33)$$

where r is the radius of the Earth and the values of 1 represent the target boat and 2 is the weather boat.

The other inputs which feature in the tuning guide were adjusted by the crew of the boat for the given conditions and were usually left the same for several of the data collection runs as the conditions remained relatively similar. The design and analysis of the two ANNs can be seen in the following sections, before comparing the results and completing the validation between predicted and actual performance.

5.6.1 ANN Alpha Design

Alpha design used the largest number of inputs for an ANN so far. With the dynamic rig loads set as inputs it was hoped that it could provide a more accurate V_b output. Various different types and designs of networks were tested for the Alpha method. It was found that the Alpha design method with the standard MLP configuration produced the optimum results. The other promising design was that of the Jordan/Elman Network (JEN), however there were stability issues, in particular with the Elman ANN in NeuroSolutions and so it

was rejected. This was disappointing as the early results proved promising. The optimum results of the Alpha method can be seen in Table 5 below, while the full set of results can be found in Appendix 3. Compared to the final ANN method which was used for the Tornado, the MSE and other errors are significantly lower. This is due to better ANN design and also the amount and the quality of the data that was used to train the ANN. In a direct comparison, the two methods can be viewed below in Table 5.

Table 5 – Illustrating the improvement of Alpha design

Design	MSE	NMSE	R	% Error	AIC	MDC
Alpha	0.07	0.724	0.58	9.09	-277.48	124.7
Beta	0.12	6.51	-0.06	24.98	-221.49	231.39

It is easy to see that design Alpha has a superior performance to that of the Tornado method that was employed beforehand. This is true for all the measures of error and the plots of the testing as can be seen in Appendix 3. However, in the initial testing phase the results of the two methods were very similar but they were trained using slightly different datasets due to the training and testing data selection procedures, which changed the outcome of the result slightly. One important feature in the testing of performance is the data selected to test the ANN as this is critical to the outcome. In NeuroSolutions there is a testing feature that uses set aside data from each of the data sets. This is usually chosen randomly and is therefore different for each ANN. This produces a wide variety of ANN performances as some data is naturally less noisy or difficult for the ANN to interpret than other sections. To counteract this, data was set aside which enabled the same test to be carried out on each of the ANNs. This therefore enabled fair testing throughout and relative performance between the methods is more important than absolute accuracy.

5.6.2 Beta Design

The Alpha design was expected to produce better results than the Beta design as more elements of a realistic sailing model and environment were being measured and used as inputs. However, the design which can be seen in Figure 48 was produced as a verification of the accuracy of the Alpha design, which did not quite reach the levels of accuracy expected. This was due to measuring too few variables on the rig. A reduction in performance of the ANN was noted when the crew were on trapeze wires as increased TWS's are accompanied by decreased rig loads, which provided confusing input for the

ANN. This problem is in theory similar to the XOR problem that was investigated in the literature and the ANN should be able to solve it with the use of backpropagation. A couple of investigatory ANNs were designed and built to explore this in greater detail and which aimed to predict TWS from the dynamic rig loads as well as V_b. This was investigated to improve the wind speed measurement data into the model. The design of the TWS prediction ANN can be seen below in Figure 50. The ANN design of predicting V_b from the rig inputs can also be seen in Figure 51. The level of ANN performance for both were lower than expected, this could be due to the only partial measurement of the sailing model. In the 49er there are many active and dynamic controls that are continually adjusted such as the mainsheet and rudder, which have the largest effect

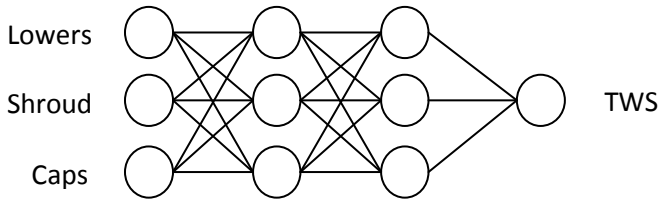

Figure 50 - ANN prediction of TWS

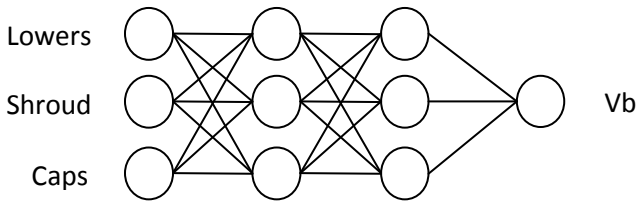

Figure 51 - ANN prediction of V_b

The results of these ANNs can be found in Appendix 3 alongside plots of the data tests. Sufficient numbers of strain gauges could have eliminated the errors produced by the incomplete set of inputs not producing a full model. The results of Beta design can be seen in table 6 below, alongside those of Alpha. Beta design is of a different type, using the Jordan design from the JEN method. There were some stability issues with the Elman methods in NeuroSolutions but the Jordan design proved to have sufficient performance.

Table 6 – A comparison of Alpha and Beta methods

Design	MSE	NMSE	r	% Error	AIC	MDC
Beta	0.039	1.29	0.55	12.66	4365.29	7247.26
Alpha	0.07	0.724	0.58	9.09	-277.48	124.71

In terms of performance comparisons between the two ANNs, the measurement errors produce some mixed answers with most of them favouring the Alpha design. In the literature review the various different error measurement techniques were reviewed and the most critical one in terms of absolute performance was the MSE measurement of error. Measurements such as the NMSE, r, % error, AIC and MDC suggest that Alpha is a better design. In terms of efficiency, the five error measures are correct in suggesting that Alpha is better in design. This is due to a more efficient design and training of the MLP as well as the additional simplicity. This was highlighted especially in the training as the Jordan ANN took three times as long as the MLP to train. However, the absolute accuracy, rather than the efficiency of the ANN is paramount in the scope of this project. In the Beta design there were further optimisations in design with the modification of the context unit which gave it an advantage over the MLP. These affects of modifying the context unit can be seen in Figure 52 and the full table of optimised results can be found in Appendix 3. The context unit is modified in increments of 0.2 and plotted against the MSE to show the effects of this optimisation process. The use of a context unit can also be viewed as a low pass filter. This has the effect of forming a weighted average for the most recent inputs. The formula that the integrator axon uses for the context unit can be seen below in Equation (34),

$$T(z, w_i) = \frac{\beta(1-w_i)}{1-w_i\beta Z^{-1}} \tag{34}$$

where β is the gain factor, w_i is the weighting and T is time.

5.6.3 Context Unit Optimisation

As the data is naturally very noisy Context Unit Optimisation is deemed to have a positive effect on the performance of the ANN although some of the context unit values produced a better performance than others. The Context Unit is a parameter in the model which governs the amount of temporal data used. Various moving averages (MA) were used in the early ANN training but this had an adverse effect on the performance of the ANN. The use of a low pass filter affect does produce a superior end result to that of the standard MLP. There

were again problems with ANN stability and program stability in NeuroSolutions for the Elman ANNs. This was experienced when CVs and GAs were used to improve the structure of the ANN. In performance terms, without these optimisation processes the performance between the Jordan and Elman ANNs was relatively similar. With the capability of using the optimisation processes the MSE could be reduced to a similar level to that of Beta design if not more.

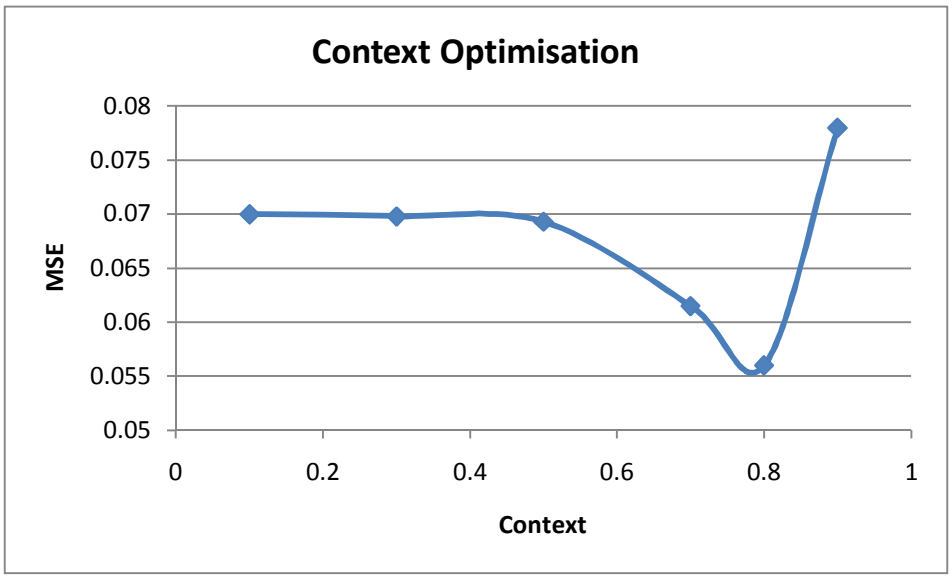

Figure 52 - A plot of context optimisation for the Jordan ANN

The context units are assigned a value between 0 and 1, with 0 using only the present time data and 1 including all the past data. It can be seen from Figure 52 that the highest performing ANN, in terms of minimising the error, is the one with a context unit at 0.8. Changes below 0.5 showed only minor variations in performance of the ANN. Context values of 0.7 and 0.8 were significantly better than the others, as the context value gets closer to 1 this shows a marked decrease in performance as the stability of the ANN reduces. Modifying the context unit in the ANN model was not a lengthy task but retraining the model took over 24 hours. Values which are over 1 lead to severe stability problems and are therefore ineffective.

An attempted improvement in the above performance was conducted with the inclusion of time as one of the inputs into the ANN. It was envisaged that the input of time would help the ANN understand the difference in time between effects measured on the RIB and experienced on the target boat. This however had an adverse affect on performance of the ANN with a reduction of MSE by 0.017. This is due to the varying time delays experienced between the weather boat and the target boat as described in Figure 36 and Figure 37. A more detailed table of this comparison can be found in Appendix 3.

5.7 49er Rig Optimisation

With the fully optimised ANN selected, the next step was to optimise the rig settings and validate them against the tuning guide. During the data collection period the conditions allowed data to be collected in virtually all of the wind ranges. All of the data collection produced successful results apart from the lighter wind range as the performance of the ANN was significantly reduced. This was due to the relatively high degree of variation in TWS and TWD, which is often found in these conditions. The data presented below was collected in the moderate range of the TWS. This was initially carried out by collecting several runs under base settings for the given conditions. This forms the benchmark of the ANN and is the same data set that was used for the ANN optimisations and can be considered the base setting. The data collected from the other seven runs was compared directly with the base line data as they fall within the TWS range of the benchmark. The other runs are labelled by the rig setting that they were adjusted to. This was measured in number of turns down or turns up on the bottle screw, which is connected to the caps and shrouds, e.g. '2d' would signify two turns down. The lowers were untouched. The comparison was made by inputting the TWS, distance and TWA into the benchmark ANN and comparing the response directly to the collected data at the different rig setting. This would not be possible without the use of an ANN, as the average TWS differed for each of the runs, ranging from 14.7 to 16.8 knots. There was also a variation of standard deviation in TWS and TWA as can be seen in Table 7.

Table 7 – Environmental variances of the 49er data runs

Setting	TWS	SD TWS	SD TWD
4u	16.43	2.25	5.9
2u	15.05	2.19	6.51
1u	15.26	1.72	6.67
0.5u	14.7	1.65	5.26
BASE	16.81	1.18	7.22
0.5d	14.94	1.73	5.03
1d	15.18	1.54	4.95
2d	15.65	2.91	8.63

Figure 53 shows the rig settings results plotted on the next page, there was one data run per setting bar the base setting which had multiple to train the ANN. Each point in Figure 50 is the difference between the ANN V_b and the raw V_b from the tuning run in knots. For example '4u' was four turns under and over 0.6 knots slower than the ANN in the same wind. The error bars are the same value as the accuracy of the modelling in knots. The wind strength for each run is shown above every data point. The table of data for the plot, which contains more details, can be found in Appendix 3. There are several interesting factors to be drawn from this plot. All of the average TWS values fall into the same rig setting bracket, which is between 16-19 knots and cover the whole of that range. One example that shows the power of the ANN is the ability to compare the performance of two similar settings in a different average TWS, which is highlighted between BASE and 0.5u setting. This is due to the ANN understanding the relationship between the wind strength and the boat performance. There are, however other factors that also affect the performance shown, which include the strength and frequency of the wind shifts and gusts as previously mentioned. During the Weymouth data collection the TWD was always in the offshore direction, producing harder conditions to sail the boat fast in compared to a steadier wind. This was most notable in the base and 2d settings which was lower than expected. There was also more variation in the TWD for the base setting compared to the other data runs. In the given TWS range, change in TWD has more of an affect than the change in TWS which would also explain why the base setting is lower than the surrounding runs

The sizes of the error bars in Figure 53 are relative to the accuracy of the equipment and the accuracy of the ANN in production mode. The difference in knots, shown on the Y-Axis, is between the output of the benchmark ANN and the individual data run at each setting. Some of the settings are shown to be faster than the BASE setting in Figure 53, which could be attributed to the other individual influences mentioned above. The only point with the error bars clearly higher than the base setting is '0.5u'. During the data collection, the author also noted feedback from the crew after each of the runs. After the '0.5u' the crew reported that it felt as good if not slightly better than the base setting in terms of performance. This could suggest either the setting suited the crew better than the squad standard or

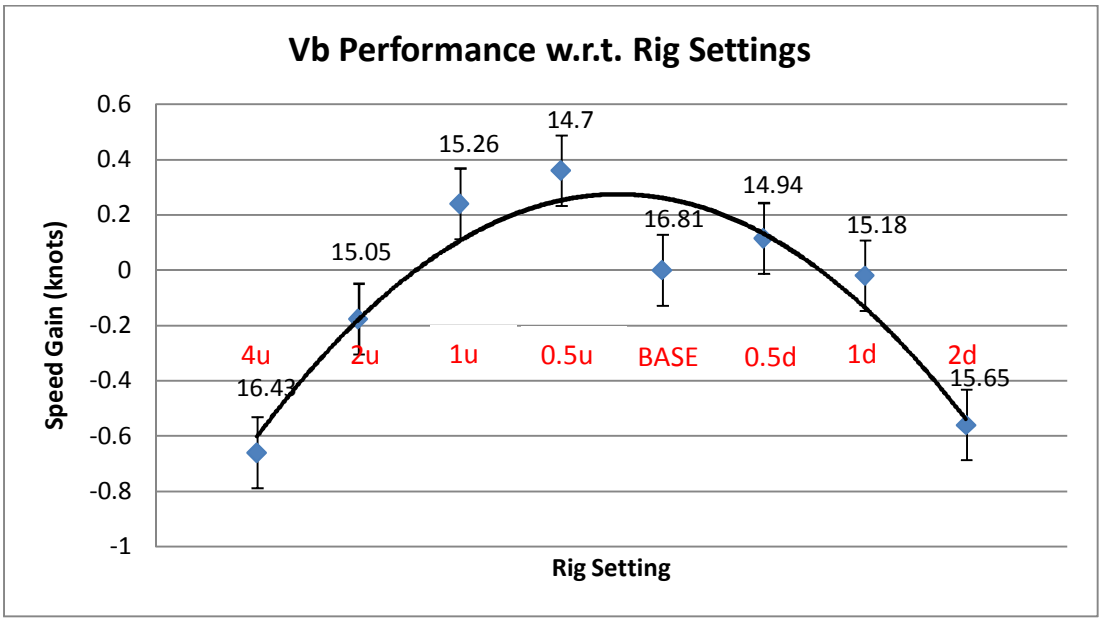

Figure 53 - Validation of 49er rig tuning guide

It is worth noting that one of the reasons why the validation was carried out with the ANN is due to the fact that the 49er is soon to have an upgraded mast and sails. This upgrade is based on the research carried out by Bethwaite, previously discussed in the literature review. The tuning time for a new rig can last for a considerable period. However, by using ANNs in the method shown in this section, that time can be cut dramatically. The Weymouth data collection period had a duration of three days with an extra two days of testing in Palma.

The two boat dynamic comparisons were also able to be calculated in a similar format to the Tornado, except with a better accuracy. An example of this can be seen below in Figure 51, with the benchmark of Evans which was collected in Weymouth compared against the raw data from Pink which was collected in Palma. This again ran the measured TWS, TWA and distance through the benchmark ANN to get a response. The performances of the two boats are very similar; however there are a few interesting points of relevance in the plot. In some places, such as around 300 and 425 seconds, there are relatively large differences in V_b, which initially produced some confusion. It was concluded that since the benchmark data was collected in Weymouth, where the conditions were offshore and relatively gusty due to the effect of the land, the performance would be naturally lower than that indicated by the data collected in Palma. The air and water temperature would also have been different between the two locations. The wind in Palma was from an onshore direction which reduced the frequency of gusts and shifts. With easier sailing conditions the boats would naturally have a higher performance. The difference in performance between Pink and Evans was very close and well within the error bars of half a meter in terms of gain over a duration of three and a half minutes sailing time.

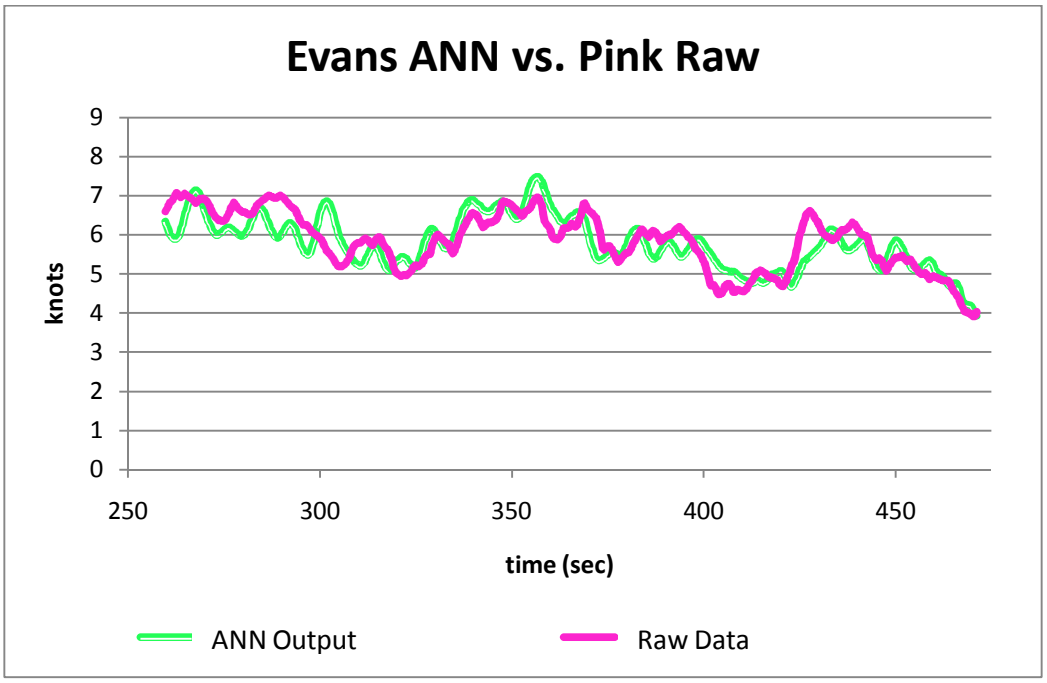

Figure 54 - Comparison of two boats through the usage of ANN

To account for the difference in wind stability the data was also collected from Evans in Palma in addition to Weymouth. This enabled the difference in performance to be corrected through two different methods. The first, which was very simple and relatively crude, was to add the difference in performance onto the output of the benchmark. This led to a sensible answer of approximately two boat lengths difference between boats. The second was to add the data collected in Palma to the benchmark's training data and build a new ANN, which would be able to recognise the change in conditions, and test it on unseen Palma data. Again there were also other factors which could affect the ANN performance, such as the improvement in sailing ability of the crew over the winter. More plots showing comparisons in boat performance, such as the Evans versus Fletcher plot, can be found in Appendix 3. The Evans versus Fletcher plot is interesting as it used the same method which produced the plot in Figure 54 but also had the two boats sailing together in a two boat testing format. This enabled the differences in the ANN to be measured directly with the relative performance between the two boats on the water. The difference in performance between beta design and beta design + with Palma data can be seen in Table 8 below.

Table 8 - A comparison of the last two evolutions of ANN 49er designs with and without Palma data included

Type	MSE	NMSE	R	% Error	AIC	MDC
Beta +	0.07	5.39	0.59	32	2658	6755

Beta	0.09	7.41	0.63	36.6	3213	7458

All of the error measurements agree that there is a significant gain in ANN performance when some of the Palma data is added to the dataset. This is due to several factors, firstly the data set is larger and more data generally produces better results. The ANN has learnt that not all gusts initially reduce the performance of the ANN due to the reduction of model error. Lastly, the data collected in Palma is also of better quality due to the steadier conditions experienced. The data that is used to test the performance of the ANN is from a different 49er crew, previously unseen by the ANN, from which the data was also collected in Palma. This is a true comparative test of the performance of both networks.

There are however some problems with the creation of the Beta + ANN which are that if Weymouth data was fed into the ANN, the performance would be reduced compared to Beta design. This leads to a condition sensitive based ANN which uses more than one ANN depending on the conditions. So for conditions with more variance in TWD and TWS the Weymouth ANN of Beta would be more suitable and vice versa for Beta +.

5.8 Conclusion

This chapter started by considering the current performance analysis methods in the sense of two boat tuning and plotting raw or lightly filtered data, such as in Bethwaite's method. It is worth noting that the typical Olympic coach still regards the two boat tuning method as the best technique for optimising boat performance. Then methods building upon both of these techniques were presented, introducing more and more sophisticated methods and analysis techniques. As the analysis progressed the results also became more accurate and it was demonstrated that it is possible to produce precise models of the boats in order to improve performance.

One of the objectives defined earlier in the thesis was to accurately model the performance of the Olympic classes. Using ANNs this has introduced a much more accurate modelling method to analyse boat performance than the existing static methods.

The two current methods of optimising boat performance were combined with the ANNs to produce a model that used the strengths from both of these methods and more. The ANNs were validated on the water in the two boat testing methods as well as against the tuning guide of the Olympic Development Squad. With the ANN model, accurate performance data was able to be fed to the squad coach. This was in various formats such as metres per

minute or seconds per mile. The end result of the development and optimisation of the ANN was a virtual tuning tool (VTT). This was able to be used as a benchmark by the sailors as shown for example in Figure 54. The VTT has several advantages over the traditional two boat tuning in multiple areas. The VTT always sails at the same performance, two boat tuning can suffer from one of the sailors having a bad day or not trying as hard as the other crew. The VTT is not influenced by these effects, it is also not affected by changes in TWS conditions or headers or lifts, which ruin a two boat tuning session. Before using the VTT, it was notable in the debrief after the training session that a significant amount of the discussion is taken up debating whether there was a header, or if the boat to leeward was faster in a tuning run.

During the data collection it was planned to produce a polar diagram from the collected data or the ANN. In some segments of the data collection runs the crew sailed in a lower and higher than optimum mode than they usually do in order to collect some additional data. This with the current ANN techniques and methods was not powerful enough to produce a full polar plot. The poor performance of the ANN downwind also made it difficult due to large TWS and TWD measurements because of poor weather boat positioning.

In the next chapter techniques used to produce accurate polar diagrams through the use of VPPs and ANNs will be considered. This will produce a full performance model of various classes for all TWS and TWA outside of the ANN model for beating and the VTT that has been created in this chapter.

Chapter 6

VPP Correction with ANNs

6.1 Introduction

It was discussed at the end of the last chapter that the VTT was able to produce a very accurate sailing performance comparison but had problems producing a full polar diagram for the different TWS. This chapter describes the development of a full polar performance model for the relevant Olympic classes using ANNs and VPPs. The methods that were used for constructing a polar diagram solely from the ANN, building upon the previous chapter, will be described, and then the explicit VPP produced to resolve problem will be presented. The final solution embraces the strengths of both of these tools to produce an accurate polar model.

The polar diagram that is normally produced by a VPP is considered a static model, whereas the ANN is able to produce a dynamic model based on the conditions it experiences. This polar is effectively a snapshot based on the conditions of the inputs that is fed into the ANN to produce a polar. The final model presented in this chapter produces a VPP polar diagram that is tuned from the ANN for the conditions experienced during the training of the ANN, and that could be considered to represent an average performance of the boat under those conditions. For this model it is considered to be flat water with gusty conditions. The weakness of the VPP is that it is usually designed for displacement yachts and has difficulty coping with dynamic and ultra light displacement small dinghies such as the 49er. The use of ANNs allows the resolution of these problems.

6.2 ANN Polar Derivations

The knowledge and experience gained during the development of the VTT was invaluable for trying to develop an ANN based polar diagram of boat performance. With a better

understanding of the application of ANNs, encouraging results were able to be obtained more quickly and an appropriate model developed. In this section methods of producing a response from the ANN that agrees with a polar diagram of actual data will be presented.

To create a polar diagram the first thing needed is an input that will produce the output in the correct form. The input has to be in the same parameters in which the polar diagram is measured, namely TWA and TWS. An example of an input can be seen in Table 13 in Appendix 3 which was used successfully in some of the early attempts. The table specifies the wind speed and angle which the ANN produces the outputted boat speed as per a VPP. 'Distance' had to be included in order to improve the ANN model as it was found to have a positive influence on the training of the model. For the input, 'distance' was taken as a fixed value, determined as the average distance between the weather and target boat as modifying the distance could have an involuntary effect on the model.

In the early pure ANN polar plots the ANN was having difficulty in recognising that at very low TWAs the boat was slowing down due to being close to head to wind. This was partially due to the fact that there was only a very small amount of data collected when the boat was almost head to wind. This produced quite a large error at small TWAs. One of the techniques used to counteract this phenomenon was for the author to artificially insert data for head to wind which was of course zero. With this data included and a new ANN trained, the ANN was able to produce a much better polar. There was however a trial and error process as too many artificial data points added for head to wind would skew the other results in the ANN. A variety of marginally modified data sets were tried and tested with the aim of the curve passing through the centre of the axis. A good example of a pure ANN derived upwind polar is shown in Figure 55. The plot used an interpolated curve with data points in the true wind axis of every five degrees.

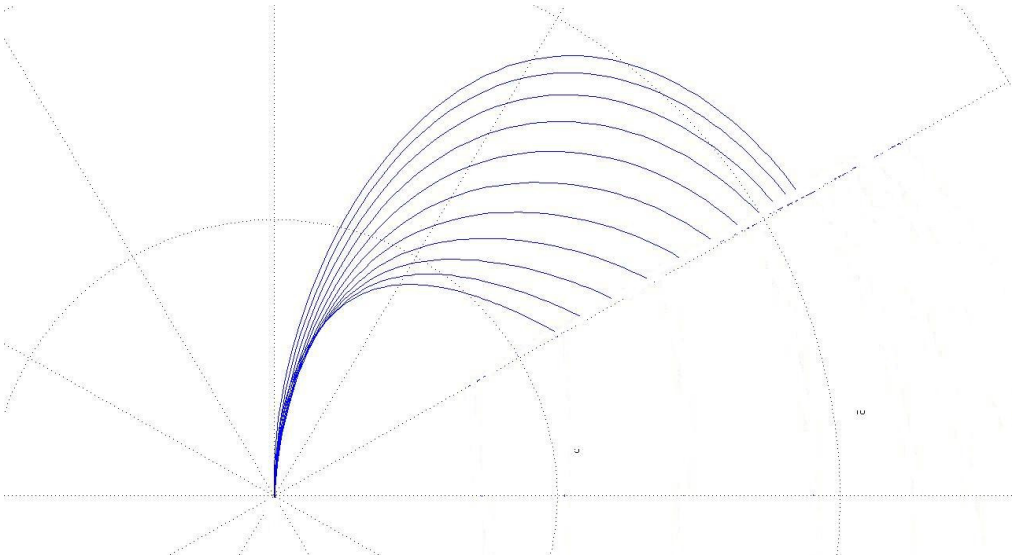

Figure 55 – Upwind 49er Pure ANN Derived Polar

In the data collection process for the 49er, downwind and reaching data was also collected, as a full ANN polar was anticipated. In the early stages the author attempted to use one ANN to produce a response for upwind and downwind. After trying several different designs and structures of ANNs an accurate enough response was not possible due to the significant reduction in accuracy over the entire wind speed and angle range. Therefore two separate ANNs were designed and trained for upwind and downwind. This was an improvement on the combined ANN for two reasons. Firstly the upwind ANN was not affected by the larger errors produced from the downwind ANN, and secondly the training of the ANNs was quicker and more robust than the previous method. Large errors were present in the downwind ANN due to the difficulty of measuring the same wind that the boat was experiencing without affecting it. There were however some issues at 60 degrees TWA due to the joining of the ANNs, these are visible in Figure 56 below. The errors above 60 degrees at the join of the two models are not that important as when the boat is racing it normally does not sail at these angles. Due to the windward leeward course the boat is either sailing upwind at an angle in the region of forty degrees or downwind at an angle of over 130 degrees true wind angle.

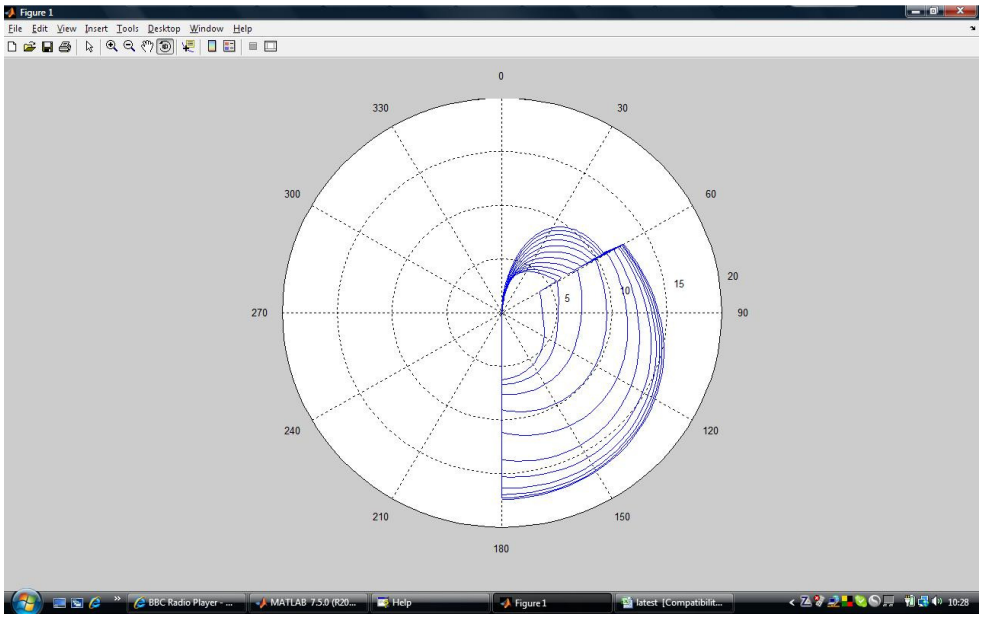

Figure 56 - Dual ANN polar response for the 49er

One of the possible factors why there was such a jump between the two ANNs is due to the small amount of data collected in this region. It was also not possible to collect data in this region in the windier conditions as the boat became too hard to sail and had a tendency to become dynamically unstable or nose dive. It is clear from looking at the downwind section of Figure 56 that the maximum VMG and V_b is continuously found to be close to directly downwind. Whereas, in reality the optimum zone is expected to be approximately thirty degrees higher and with a large reduction in VMG performance close to 180 degrees TWA. This was attributed to the errors from the data collection for the downwind data in a similar scenario to Figure 36 and in Figure 37 but with an increased magnitude. Positioning the weather boat for downwind data collection was difficult as measuring the wind alongside the target boat affected the wind and there was also interference from the wake of the weather boat. Measuring the wind in front of the target boat would have affected it even more from the wake of the weather boat. Hence the only position to collect data without affecting the target boat was from directly behind. This would produce the situation where the 49er would catch up with gusts in front and it would take a significant time for the weather boat to measure the increase in TWS or change of direction. Another factor was that since the weather boat was travelling faster, errors in corrections in dynamics for the TWS and TWD readings also increased as the motions of the rib were more violent.

Due to the difficulty in producing polars with just the ANN it was decided to use a VPP to complement the ANN. A VPP was written by the author based on the work by Martin (2001) as discussed in Chapter 2. The sophistication of the VPP is not as advanced as today's commercial packages with full hull form modelling, but this is not important as the

VPP will have been calibrated using ANN in those areas known to be accurate and validated. Using the ANN to 'tune' the VPP also produces an improvement in the standard VPP. VPPs are regarded as static models whereas the ANN is a dynamic model. One example of this in reality is when the helmsman anticipates a gust and is able to sail higher than in theory by luffing. The ANN is able to model this and correct the VPP for the wind speeds when this technique is being used. In the next section the methods used for constructing the VPP and correcting it with the ANN will be described. The VPP methods shall be covered in brief with the full workings and equations in Appendix 4.

6.3 VPP Building Methods

It was discussed in chapter two that the forces and moments in the VPP model need balancing in order to satisfy equilibrium conditions. Each of these components is produced from several different calculations and factors. For the simplified VPP developed for the project the forces needing balancing are listed as below:

- $M_{heel} = M_{right}$
- $F_{heel} = F_{side}$
- $F_{drive} = R_{total}$

M_{heel} is the sum of the components that produce a heeling force on a yacht. This is produced from the sails and is calculated from the nominal sail areas of the main and jib. Other factors such as calculating the TWS at the CoE of the sail plan is also taken into account. The counteracting force to this is the righting moment of the yacht, known as M_{right}, which from the balancing equations has to be equal to the heeling force. The righting moment is calculated using Larsson's principles (Larsson, 1994) based on the characteristics of the hull and the centre of gravity of the yacht.

F_{heel} is the third component is produced from the lift and drag of the yacht's sails with respect to the TWA at several different angles. It is worth noting that F_{heel} must be calculated first in order to determine the componentM_{heel}. F_{side} is one of the smaller components and one of the most difficult to calculate accurately or even measure in reality without sophisticated equipment. In the scope of this project the F_{side} is calculated using a look up table derived by Gerritsma. (Gerritsma et al, 1991) The table enables the calculation of F_{side} through several different coefficients of heel at different angles. In between these

angles the standard cubic interpolation method produces an accurate enough answer. The rudder angle is not included in these equations due to the assumption of a balanced model.

The penultimate component that needs balancing is F_{drive} which is the driving force of the yacht generated from the sails and is similar in calculation methods to the drag of the heeling force of the yacht that was covered earlier. The driving force is calculated from initially determining the sail areas, before the coefficient of lift, which in turn calculates the lift generated by the yacht. The lift is then calculated with the TWA and the drag to produce F_{drive}. The counteracting and final force to F_{drive} is the resistance of the yacht in a hydrodynamic perspective known as R_{total}. This is one of the more complex areas of the VPP as there are several factors that influence the resistance. These range from the appendages to the calculation of the canoe body resistance in several different forms of resistance ranging from residual to frictional.

In order to balance the forces discussed on the previous page an optimisation process must be used. In this case the VPP was written in Microsoft Excel which enabled the author to use the well known Solver tool, which used the Generalized Reduced Gradient (GRG2) method to optimise a variable based on various constraints set by other functions. There are nine constraints that need to be followed as well as maximising the speed of the yacht for every TWA and TWS. Maximising the speed of the yacht is crucial as without this feature it would be very easy to balance the equations with the yacht stationary or travelling at a slow speed. Maximising the theoretical performance at each different TWA is also the aim for producing a realistic and more accurate model. In the next paragraph the constraints shall be examined in turn. One of the important features to note from using an iterative process like solver is that every time it is run it could produce a very slightly different answer to the previous run for the same inputs and conditions. The size of these differences in results is insignificant in relation to the result produced as it is several order of magnitudes smaller than the error of the modelling technique. This is due to the nature of the GRG2 and also the size of the error bands that were specified by the author in the design of the VPP.

The nine constraints are split into two different sections, the first is designed to ensure that the model works effectively and the second part is the balancing equations as mentioned previously. It is worth noting that not all of the constraints are necessary but without all of them the reliability of the program is reduced. This is found when solver is not able to find a solution based on the constraints and inputs that the user has specified. It is worth noting that some of the forces are left out and assumed to be in equilibrium, such as the weight and the buoyancy being in balance. There is no yawing moment as the keel and mast are assumed to be in the optimum location.

6.4 VPP First Section Constraints

The first constraint is leeway which is specified to be greater or equal to zero for the model to balance. Without this, solver could start to use negative leeway which would greatly reduce the validity of the VPP. Reefing and flatteners are used by the VPP in the higher wind ranges when the heeling force becomes too large in order to still balance the model. In all but one of the Olympic classes the sailors do not have the option to reef or to use a heavy weather jib, so the reef and flattener were regarded as other depowering components used by the crew, such as increased bending of the mast, using more Cunningham or changing the sheeting angle as this would have a similar effect. It is worth noting that the depowering constraints were changed for each of the classes, as the boats with larger sail areas were overpowered much quicker than something like an Yngling. This constraint was added in order to limit the size of the reefing and flattener as the model could change this to over 1 in the lighter conditions in order to improve performance.

In the VPP described by Martin (2001) he uses a constraint on the distance that the crew are able to sit to windward measured from the amidships (CRARM). As Martin's VPP was designed to be used for large displacement yachts it assumes that the crew is hiking. For this project most of the crew have their body weight outside the sheer line of the boat by either hiking with toe straps or trapezing by wire, which means that a change in constraint is needed for the formula, hence Equation (35) changes to Equation (36) for hiking boats and Equation (37) for trapeze.

$$0.01 <= CRARM <= \left({}^{B}/_{2}\right) - 0.015 \tag{35}$$

$$0.01 <= CRARM <= \left({}^{B}/_{2}\right) + 0.5 \tag{36}$$

$$0.01 <= CRARM <= \left({}^{B}/_{2}\right) + 1.4 \tag{37}$$

The final variable at the end of each of the equations is changeable based on the height and mass of the sailor as this varies considerably between the different Olympic classes. There are also several different hiking techniques that are used, for example the straight legged Laser hiking technique is very different from the crew of a Star which is drop hiking which would result in a change of performance.

One of the assumptions that the VPP makes is that since there is wind there will always be a heel of some magnitude in order for the balancing equations to function. This is due to not being able to an angle of heel of zero which would produce invalid results. Hence Martin (2001) specified a minimum heel close to zero and up to a maximum of thirty five degrees. In the VPP for this project, it is a known fact that the sailors do not sail the boats heeled anything close to thirty five degrees. In some classes such as the Tornado or Star heel at a certain angle is good in order to reduce wetted surface area by lifting a hull or using a chine. The maximum heel will have to be changed dependent on each of the classes.

The final constraint from the first section is the minimum speed that the boat is travelling at. This was set to be greater than 0.5 knots as below this speed there are larger errors in the calculations of drag and lift for hydro and aero forces.

6.5 VPP Second Section Constraints

The second set of constraints that solver has to optimise are similar to those which Martin used in his program. However, the error bands that solver has to work within are increased as initial work found some problems with stability in finding a solution. The acceptable error bands have increased from 0.05 percent to 0.1 percent. One of the reasons why there was an increase in the allowable error was that modelling smaller yachts than those which Martin modelled were often harder to solve, especially at the higher wind speeds when beating upwind. The three equations can be seen below which relate back to the equations specified at the start of this section.

$$(F_{drive} - R_{total})/\ R_{total} <= 0.001 \tag{38}$$

$$(F_{heel} - F_{side})/F_{side} <= 0.001 \tag{39}$$

$$(M_{heel} - M_{right})/M_{right} <= 0.001 \tag{40}$$

There are several inputs which are used in a VPP to specify the parameters and dimensions of the yacht which is being modelled. However some of these inputs need to be inserted as an initial estimate into the solver program to start the iterative process. Inputs such as principal dimensions also need to be defined for the model to function. The values inserted are only a starting point but solver needs them to be specified in order to begin the process. A guess of boat speed is needed, the closer the guess for each of these inputs the quicker the

solution can be found. The other inputs that need an initial input are also the constraints listed in the first section.

6.6 The VPP Program

Since the program is based on various formulae and relations in an Excel spreadsheet, the data is easy to manipulate. However inserting data for every different TWA, TWS and estimating the values for the starting points is a very laborious task. Therefore the author decided to write a program in Visual Basic that was able to manipulate the Excel spreadsheet that the VPP was in by automatically changing the values and presenting the results. This was done through the use of Excel Automation. This enabled a full program to run but also small adjustments to be made to the VPP as well. The program was initially validated against a program called Sail Performance Analysis, SPAN, developed by the company Formation Systems. Further details of the formulae used and some of the techniques employed can be found in Appendix 4.

6.7 VPP Correctional Methods

When the particulars for the Star were initially entered into the VPP it was impossible to determine how accurate it was. The Star is a difficult boat to measure in a traditional VPP as it has an unusual hull form due to a very prominent chine. The Star is also considerably smaller than the usual yacht that would be analysed with a VPP. However, once data was collected from the Star and processed using the ANN it was possible to produce an upwind optimum sailing angle for a variety of conditions. This then allowed the author to modify the VPP by matching the optimum upwind points of the ANN with the VPP. It would also include the crew interaction correction into the VPP polar plot. The methods that the author's VPP is based on are a generic interpretation of performance which means that several of the calculations are approximations, such as the lift and drag calculations with respect to the sail coefficients. In some of the TWSs and TWAs the performance of the ANN and VPP were relatively similar. However especially in the windier conditions the results tended to differ due to the VPP having difficulty in balancing the equations and a difference in theoretical and actual hull shape. This was due to the fact that the VPP finds it harder to balance the yacht in those conditions. The results before the ANN correction are method alpha and post correction from the ANN method beta.

Table 9 - Before and after correction has been applied

	Alpha method		Beta method	
TWS	TWA	V_b	TWA	V_b
5	47	4	44.6	4.03
10	40	5.5	37.6	4.98
15	38	5.6	36	5.28
20	40	5.8	36.1	5.39

There are clearly differences between the two methods. After the correction had been applied to the polar the difference in the plot was clear to see. The largest difference in performance was between 45 and 90 degrees. The downwind performance was relatively similar between the two methods. This is due to the fact that the coefficients of lift are no longer as important due to the driving force on the sail changing from lift to drag. The comparative polar can be seen on the next page, to keep the diagram simpler the plot for 10 knots TWS is only shown in Figure 57. Method Alpha is the plot in red and Beta in black is the corrected version.

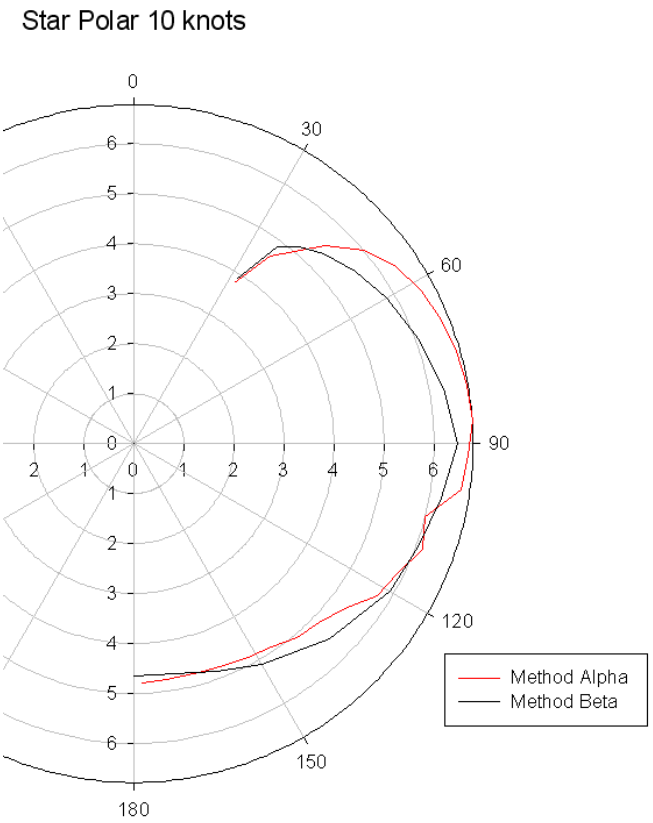

Figure 57 - Alpha versus Beta method for the Star in 10 knots TWS

In the final year of the PhD, a set of polars were needed for each of the classes for the Olympic Games in order to enable tidal calculations to be performed. With a very accurate knowledge of the tide at locations across the race course and an accurate polar performance known the strategy could be determined before the race. This involved a more sophisticated VPP as the author's VPP was not very reliable and did not cater for smaller yachts or planing dinghies. Hence work began with Dr. Martyn Prince of the Wolfson Unit at University of Southampton. More on this further step can be found in the next section. A few other examples of the Star polar can be found in Appendix 6 for different TWSs. It is interesting to note when examining the other wind speeds that at the higher wind speeds the VPP has difficulty balancing the boat when it is beating.

6.8 Wolfson VPP

Using the author's VPP and the ANN method, as described in the previous section, produced good results for the Star class as there was sufficient data and the type of boat is significantly closer to a conventional keelboat than the other Olympic classes. The author's VPP was not able to cope with the lighter displacement classes even with the ANN corrections as there were severe problems with model stability. This is due to the nature of the VPP that was used especially in areas such as calculating resistance.

A solution was found for this problem and that was by using the Wolfson VPP (WinDesign). The Wolfson VPP is also partially based on the Delft series that was used in this project but has a higher level of sophistication. The Wolfson VPP is a much more accurate VPP than the author's but the most important factor is that it has a dinghy section. This dinghy section is simpler than the rest of the VPP and focuses more on length and wetted area for the calculation of performance. It is able to model the performance of the boat when it planes significantly better than the author's VPP. It does have a reduced performance in the transitional zone when the boat is just starting to plane but this is usually limited to a ten percent error.

Therefore using the Wolfson VPP and correcting it with the ANN in a similar way to the Star method was the logical step. This was enabled through better modelling from the VPP and also the expertise of Dr. Martyn Prince of the Wolfson Unit. The difference between the Wolfson VPP and the ANN was significantly smaller than the previous attempt of the author but correction of the VPP was still needed. There were differences in the TWA in the higher wind ranges as expected upwind as the ANN was able to sail the boat higher than the static

VPP as it included the input from the crew. There were usually a couple of iterations before the final polar was produced for each of the classes. One of the first polars was that of the 49er as the author had a well trained ANN and the Wolfson Unit had some good data for that boat. The ANN was able to correct the VPP upwind through manipulation of the sail coefficients, and the VPP is able to produce a downwind performance. An example of the finished 49er polar can be seen on the next page in Figure 58. As mentioned previously in the chapter the Wolfson VPP was corrected to known points derived from the ANN and the two were joined together. In the majority of the curves the transition is smooth, however for the wind speeds between 4 and 7 knots this transition is less smooth between 60 degrees and 80 degrees. This could be due to the sudden drop off of apparent wind sailing with reduced wind speed and no spinnaker hoisted.

The interesting part of Figure 58 is that the VPP is powerful enough to determine the optimum downwind angles. This was not possible with Carrico's VPP which was discussed in *chapter two* possibly due to the sail coefficients as it determined the optimum angle to be at 180 degrees TWA. This problem was initially found in the Finn as VPPs in general struggle with the aerodynamics of single sails close to dead downwind due to the difficulty in determining the lift coefficients of the sail. However with the sail coefficient correction it produces a much more realistic polar diagram. A couple of the other combined polars can be found in Appendix 6 from the Tornado and the Star classes. In the next section further data analysis techniques shall be examined using the software and ANNs written by the author.

49er Polar Diagram

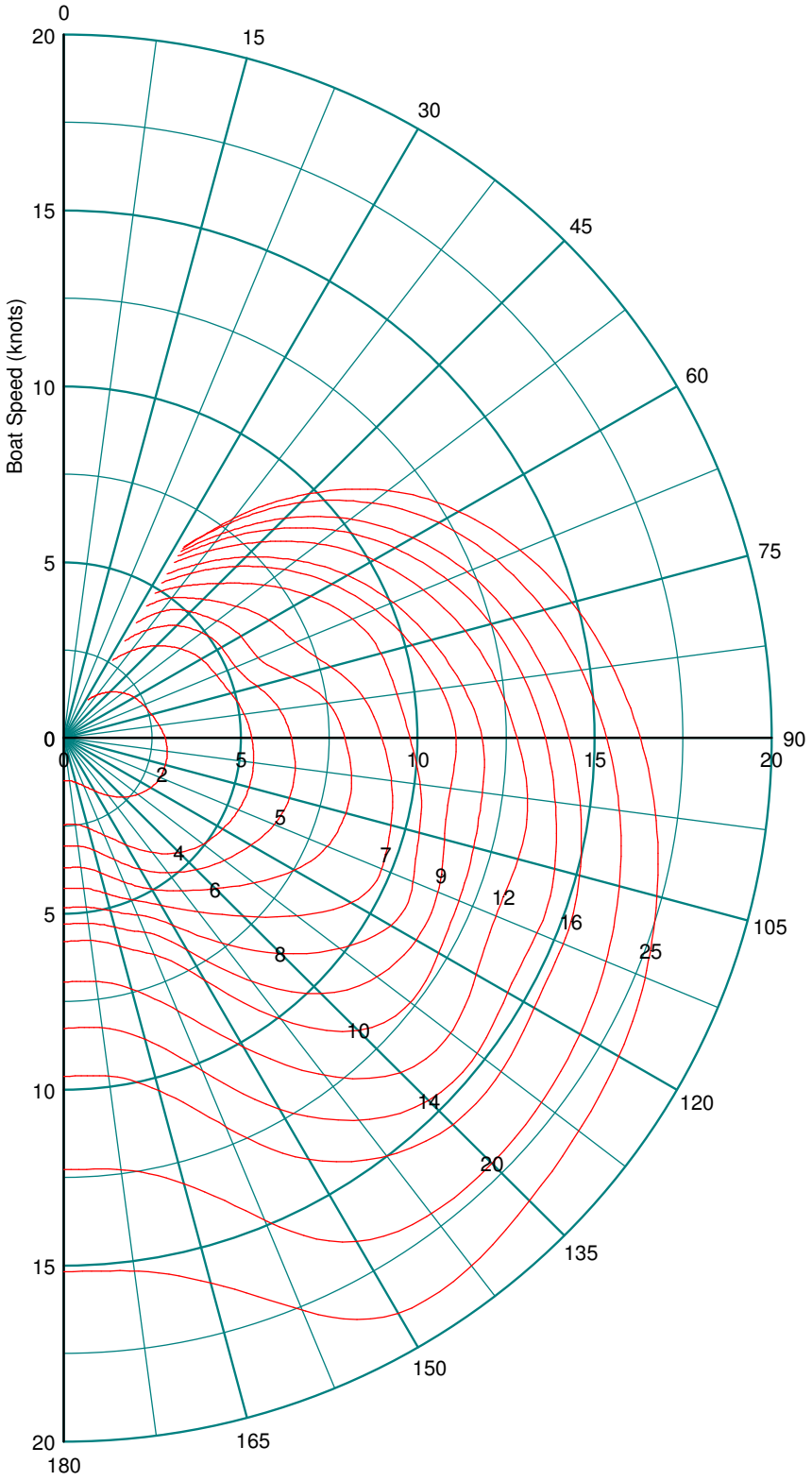

Figure 58 - The final 49er polar based on the results from the ANN and the Wolfson VPP

6.9 Custom Software

Near the end of the development of the ANN and its analysis techniques, a need arose to use the new methodology in a user friendly format with a few other additional features added. This requirement originated from the RYA technical department who intended to use the package after the end of the project, under the title of the RYA Performance Analysis Tool (RYAPAT). The software revolves around the use of the ANN and also some of the work that was carried out with the Dr. Prince at the Wolfson Unit. In the next section an examination of the features and functions of the program will be presented and it will be explained how they help in modelling the performance of yachts quantitatively.

6.9.1 Program Features

The program has multiple features and tools, all designed with the aim of providing the user with answers to boat performance queries. In the software an attempt has been made to eliminate qualitative assertions about performance and replace them with accurate quantitative performance descriptors. These can take a variety of formats such as 'the yacht is twenty seconds per mile quicker than the baseline performance' or alternatively, for the non technical user, that it is simply quicker. In the next section the various aspects and segments of the program shall be described. Further information and illustrative screenshots can be found in Appendix 10. The features discussed will include the data pre-processing and fusion, the ANN response and running the data analysis tool.

6.9.2 Data Pre-Processing

During a training or testing session the data is usually offloaded into Pi Toolbox for quick analysis. It is then possible to export the data from the weather boat and the target boat into Excel. Pi Toolbox exports data using a procedure named RYAPAT that, fuses them into a pre-determined format ready for the analysis program to process. Once this is complete the data is displayed in the windows in its raw format in a time distance plot and in polar format. The trace of the yacht can also be seen in a bird's eye plot. If there is any tide where the data has been collected this can be corrected for in the program by entering the tidal speed and direction. The vectors are then resolved to remove the tidal component. Ideally, the data collection is carried out in non tidal waters as the tidal effects can only be represented approximately and are a source error, however small.

6.9.3 ANN Processing

In the software, as mentioned earlier, the ANN is the main component and it acts as a very powerful and flexible performance analysis tool. The ANN is produced by using a feature in NeuroSolutions, Custom Solution Wizard, which builds a .dll file, based on the ANN that has been created. This effectively produces six different files that are used for producing a response from the ANN based on the input data. To produce a new ANN and six new files, the new ANN has to be trained in NeuroSolutions first before loading it into the software. It is possible to allow the training and testing of ANNs in the software but this was disabled due to the cost of the higher user level and the complexity involved in the training of the ANNs, which produced a recall only ANN. The recall only facility allows users to evaluate themselves against the benchmark but not train new ANNs.

Once the data has been successfully loaded into the ANN from the pre-processing method or directly from a complete file it is simply a matter of using two buttons to produce a numerical and graphical response of the ANN against the raw data in terms of the boat speed.

The next step is to investigate how the raw data compared against the ANN in a variety of terms, as illustrated in Figure 59. The figure shows (1), the data analysis tab which consists of a time distance plot of both boat performance; (2) a dial which shows how it compared with colour coding; and (3) tables with more detailed numerical data. This display can be altered depending on the needs of the user, which are graduated at four different levels. The first gives a basic view which shows the dial and the percentage difference in performance with the time distance plot showing all the available features for the advanced user. The level above this enables the selection of different ANNs and allows the capability to load them in. This level is secured in order to reduce the chance of the user changing the ANN loaded in mistakenly. A screen shot of this tab can be seen on in Figure 56 with the important features labelled.

The next level allows the user to select different segments of the data collection run and analyse them individually. When a section is selected the analysis is automatically run and can be compared to the overall performance. This feature is particularly useful when a sailor or coach feels that the sailor was faster or slower in one section through a change in technique or setting on the boat.

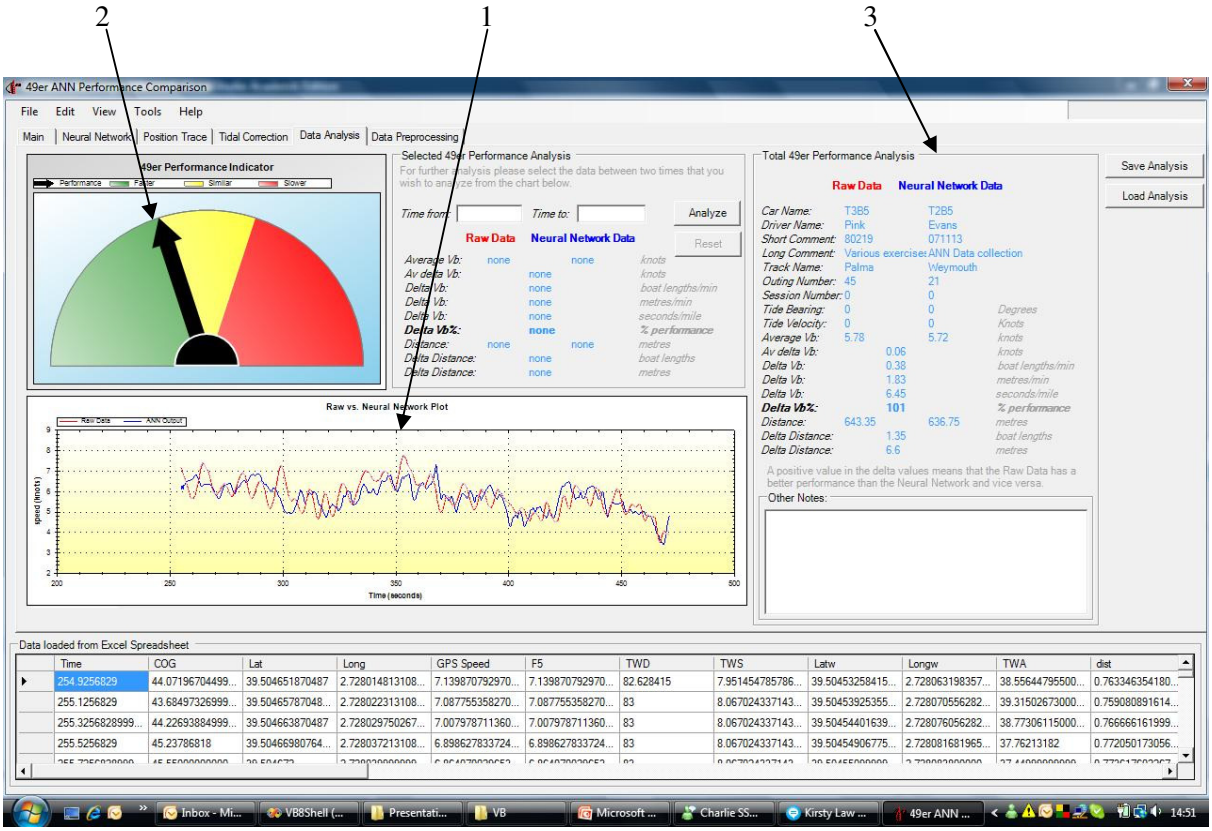

Figure 59 - Showing the data analysis tab after processing 49er data

The results of the data analysis can be saved into an Excel file if desired. One of the later features that was added to the program is one of the most important, which is the re-importing of data into Pi Toolbox with the ANN included. This feature included the information of the data analysis tab but with the added function of producing a latitude and longitude trace of the raw and the ANN data. This produced a feature that displayed the raw data sailing, with the ANN sailing alongside in the same conditions, almost as a ghost boat. A screenshot of this feature can be seen on the next page in Figure 60.

The method for producing the comparative trace was based on using the spherical trigonometry calculation with the new bearing and speed of the ANN for the inputted wind conditions. Dr. Martin Smith of Nottingham University contributed some invaluable help with this feature. The method is an approximation and there are two other methods which can be used for the calculation. Due to time constraint these other methods were beyond the scope of the study. The first of these alternative methods involved using the Haversine method while the third and most complex approach was to build and use a Kalman filter.

The spherical trigonometry method used the sine cosine rules and assumed that the Earth was a perfect sphere. The notes for this method were kindly provided by Dr. A Sowter of the same department.

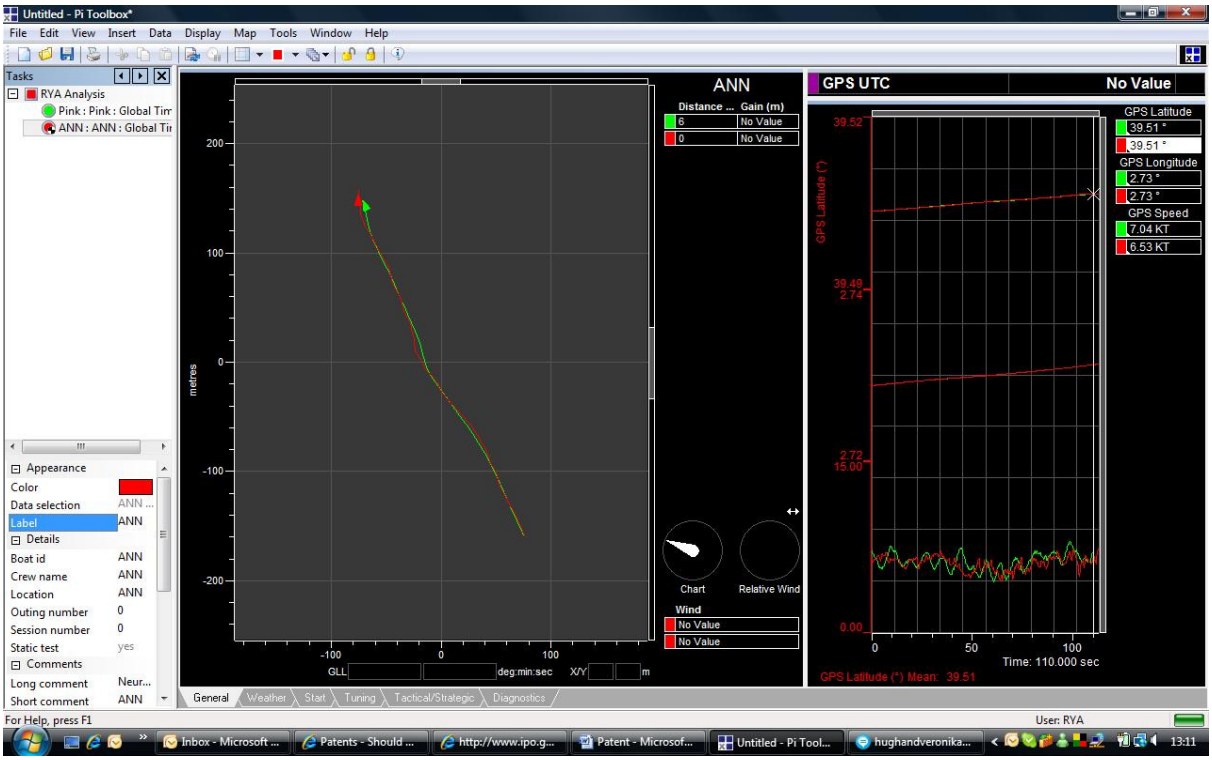

Figure 60 - The comparative analysis of performance through producing an artificial latitude and longitude ANN trace

Figure 60 clearly illustrates a very powerful tool for the sailors in the debrief and when analysing various aspects of performance. One of Pi toolbox's features is the synchronisation of data with video, with the trace running in synchronisation with video, further techniques can be analysed by the coaches as it would show direct indications in the performance of the trace. In the next section the uses of VPPs shall be examined in the program.

6.9.4 VPP Analysis

One of the additional benefits of producing the Wolfson based polars for the Olympics was that they could be used in performance analysis. The technique in which they were used is similar to the method that Deckman uses, which is by interpolating between the values for a given TWA and TWS. This feature was added to enable performance analysis for classes where there was little or no collected data, such as the 470. Since the performance is relative

to the ANN corrected polar, the modelling technique would be a static one. In a comparison of how the VPP based analysis compares to the raw data and the ANN analysis, a comparison was conducted which can be seen below in Figure 61.

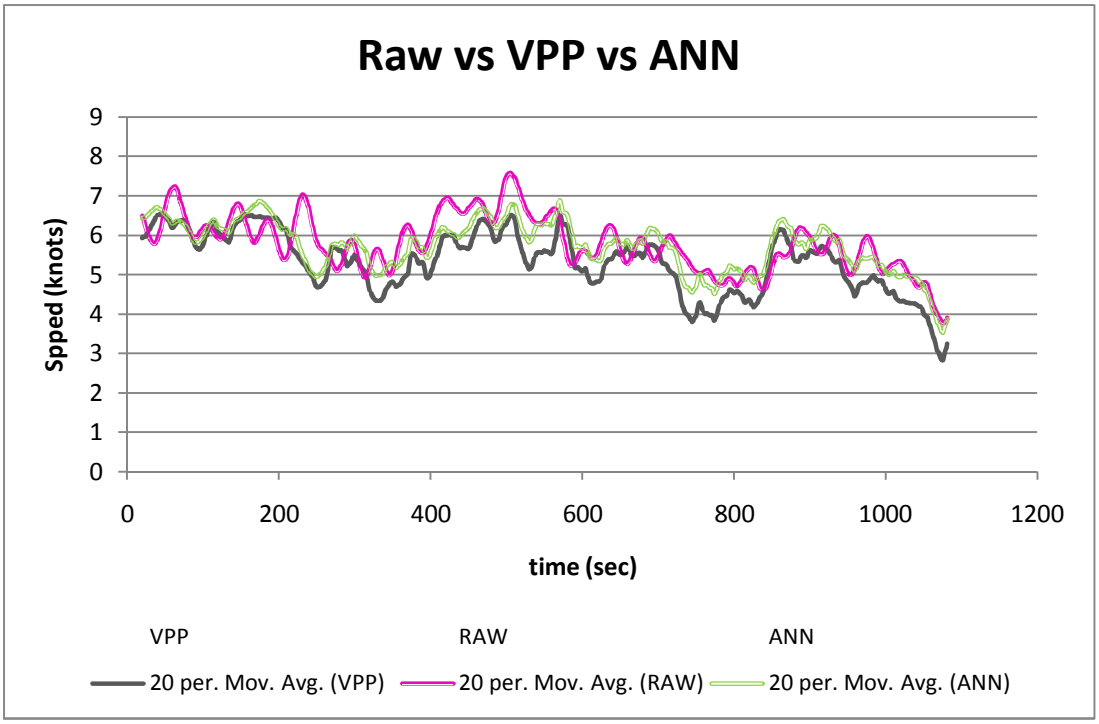

Figure 61 - A comparison of the VPP interpolation, the ANN and the raw data

The differences in performance between the VPP output and the ANN show the difference in modelling technique between the static and dynamic methods. Since the VPP is static, as soon as the TWS drops, the VPP produces the relevant drop in performance whereas in reality it takes time for the yacht to slow down due to momentum. This also happens with gusts and changes in the direction of the wind. However, it is clear to see from Figure 61 that in constant conditions the VPP and ANN produce similar results. This is encouraging to see as the VPP was tuned from the ANN. The plot in Figure 61 is from a 49er, which is hard to model accurately with just the VPP. A heavier displacement boat such as a Yngling or Star would be better for modelling.

This concludes the chapter on ANN and VPP based data processing and analysis. In the next section the results shall be looked at in a broader sense before concluding in the following chapter.

Chapter 7

Sail Based ANN Performance Analysis

7.1 Introduction

One of the common themes throughout the project was that for every question answered or problem solved further issues of interest were identified. One example of this is that after the initial development of the ANN for the Tornado class it was considered desirable to include a further input to the ANN to try and improve the accuracy of the model. The input selected, because of its influence on the performance of this class, was shroud tension as measure by strain gauges located on the shrouds. As a corollary of this, another input that was considered worthy of exploring was the resulting sail shape. To do this an image recognition system was used to monitor characteristics of the sail shape and this was time stamped to allow it to be synchronised with the other logged data, to provide a further input to the ANN. It was hoped that the change in sail shape could then be directly related to the performance of the boat and vice versa.

Image recognition may seem like a significant change of direction from the main focus of this study but it was initiated with the idea of being able to use the sail characteristics as inputs for the ANNs. In the following sections the history of sail image recognition is discussed along with existing sail image recognition tools. The static and dynamic sail image recognition techniques investigated are then compared.

7.2 Sail Image Recognition Background

One of the key skills of sailors is the ability to trim a sail correctly. Trimming a sail effectively may be considered to be a skill developed from both understanding and experience that relies on qualitatively judging the correct sail shape by eye as there is no quantitative measure of sail shape used. Nevertheless, the experienced sailor can trim sails very effectively to allow the maximum performance to be obtained. A related and more difficult skill is to take this understanding of sail shape and apply it to the design of sails. In designing a sail there are several parameters and dimensions that need to be ‘optimised’ as well as observing constraints on the maximum allowable size of the sail. When trimming, or

designing a sail, there are several key factors that need to be considered, these are apparent in the points labelled in Figure 62:

- Maximum draft position in the sail (Point 2);
- Maximum camber of sail (Point 3);
- Entry angle (Point 4);
- Exit angle (Point 1);
- Twist in the sail.

The twist is not visible in the Figure as the picture is taken looking upwards. The twist measurement is defined as the angular difference between the boom and the top draft stripe. Figure 62, (Halsey, 1999), is from the literature used to describe the commercial sail makers sail program 'AccuMeasure'. It is one of the more widely used manual fitting programs currently in use and shall be discussed further in the next section.

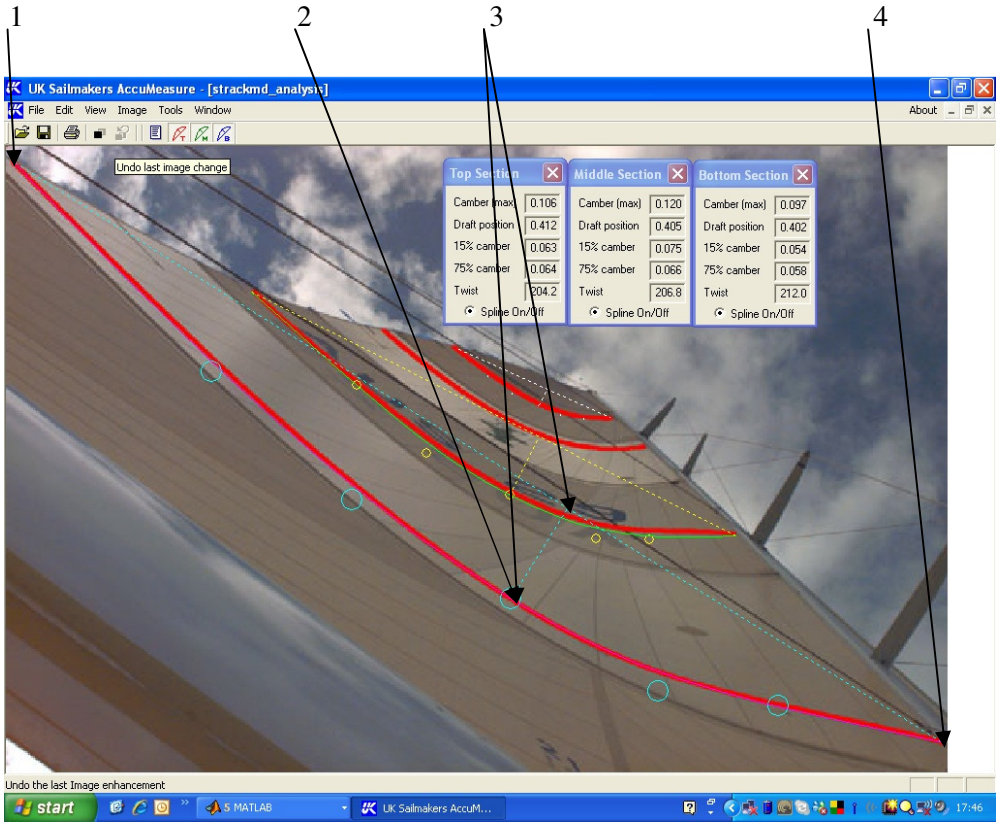

Figure 62 - Looking up a mainsail (taken from UK Halsey, 1999)

7.2.1 Fitted Spline Sail Analysis (FSSA)

There are two different types of sail analysis programs, fitted and automated. The fitted method has been in existence for around a decade, originally coming from the work carried out in preparation for the America's Cup (AC) races. However, it has found its way into the commercial market and is now more widely available for use by sail makers. Normally the shape of the sail is measured at three or four different heights in order to get a good understanding of the overall sail shape. These points can usually be recognised by sail stripes, which can be seen in Figure 62 above in red. In the fitted method the user takes a picture from the bottom of the sail at a known reference point that is sometimes marked on the sail. The aim is to fit in all the sail stripes from a view point that is almost underneath the sail. If the picture is taken from the wrong place then the sail dimensions will become distorted.

The characteristics of the sail are measured by the user manually fitting a spline to each of the sail stripes. There are various control points along the spline that are adjusted until they align with the sail stripe. Once the two have been aligned properly the program is able to calculate the various characteristics of the sail at that point. This process takes approximately ten minutes per picture and is regarded as a relatively laborious task. There is also scope for errors in aligning the spline with the sail stripe as can be seen in Figure 63 below.

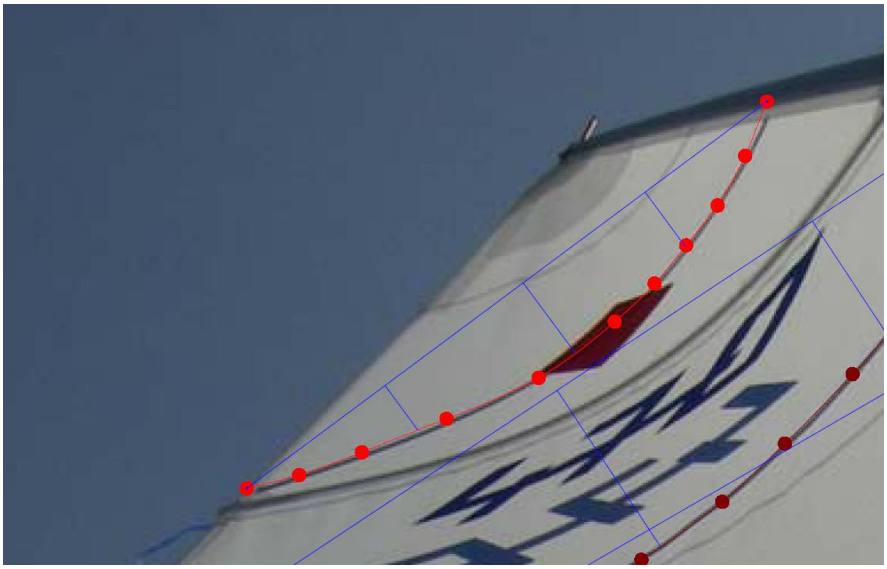

Figure 63 - An example from the North Sails program

Since it is such a labour intensive process, multiple pictures in a sequence can be very time consuming to analyse. While this method has proved effective for larger keelboats it would not be as suitable for most of the Olympic classes as the rigs are very dynamic, namely they tend not to be in a steady state; one image could look very different to another in the same wind conditions if one of them is taken at the time the boat encounters a wave. This problem has led to the recent development of an automated system, which has a number of potential benefits.

7.2.2 Automated Spline Analysis System (ASSA)

The automated system has again come from the AC arena and is the Sail Vision software (Sail Vision). This is a significant step forward from the manual fitting version, as all the splines are fitted automatically, saving a lot of time and ensuring better accuracy. One of the most important features of the software is that it is time stamped and included in the dataset. This means that the usual performance analysis of the yacht can be carried out but the sail data can be added to this as well in order to assess the performance of the trimmers or the design of the sail. The principal disadvantage of using such a system is that multiple cameras need to be fitted to the boat with two on the mast head and two a little lower than the forestay fitting on the mast. The two at the top are able to analyse the mainsail and the twist of the mainsail from the boom reference. The two below the forestay are for analysing the genoa; the twist in this case is from the sheeting position. A sample of the main sail analysis can be seen below in Figure 64 (Sail Vision Report, 2007) and the genoa in Figure 65 (Sail Vision Report, 2007).

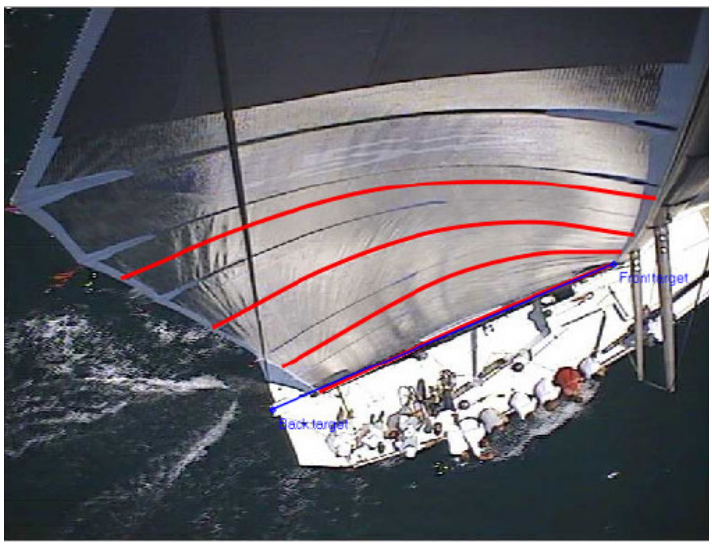

Figure 64 - Sail Vision Mainsail Analysis (Sail Vision Report, 2007)

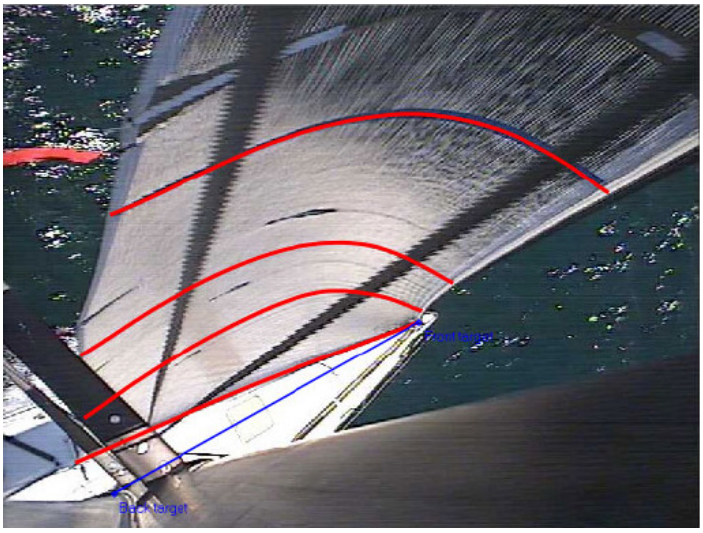

Figure 65 - Sail Vision Genoa Analysis (Sail Vision Report, 2007)

There are other advantages of using an automatic system such as the analysis of more than one sail at the same time. Taking images from the top of the rig enables all of the sail to be included in the image. Quite often in the manual process, when taking a photograph from under the boom, it is not possible to fit all the draft stripes in. The smallest draft stripe which is the one near the top of the sail is normally the hardest to see, so having the camera at the top of the rig enables it to be the closest.

7.2.3 Assessment of Current Sail Vision Systems

Having discussed the main positive and negative features of both systems, the automated system is potentially the better system for application to the types of boats considered in this study. As mentioned previously, for boats with highly dynamic characteristics, such as the Olympic classes, it is difficult to analyse sail shapes without an automated system. A static system only gives a single snapshot at one moment in time of the overall dynamic system.

The use of image recognitions systems in the past have been met with varied results. The FSSA and ASSA techniques can be viewed as static and dynamic methods as the Fitted Spline method is based on a brief snapshot of the sail whereas the Automatic Spline method can be applied at specified time intervals.

In the Olympic classes the coaches regularly work with sail designers and manufacturers in the build up to the Olympic Games with the aim of optimising the sail design. In this process they use manually fitted spline method with the sail designers. An option was to use the Sail Vision system but it was not deemed suitable due to space requirements and cost.

With the author's dynamic system it differs to the Sail Vision system that was reviewed in *chapter two* as the data processing is not analysed in real time. This means that the data can be captured and analysed at a higher rate, as time and processing power is no longer a constraint. In the Sail Vision system the processing has to be instigated by the user and cannot be carried out readily.

Hence a program was written in Matlab using the image processing toolbox. The program used several well known techniques that shall be discussed in the next section before looking at the program in action in the demonstration.

7.3 Image Recognition Methods

The image recognition system consists of two major components, the camera and recording system hardware and the accompanying software that processes the information recorded. The aim of the software is to extract the sail stripe from the image and then calculate the shape of the sail from analysing the extracted stripe. In the initial investigation into the sail image processing techniques the colour day glow red was chosen. This was used as it stands out well from the colour of the water and from the white boats and sails. In this section the methods used by the software to isolate the stripes is outlined.

7.3.1 Pixel Labelling

The first step in the process is to apply a colour space transform to the image. A colour transformation structure is created which changes each of the pixels from the RGB format to an *L*a*b** format which is a different colour system encoding. It is then possible to apply this colour transform to the image using the three different areas such as luminosity '*L*'. The second of the three processes in the *L*a*b** format '*a*' determines how much green and red the pixel has. The third and final section '*b'* performs the same analysis as '*a*' but in the respect of blue and yellow. This is done for each of the pixels and a colour marker is then attributed to it. The time needed to label all of the pixels is related to the processing power of the computer and the resolution of the image.

7.3.2 Cluster Indexing of Pixels

After each of the pixels have been labelled by the *L*a*b** method the next step is to label all the pixels with a cluster index. The cluster index can be optimised with respect to the distance between clusters and partitions. This, through the use of *K*-means, enables the clusters to be arranged in an optimum format. *K*-means allows natural clusters of data to be identified through an iterative procedure. There are various controls of the K-means clustering such as using replicates to avoid local minima in the iterative process. Other factors such as the calculation of distance between the clusters can be altered and in this case the squared Euclidean method was used. One other variable of the *K*-means method is the alteration of the number of colours that are used in the process. In this application, isolating red sail stripes made the process easier and the value was set at 3 accordingly.

After this process is complete it is then possible to label each of the images with the results from the *K*-means segmentation. This has the effect of producing three images that all consist of segmented pixels. In these three images the sail stripes are finally isolated from the rest of the colours with two other segmented images. An example of the extracted sail stripe can be seen in Figure 66.

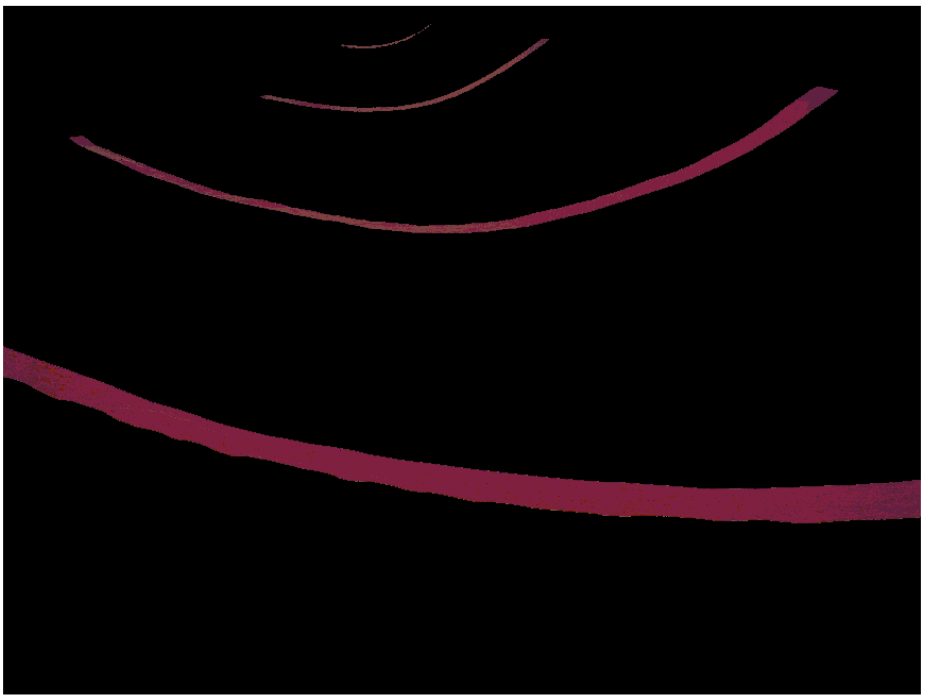

Figure 66 - A segmented image taken from looking up the author's RS 400 jib

Once the sails stripes are isolated, further processing is needed to produce an image that can be analysed. This is done by firstly changing the RGB image to a greyscale image for the desired segmented image. The next step is to detect the edge of the stripes through the use an edge detection algorithm. This can be done using several different such methods, ranging from the Sobel to the Prewitt methods. During early testing, several different methods were tested and the best performance was judged to be given by the Canny edge detection method. Once the edges have been isolated the last image processing step is to trace the edge with the boundary tracing method. After it has been traced the image is then ready for calculating the actual variables of the sail shape, such as maximum draft and entry angle. After this process is complete it can be plotted graphically as shown in Figure 67.

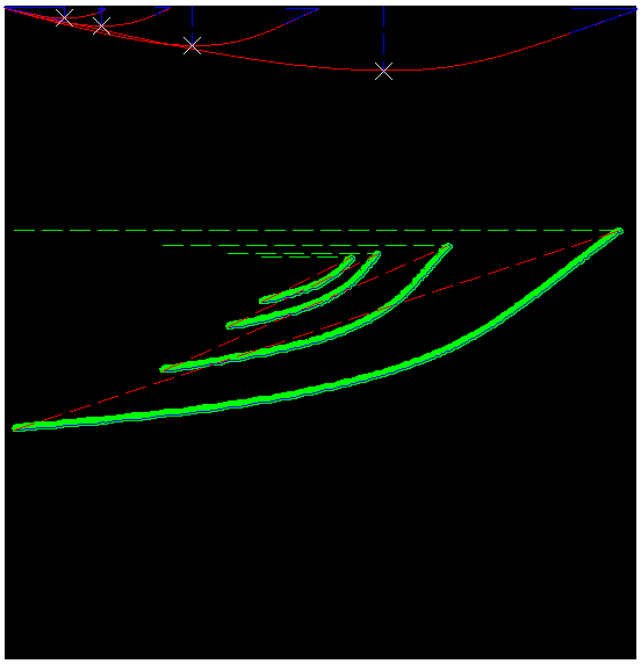

Figure 67 - An example of graphical analysis

An example of the other segmented images can be found in Appendix 5. The important output of the software is not in the graphical representation of the sail but quantifying the parameters required and providing them as numerical output characterising the sail shape. An example of this can be seen in Figure 68. The values for each of the parameters are time stamped at the same frequency as the other logged data in order to aid the synchronisation process.

The software was originally written a few months before the hardware testing began as the initial work was based on static pictures of sail shapes.

Deciding on the best hardware proved to be more difficult than the software development as there was a trade off between the cost of the required camera(s) and the quality of the image that they provide. There were four demonstration tests in total which used hardware from two different companies. The first test used the hardware that the RYA already possessed, which consisted of a bullet camera and a waterproof MiniDV tape recorder. This system was tested on the author's RS400 with red sails stripes and the camera taped to the top of the mast. The results of the first demonstration indicated that the hardware was not of a sufficient quality with respect to the resolution of the camera and the length of the analogue cabling. The quality of the captured image was so poor that an almost random colouring on the edges of the images was experienced. This had a drastic affect on the segmentation process and produced a lot of scatter, which can be seen in Figure 82 in Appendix 5. Hence an investigation into finding more suitable equipment began.

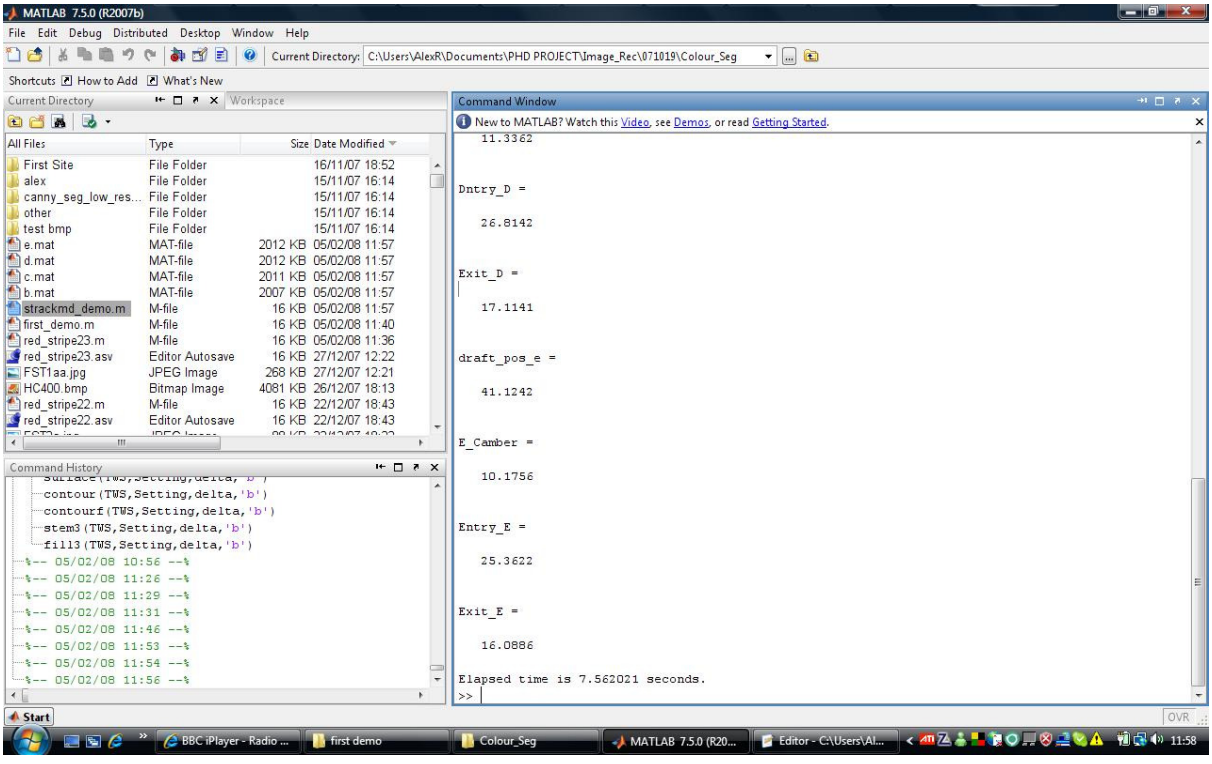

Figure 68 - Showing the output of the image recognition

The first search for better image acquisition hardware resulted in two demonstrations with a company called First Site. The hardware that was trialled was significantly superior to that of the initial demonstration with the RYA equipment. This was due to a better camera, which used Ethernet connections to a computer, producing a much better image quality with better saturation and there was also significantly less reduction of the signal quality. The

computer or tablet was able to store the images in a more efficient manner than the MiniDV tapes, as there was a function to 'rip' the desired images as they were recorded. An example of one of the ripped images can be seen in Figure 70. This however added to cost and weight of the hardware, which was considerably more expensive than the RYA equipment, and also needed water proofing.

7.4 Hardware Selection Trials

The camera system was tested with an old B14 jib simply held so as to provide a shape representative of a set sail. Again the jib had red day glow stripes on the battens and the camera was filming from above the head of the sail. This test was far more successful than the first one with the acquisition system producing a much better image. The results of this image processing can be found in Figure 70. Compared to the RYA equipment the results are far superior. The conditions for testing were not as good as the first demonstration as the light level was falling but the results were nevertheless encouraging. The other segmented images can be found in Appendix 5. First Site were also able to provide a camera calibration service that corrects the 'fish eye' effect that is found from using a digital camera. This mainly affects the top draft stripe as it is close to the edge of the image. It is worth noting that the Sail Vision system does not include this image calibration.

Figure 69 - Raw image from the second demonstration

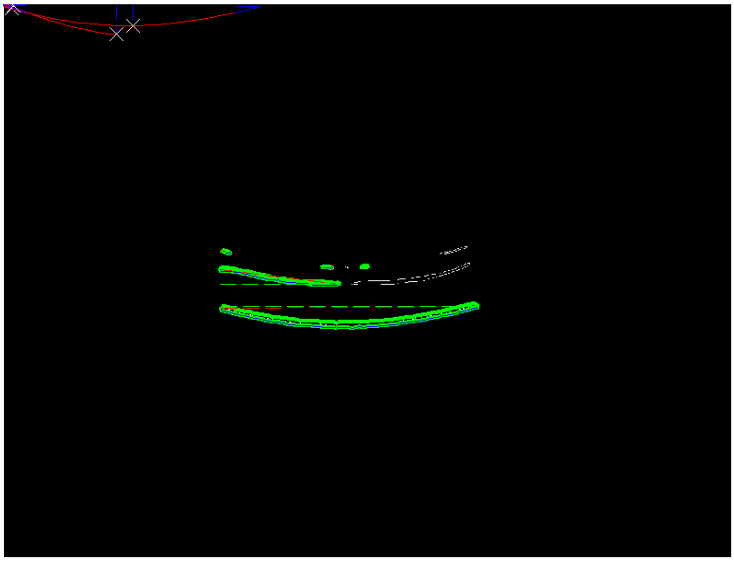

Figure 70 - Analysis from the second demonstration

In the image analysis process the bottom and middle stripes were partially hidden from the camera that meant that a full analysis could not be conducted on the two stripes. This was due to the fact that the jib was very old and the battens had stretched the material around the draft stripes and this was therefore sagging compared to the surrounding areas of the sail so were hidden from view. The bottom draft stripe could also be larger as it is the most difficult to view. This is a common technique used on the AC yachts, the bottom stripe can sometimes be as wide as a meter since the location of the camera is relatively far away. Moving the camera away from the mast would improve the view of the draft stripes but this would then effectively distort the shapes of the stripes further.

A second test session was conducted a couple of months later by First Site in determining the optimum location of the cameras on the author's RS400. This however was a flawed test as the camera was not set up correctly and the colours captured were distorted or faded. Correction to the images was attempted but was not to a sufficient level of accuracy.

At the time of the third test another company, DogCam, was found producing suitable hardware. Their hardware represented a good compromise between the RYA and the First Site hardware in terms of quality and price. It had the advantage of the RYA equipment in terms of ruggedness, but not as high quality as the First Site hardware. The final demonstration was conducted at DogCam using the ME1 configuration which can be seen in Appendix 5. This demonstration was by far the most successful with the acquisition and processing systems functioning well on the first attempt. This was mainly due to the functionality of the hardware and software provided by DogCam. The Matlab code was also

updated which sped up the processing and improved the stability of the program. The segmented images can be found in Appendix 5 and the processed image can be seen in Figure 68.

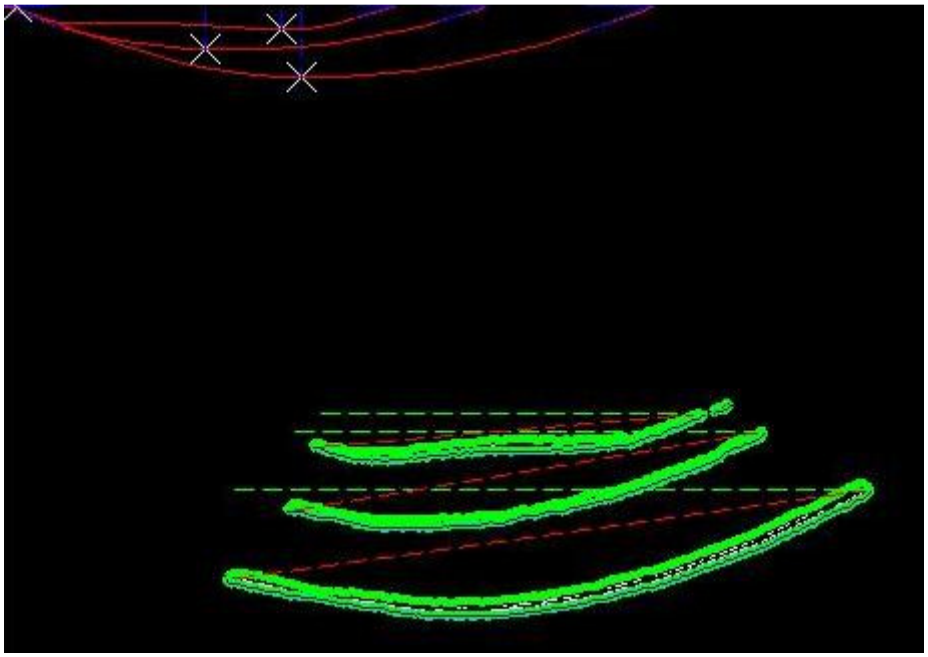

Figure 71 - The final image recognition output

After this successful test, a proposal was written to purchase the equipment for further on the water testing. However this was not possible due to a change of financial constraints at the RYA so this aspect of the study was not able to be progressed further but these experiences and the method developed are considered to provide a useful starting point for further work in this area.

7.5 Conclusion

With the finance to purchase the camera system hardware, and the time to develop it into a useable system, a very powerful tool could be created. This tool would be different to Sail Vision as all the analysis is done in a post processing format and the characteristics and dynamic behaviour of the sails could be analysed in greater detail. This is due to the high frequency of capture and the automation of the software. This tool could then be used to provide additional inputs for inclusion into the ANN model. This could give the user the performance of the sails with respect to the performance of the boat and crew. After the ANN learns several similar sail shapes it could be used as a performance prediction tool where future sail shapes could be entered in order to determine the performance of the yacht.

This is just one example of how the method presented could be extended; in Chapter 8 further comment is made about future work in the application of ANN to performance prediction.

Chapter 8

Conclusions and Future Work

8.1 Conclusions

A novel approach in modelling yacht performance analysis has been developed in this project through taking advantage of the power of ANNs. The new approach has advanced yacht performance analysis from quasi static analysis and modelling to a truly dynamic performance evaluation technique. In contrast to the majority of current performance analysis and prediction techniques it is able to provide both a higher level of accuracy and also to include, for the first time, the performance of the crew in the model. This ability to include explicitly the performance of the crew in the model is considered to be a very significant original contribution of the work presented.

Determining the final ANN design was a lengthy process with many alternative solutions investigated in order to establish the most appropriate ANN design types and configurations for each class of boat modelled. Some designs were found to be more suitable than others for different applications and had various advantages and disadvantages. For example in Chapter 5, the Jordan ANN produced the best performance for the 49er, but had the longest training time. In contrast the MLP design trained quickly and was able to give approximate answers relatively quickly and robustly for new or exploratory methods. Similarly, the performance of the MLP proved to be superior compared to the Jordan ANN when the rig settings were used for the 49er.

Throughout the project data collection techniques improved which also helped the training and accuracy of the ANN model. Dedicated days of data collection runs were implemented which improved the whole process further as described in Chapter 5.

In terms of advancing the field of performance monitoring and evaluation, the use of an ANN allows the development of a novel and purely quantitative model by reducing the reliance on the qualitative inputs and responses. It represents a step change from current methods where modelling performance is at best based on regression of raw or filtered data

integrated with qualitative assumptions. With this core tool, various other features can be created that can be used to monitor the performance of sailing yachts; examples include the rig optimisation tool, and the ANN comparative positional trace plot. Chapter 6 demonstrated that the main additional feature that was created was the facility to produce an accurate polar diagram from a corrected VPP. This capability enabled the sail designer for the UK Olympic team to produce better designed sails for various classes of boats. The technique was used in the Star and Finn classes for the sail design. It enabled the sail designer to improve the CFD model allowing better sails to be designed.

The project was used as the basis for developing new methods and approaches to training the Olympic sailing team. Implementing this culture change was one of the more challenging aspects of the whole project. Up to this point the sole approach had been based on the conventional technique of changing various parameters on the boats in order to improve the performance through qualitative inputs and outputs. The project introduced new concepts and methods that were able to model performance more efficiently and objectively than before by almost removing the human factor in the assessment through the use of ANNs and allowing, for the first time, the human influence on sailing performance to be assessed objectively. This improvement in modelling more than satisfied several of the original pragmatic requirements of the project. An aspiration of the work was to transform the level of yacht performance analysis techniques and modelling to that of performance prediction used in Formula One motor racing. A good indicator of this increased investment at a higher level in sailing is the converging professionalism and budgets of the America's Cup with Formula One.

This project has gone some way to changing attitudes to training in the sport, with many coaches working with different Olympic class recognising the associated benefits in preparing for the 2008 Olympics. This shift in attitude has not been altogether universal with some classes, such as the 470 and RSX windsurfer, yet to benefit from these approaches. Some classes are continuing to use these tools to prepare for 2012, particularly those where early data collection was accepted. For these classes there has been a change in attitude in the team from initial reluctance to mounting the GPS units to the boats, to proactive requests for data collection and access to the performance analysis techniques developed from this project. This has acted as a major factor in closing the loop of including the influence of boat and crew performance on boat design, the training of crews and sail design.

8.2 Future Work

The use of ANNs has proved to be a very powerful tool in the area of performance analysis of yachts. Their unique ability to model complex environments much more effectively than previously used methods opens up a world of alternative and future uses of ANNs in the sailing environment. This project has only scratched the surface in terms of using ANNs for modelling sailing performance. There are several different routes that were discussed and envisaged to be of potential interest in further research past this project.

8.2.1 Separating out Boat and Crew Performance

During a training session it is often difficult to determine whether the improvements in performance of the crew and the yacht are in relation to the improvement of the crew; a technical enhancement of the yacht; or just that the yachts being compared are sailing in different environmental conditions. ANNs would provide an approach to solving this problem. A model would be trained with the original boat and crew, then the crew would be replaced or elements of the crew replaced and they would sail against the model. With the yacht remaining the same and the only difference the crew it would be possible to ascertain the individual performance characteristics of the crew. If sufficient data were collected, this approach could be extended to modelling different members of the team sailing the same boats in identical environmental conditions, thus isolating crew performance. By the same token different rig configurations can be tested by having the same crew sailing the yacht repeatedly in the same environmental conditions, but with different rig settings. Additionally, using similar techniques, the best yacht in a group can be identified for particular weather conditions.

8.2.2 Rig Optimisation

At the time of writing, the 49er class has recently adopted a new mast and sail plan. This provides an opportunity for the settings of the new rig to be optimised in preparation for the next Olympics. This could be based upon the techniques described in Chapter 5 and could potentially be developed further with the use of more sophisticated measurement techniques. Improved GPS units would improve the accuracy of the measurement of V_b by almost an order of magnitude. More advanced methods of producing and comparing boat performance could be developed with the use of ANNs primarily by building upon the ‘Alpha’ design that

was also discussed in Chapter 5. The 'Alpha' design could be improved upon further by the addition of further inputs, such as mainsheet load, trapeze line load, forestay load and various other controls such as kicker and Cunningham that could all be logged at the same time as the other variables. This increase in inputs could potentially improve the performance of the 'Alpha' design over that of the 'Beta' design method and also reduce the amount of data collection time. It would however require significantly more time setting up the equipment in the target boat.

8.2.3 Telemetry and Real Time Modelling

A telemetry system does exist for the GPS units that the RYA currently employs and which was used in the early part of this project. One of the ideas for further work in this area is to use the telemetry system to show the performance of the target boat compared to the ANN. This system would function by sending the V_b and *COG* to a receiver in the weather boat. The receiver would be connected to a tablet computer that also has the input for *TWD* and *TWS*. With these inputs the ANN could produce an output of predicted boat speed in a similar manner to the results previously described for desired and actual V_b but in real time. The result of the comparison of the raw data to the ANN could then be shown in real time on a display for the coach in terms of the relative performance of the boat with respect to the target ANN prediction. A further development could be sending the results back to the subject boat via telemetry on a small display for the crew to monitor their relative performance also. This could be conducted more easily on a larger yacht with onboard computers.

8.2.4 Integration with Existing Software

An extension of the previous idea of real time performance monitoring and benchmarking performance would be to apply it to larger displacement yachts, such as Americas Cup Class boats, which have the space and capability to have significant computing resources onboard. This could be integrated with existing proprietary software packages used to monitor performance and augment their functionality further. The main advantage of this would be to allow much quicker analysis and subsequent comparisons as the data bandwidths would be significantly higher than via telemetry. It would also be a useful tuning tool for large

yachts as in most cases the testing is conducted in secret or where there are no other identical types of yachts to conduct boat on boat testing with.

8.2.5 Performance Prediction for Boat Design

One of the areas in which ANNs have been used in the marine industry is with respect to predicting resistance in the design process for larger vessels. The ANN uses tank test data and provides an alternative to traditional statistical regression approach for interpolation.

The work involving ANNs in this project with performance analysis could potentially be combined with the towing tank data for various yacht forms to produce a resistance evaluation tool for use in design. The various design parameters that would have an effect on the performance of the yacht in the towing tank or in reality could be investigated using the ANN model with a view to identifying forms with improved resistance and performance characteristics.

8.2.6 Virtual Racing and Benchmarking

Since the performance of the yacht and the crew can be modelled with ANNs it should be possible to combine this with a virtual racing simulation. Several papers have been written on decision making and simulation of a fleet race or match race. The work by Scarponi (Scarponi, 2007) is a good example of an approach that it could be combined with.

References

Adams, J., et al (1996) 'Technologies for Spacecraft Formation Flying' *Stanford University* 1996

Agnew, D., Larson, K., (2007) 'Finding the repeat times of the GPS Constellation' *GPS Solutions* 11 pp 71 – 76. 2007

Anderson, J., Rosenfeld, E., (1988), *Neurocomputing: Foundations of Research*, Cambridge: MIT Press

Aparicio, M., et al (1996) 'GPS Satellite and Payload' *Global Positioning System: Theory and Applications,* Vol. I pp 209 – 244. 1996

Bao, P., (1999), 'PCA Neural Network for JPEG Enhancement', *Conference Record of the Asilomar Conference on Signals, Systems and Computers*, v 2, pp 976-980, 1999.

Bethwaite, J., (2007) 'Internship Report 49er Performance Enhancement' *May-July 2007*

Bethwaite, J., (2008) 'The Case for Change 49er Development - Part 3' *January 2008 Seahorse International Sailing'* 2008

Braasch M., et al (1992) 'Improved modelling of GPS selective availability' Langley Research Center, FAA/NASA Joint University Program for Air Transportation Research, 1992-1993 p 45-54

Cane, J., (1995) 'Scoring IMS Regattas – An Empirical Study of Alternative Methods'. *The 12th Chesapeake Sailing Symposium.* Chesapeake, 28th January 1995, pp1-13.

Carrico, T., (1995). 'A Velocity Prediction Program for a Planing Dinghy'. *The 12th Chesapeake Sailing Symposium.* Chesapeake, 28th January 1995, pp183-192.

Cassella, G., Robert, C., (1999) *Monte Carlo Statistical Methods, 1st edn, 1999*

Claughton, A., (1999) 'Developments in the IMS VPP Formulations'. *The 14th Chesapeake Sailing Yacht Symposium.* Chesapeake 1999.

Clauser, M., (1979) 'A Microcomputer Beats to Windward'. *The fourth Chesapeake Sailing Yacht Symposium.* Chesapeake 1979.

Dana, P., (1996) *Global Positioning System Overview*. Available at: http://www.colorado.edu/geography/gcraft/notes/gps/gps_f.html (Accessed: 060116)

Danchik, R., et al, (1990) 'The Navy Navigation Satellite System (TRANSIT),' *Johns Hopkins APL Technical Digest*, Volume 11, numbers 1 & 2, 1990

Danielson, et al (2003) *Meteorology,* McCraw Hill, 2003

Elliot, J., (2004) 'British Americas Cup Challenge performance analysis software manual'. 2004

Elman, J., (1990), 'Finding Structure in Time', *Cognitive Science* 14, pp 179 – 211, 1990.

Fassardi, C., (2003) 'Tank Testing and Data Analysis Techniques for the Assessment of Sailboat Hydrodynamic Characteristics', *International Journal of Small Craft Technology,* Vol 145, Part B2.

Featherstone, W., (2003) 'Improvement to Long – wavelength Australian gravity anomalies expected from the CHAMP, GRACE and GOCE dedicated satellite gravimetry missions' *Exploration Geophysics 34,* pp 69 – 76 2003.

Fisher, B., (1980) '*The Fastnet Disaster and After*'. 1st edn. Pelham Books

Francisco, S., (1996) 'GPS Operational Control Segment' *Global Positioning System: Theory and Applications*, Vol I pp 435 – 468

Gautier, L., (2001) 'EGNOS: The First Step in Europe's Contribution to the Global Navigation Satellite System' *European Space Agency* Toulouse, France 2001

Gautama, T., et al, (2003), 'A Different Entropy Based Method for Determining the Optimal Embedding Parameters of a Signal', *Proceedings of the International Conference on Acoustics, Speech and Signal Processing*, 29-32 2003.

Gerritsma, J., Keuning, J., Omnink, R., (1991). 'The Delft Systematic Yacht Hull (Series II) Experiments'. *The Tenth Chesapeake Sailing Symposium*. Chesapeake, 9th February 1991, pp27-39.

Gerritsma, J., Keuning, J., Versluis A., (1993) 'Sailing yacht performance in calm water and in waves', *The 11th Chesapeake Sailing Yacht Symposium.* Chesapeake 1993.

Gilbert, R., (2006) *Private Correspondence*. Investigation into optimum performing settings for RYA GPS and early trials

Graf, K., Böhm, C., (2005) 'A New Velocity Prediction Method for Post-Processing of Towing Tank Test Results'. *The 17th Chesapeake Sailing Symposium*. Chesapeake 4th-5th March 2005, pp 67-78.

Guier, W., Weiffenbach, G., (1998) 'Genesis of Satellite Navigation' *John Hopkins Technical Digest,* Volume 19, Number 1. 1998

Guler, M., Artir, R., (2005), 'Modula Neural Network Modelling of Compressive Strength of High Alumina Bricks by using Tangent Function', *Materials and Design 28, pp 112 – 118, 2007.*

GPS World (2008) Available at: http://www.gpsworld.com/gpsworld/issue/issueDetail.jsp?id=13717 (Accessed: 080501)

Haines, B., et al (2003), 'Initial Orbit Determination Results for Jason-1: towards a 1 cm orbit' *Inst. Navigation* 50 (3), pp 171-179, 2003

Han, J., et al (1996) 'Optimisation of Feed Forward Networks', *Engineering Applications of Artificial Intelligence*, Vol. 9, No. 2, pp 109 – 119, 1996.

Hansen, H., Jackson, P., Hochkirch K., (2002) 'Comparison of Wind Tunnel and Full-Scale Aerodynamic Sail Force Measurements'. *High Performance Yacht Design Conference.* Auckland 4-6 December, 2002

Hazen, G., (1980) 'A model of sail aerodynamics for diverse rig types', *New England Sail Symposium*. 1980

History of GPS. Available at: http://usinfo.state.gov/ (Accessed: 051103)

Helvacioglu, S., Insel, M., (1995), 'Sailing Yacht Performance: The Effects of Heel Angle and Leeway Angle on Resistance and Sideforce', *I. International Yachting Technology Conference* 3rd – 10th October 1995, Çeşme.

Hodge, L., Auda, G., Kamel, M., 1999. 'Learning decision fusion in cooperative modular neural networks', International Joint Conference on Neural Networks: IJCNN'99, Vol. 4, Piscataway, NJ, USA, pp.2777–2781.

Holley, J., Bull, L., (2007), 'Multiple Model Analysis of Tornado Class Polar Data', *University of the West of England*, November 2007.

Huang, J., Liu, H., (1997) 'Object recognition using genetic algorithms with a Hopfield's neural model', Expert Systems Applications, Vol. 13, no. 3 pp. 191–199, 1997

Hwang, J., (1993), 'What's wrong with a cascaded correlation learning network: A projection pursuit learning perspective', *Dep. Elect Eng, University of Washington*, FT-10, 1993.

Ignizio, J., Soltys, J., (1996) 'Simultaneous Design and Training of Ontogenic Neural Network Classifiers', *Computers Ops Research.* Vol. 23, No. 6, pp 535 – 546, 1996.

Juan Garay (2008), Private correspondence.

Jordan, M., (1986), 'Attractor dynamics and parallelism in a connectionist sequential machine', *Proc. Eighth Annual Conf. of the Cognitive Science Society*, Amherst, MA, pp.531–546, 1986.

Kang, Z., et al (2007), 'Impact of GPS Satellite Antenna Offset on GPS Based Precise Orbit Determination' *Advances in Space Research 39*, 2007, pp 1524 – 1530.

Kaplan, E., (1996) *Understanding GPS Principles & Applications.* Artech House, London

Kerwin, J., (1978) 'A Velocity Prediction Program for Ocean Racing Yachts Revised to June 1978', *Irving Pratt Ocean Race Handicapping Project Report*, 78-11, MIT/H.

Keuning, J., Binkhorst, B., (1997) 'Appendage Resistance of Sailing Yacht Hull' *The 13th Chesapeake Sailing Symposium.* Chesapeake 1997.

Keuning, J., Sonnenberg, U., (1998) 'Approximation of the Hydrodynamic Forces on a Sailing Yacht based on the Delft Systematic Yacht Hull Series'. *International HISWA Symposium on Yacht Design and Construction.* Amsterdam November 1998.

Kong, C., (1998), 'Radar Tracking System Using Neural Networks', *International Journal of the Computer, the Internet and Management*. Vol. 6 No. 2, 1998.

Korpus, R., (2007) 'Performance Prediction without Empiricism: A RANS-Based VPP and Design Optimisation Capability', *The 18th Chesapeake Sailing Yacht Symposium.* Chesapeake 7th – 8th March 2007.

Lachapelle, G., (1997), 'Lecture Notes of GPS Theory and Applications' *The University of Calgrary,* Calgary, Canada

Lanyi, G., (1984), 'Troposheric Delay Effects in Radio Interferometry' *TDA Progress Report*, 42 – 78

Larsson, L., Eliasson, R., (1994) *Principles of Yacht Design.* 2nd edn. London: Adlard Coles Nautical

Leik, A., (1995) *GPS Satellite Surveying* 2nd edn, New York: John Wiley and Sons

Letcher, J., McCurdy, R., (1987) 'Data Collection and Analysis for the 1987 Stars & Stripes Campaign'. *The 8th Chesapeake Sailing Symposium.* Chesapeake 1987

Lunt, et al (1999) 'Effects of the Protonsphere on GPS Systems: modelling and observations' *Antennas and Propagation, IEEE National Conference.* August 1999, pp 200 – 203

MacMillan, D., (1995), 'Atmospheric Gradients from Very Long Baseline Interferometry Observations', *Geophys. Res. Letters.* 22(9), pp 1041-1044, 1995

Marchaj C., (2003) *Sail Performance.* Rev edn. London: Adlard Coles Nautical

Martin, D., Beck, R., (2001) 'PcSail, a Velocity Prediction Program for a Home Computer'. *University of Michigan, 2001* 623.8223 CHE

Massat, P., Wayne, B., (2002) 'Optimising Performance through Constellation Management' *Crosslink*, 2002 pp 17-21

Masuyama, Y., Nakamura, I., Tatano, H., Takagi, K., (1993) 'Dynamic Performance of Sailing Cruiser by Full-Scale Sea Tests' *The 11th Chesapeake Sailing Symposium.* Chesapeake 1993

Masayuma, Y., Fukasawa, T., Sasagawa, H., (1995) 'Tacking Simulation of Sailing Yachts – Numerical Integration of Equations of Motion and Application of Neural Network Technique'. *The 12th Chesapeake Sailing Symposium.* January 28th 1995.

McCulloch, S., Pitts, W., (1943) 'A logical calculus of the ideas immanent in nervous activity', *Bulleting of Mathematics Biophysics* 5: 115 – 133

Meza, A., et al (2002), 'Global Behaviour of the Ionosphere Electron Density Using GPS Observations' *Advanced Space Research.* Vol. 30, No. 2 pp 307 – 312 2002.

Minsky, M., Papert, S., (1969), 'Perceptrons' *Cambridge,* MA: MIT Press.

Mitra, A., (1974), *Ionospheric Effects of Solar Flares*. 1st edn. Dordrecht: Reidel.

Moller. M., (1990), 'A Scaled Conjugate Gradient Algorithm for Fast Supervised Learning', *Computer Science Department, University of Aarhus, Denmark*, 1990

Neumann, J., et al (1996) 'Test Results from a New 2cm Real Time Kinematic GPS Positioning System' *ION GPS – 96.* Kansas City, September 17-20 1996

NAVSTAR GPS User Equipment Introduction. September 1996

Oossanen, P., (1985) 'The Development of the 12 Metre Yacht "Australia II"'. *7th Chesapeake Sailing Symposium. Chesapeake* 1985

Pedrick, D., (1979) 'Evolution of Offshore Ratings – To the Limit'. *The Fourth Chesapeake Sailing Symposium.* Chesapeake, 20th January 1979, pp2-18.

Petriu, E., (2004), 'Neural Networks: Basics', *School of Information* Technology and Engineering. Available at: http://www.site.uottawa.ca/~petriu/ (Accessed 061201).

Pham, D., Karaboga, D., (1999), 'Training Elman and Jordan networks for system identification using genetic algorithms', *Artificial Intelligence in Engineering 13 pp 107–117*, 1999.

Philpott, A., Mason A., (2002) 'Advances in Optimization in Yacht Performance Analysis', *High Performance Yacht Design Conference.* Auckland, 4-6th December 2002.

Plumer, E., (1996) 'Optimal Control of Terminal Processes Using Neural Networks', *Neural Networks, IEEE Transactions on Volume 7*, Issue 2, pp 408 – 418, 1996.

Principe, J., et al, (1999) *Neural and Adaptive Systems: Fundamentals through Simulations*, New York: Wiley, 1999.

Rama, B., (1996), 'Technique to Reduce Multipath GPS Signals' *Current Science,* Vol. 90. No. 2, 25th January 2006.

Reid, A., (2005) *GPS Based Performance Analysis in Small High Performance Boats*. MRes thesis. University of Newcastle upon Tyne.

Rosenblatt, F., (1958), 'The Perceptron: a Probabilistic Model for Information Storage and Organization in the Brain', *Psychological Review* 65: 386 – 408

Rumelhart, D., et al (1986), 'Learning Representations by Back - propagating errors' *Nature, Vol. 323*, 9th October 1986.

Rumelhart, D., McClelland, J., (1987), *Parrellel Distributed Processing* – Vol. I, Cambridge: MIT Press

Sail Vision Report Team Cristabella training from BSG Developments. 10th May 2007.

Sail Vision Software available at: (http://www.bsgdev.com/) accessed (080610).

Sanchez, E., Sinencio, E., Lau, C., (1992) 'Artificial Neural Networks', *IEEE Press, 1992*

Scarponi, M., (2007) *Including Human Performance in the Dynamic Model of a Sailing Yacht: A Combined Ship Science – Behavioural Science Approach Towards a Winning Yacht-Sailor Combination*. Ph. D thesis. University of Southampton.

Selmic, R., (2000), 'Deadzone compensation in motion control systems using neural networks', IEEE Trans. Autom. Control 45 (4) pp 602–613 2000.

Sharma, S., et al (2003), 'Learning soft computing control strategies in a modular neural network architecture', Engineering Applications of Artificial Intelligence 16 pp 395–405 2003.

Shu-Heng Chen, (2006), *Handbook of Financial Engineering*, Kluwer Academic Publishers, 2006.

Siegelmann, H., (1999), *Neural Networks and Analog Computation*, Berlin: Birkhäuser

Singh, S., (1998), '2D Spiral Pattern Recognition with Possibilistic Measures', *Pattern Recognitions Letters*, 19, pp 141 – 147. 1998.

Strohmeier, D., (1979) 'The Measurement Handicapping System of USYRU', *The Fourth Chesapeake Sailing Symposium.* Chesapeake, 20th January 1979, pp35-45.

Srivaree, C., et al, (2000), 'Estimation of all Terminal Network reliability using an Artificial Neural Network', *Computers & Operations Research*, 29 pp 849 – 868 2000.

Tatano, H., Kaneda, T., Kono, S., (1978) 'Hydrodynamic Analysis on Sailing (2nd Report) Performance Prediction of International Flying Fifteen Class Yacht' *J. Kansai Soc. N.A., Japan, No. 175. December 1979*

Todter, C., et al (1993) 'Stars and Stripes Design Program for the 1992 America's Cup' *The 11th Chesapeake Sailing Yacht Symposium.* Chesapeake 1993

Tomandl, D., (2001), 'A Modified General Regression Neural Network (MGRNN) with new, efficient training algorithms as a robust 'black box'-tool for data analysis', *Neural Networks*, Vol. 14, Issue 8, pp 1023 – 1034, 2001.

Townsend, B., Fenton, P., (1994) 'A Practical Approach to the Reduction of Pseudorange Multipath Errors in a L1 GPS Receiver', *Proceedings of ION GPS – 1994,* Salt Lake City, September 20 – 23, pp 143 – 148

Tzafestas, S., Dalianis, P., Anthopoulos, G., (1996) 'On the Overtraining Phenomenon of Backpropagation of Neural Networks' *Mathematics and Computers in Simulation 40.* 1996 pp 507-521

u-blox 2001 *Reference Document The GPS Dictionary* written by u-blox 2001

US Department of Homeland Security Navigation Centre. Available at: http://www.navcen.uscg.gov/faq/gpsfaq.htm (Accessed: 060223)

Werbos, P., (1974) 'Beyond regression: new tools for prediction and analysis in the behavioural sciences' PhD thesis, Harvard University, 1974.

Widrow, B., (1987), '30 Years of Adaptive Neural Networks: Perceptron, and backpropagation', *Proceedings of the IEEE, Stanford University,* September 1990

WinDesign, Wolfson Unit Software, Available at (http://www.wumtia.soton.ac.uk/brochures/WindesignBrochure.pdf) (Accessed: 080416)

Zhang, K., (2004), 'GNSS – for Sports – Sailing and Rowing Perspectives', *Journal of Global Positioning Systems (2004),* Vol. 3, No. 1-2, pp 280 – 289

Zogg, J., (2002) *u-blox Reference Document GPS Basics* 2002

Appendices

Appendix 1 GPS Board Specification

u-blox AG
Zürcherstrasse68
8800 Thalwil
Switzerland
www.u-blox.com

Phone +41 1722 7444
Fax+41 1722 7447
info@u-blox.com

SAM-LS
GPS Smart Antenna Module

Data Sheet

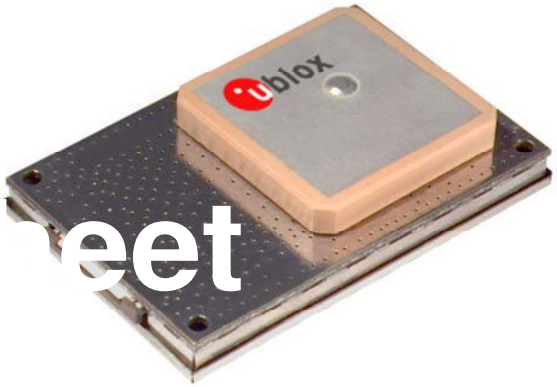

Abstract

This document describes the features and specifications of the SAM-LS Smart Antenna Module, a low power GPS receiver macro-component with integrated patch antenna. Based on the ANTARIS GPS technology, it offers high GPS performance combined with easy and fast systemintegration

your position is our focus

Features

- 16 channel GPS receiver
- 8192 simultaneous time-frequency search bins
- 4Hz position update rate
- ANTARIS Positioning Engine
- ATR0620 Baseband IC with ARM7TDMI inside
- ATR0610 Low noise amplifier IC
- FLASH memory (min. 4 Mbit)
- DGPS and SBAS(WAAS, EGNOS) support
- FixNOW™ power saving mode
- Operating voltage 2.7 to 3.3 V
- Battery supply pin for internal backup memory and real time clock
- Industrial operating temperature range ´0 to 85°C
- Small size
- Size 31.5 x 47 x 9.5 mm
- Weight 23g

your position is our focus

2 Performance Specification

Parameter	Specification			
Receiver Type		L1 frequency,C/A Code, 16-Channels 8192 search bins		
Max Update Rate		4 Hz		
Accuracy (SelectiveAvailability off)	Position	2.5 m CEP [3]	5.0 m SEP [4]	
	Position DGPS/ SBAS	[2] 2.0 m CEP	3.0 m SEP	
Acquisition		[5] FastAcquisition Mode	Normal Mode	High Sensitivity Mode
	Cold Start [6]	34 s	36 s	41 s
	Warm Start	33 s		
	Hot Start	<3.5 s		
Signal Reacquisition		<1 s		
Sensitivity		FastAcquisition Mode	Normal Mode	High Sensitivity Mode
	Acquisition	-132 dBm	-136 dBm	-138 dBm
	Tracking	-141 dBm	-144 dBm	-147 dBm
Dynamics		δ 4 g		
Operational Limits		COCOMrestrictions		

Table 4: Performance Specification

[2] Dependson accuracyof correction data of DGPSor SBASservice

[3] CEP= CircularError Probability: Theradiusof a horizontal circle,centered at the antenna'strue position, containing 50% of the fixes.

[4] SEP= SphericalErrorProbability. Theradiusof the sphere,centered at the true position, contains50% of the fixes.

[5] Thedifferent start-up modeslike cold, warm and hot start are described in the System Integration Manual [1]

[6] Measured with good visibility and -125 dBmsignalstrength

During the data collection sessions the performance of the GPS was continually monitored in order to produce the best results possible. This was accomplished using a program from u-blox who are also the manufactures of the GPS. A screenshot of the performance monitoring in action can be seen below in Figure 72.

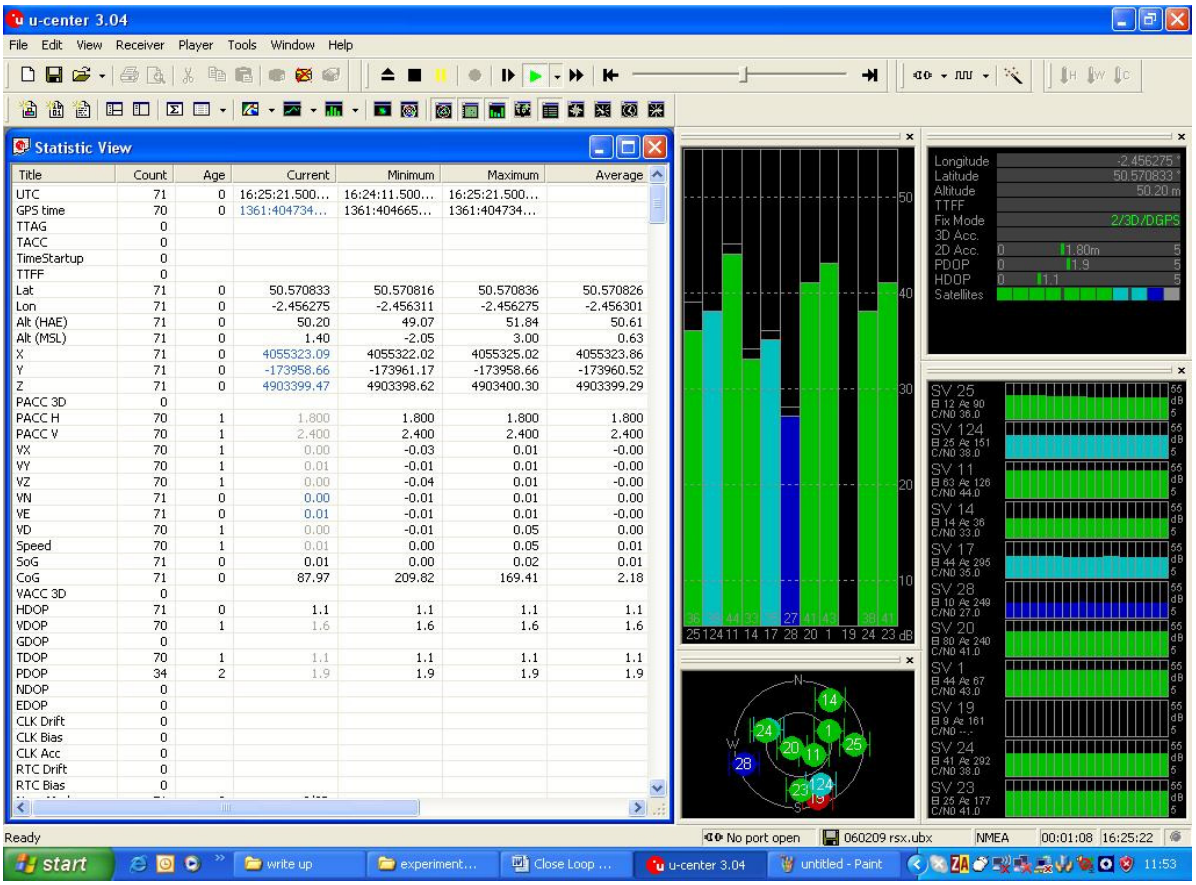

Figure 72 - Showing the performance of the GPS with the u-blox program

Appendix 2 49er Optimisations

Table 10 - The Olympic squad tuning guide for the 49er

TWS (knots)	Shroud (turns)	Cap (turns)	Lower (turns)	Tack/Jib (mm)	Board (inches)	Outhaul (inches)	Notes
0-7	-1	14.5	0	+ 9-14	Down	1.5	
6-9	0	14.5	0	+ 7-10	Down	1.5-2	
8-12	+5	14.5	0	+2-7	Down	2-2.5	
11-15	9-10	14.5	0.5	+0-4	Down	2.5	
14-17	14	14.5	0.5	-0-4	Down	2.5	
16-19	16-17	14.5	0.5	-4-10	Up 2.5	2.5	
19+	35	14.5-13.5	0.5-1	-10-18	Up 5-10	2-1.5	

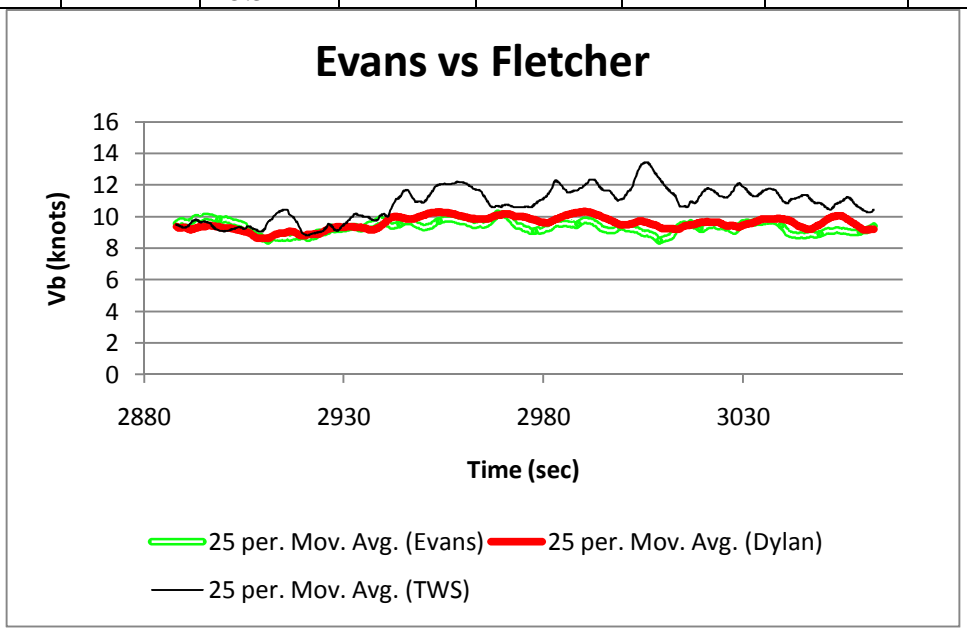

Figure 73 - More comparisons of performance with ANN predictions, TWS is included in this plot

Table 11 - Showing the optimisation process of the context unit

Context	MSE	NMSE	r	% Error	AIC	MDC
0.1	0.07	3.71	0.54	20.76	4374.7	7532.7
0.3	0.0698	3.684	0.55	20.63	4370.1	7528.9
0.5	0.0693	3.672	0.57	20.61	4369.4	7527.4
0.7	0.0615	3.23	0.57	19.05	4305.9	7463.9
0.8	0.056	2.97	0.58	18.3	4264.1	7422.4
0.9	0.078	4.13	0.56	22.17	4428.5	7586.5

Table 12 - Alternate ANN methods

ANN type	MSE	NMSE	r	% Error	AIC	MDC
TWS						
V_b	0.269	2.63	0.42	17.31	-173.6	12.33

Appendix 3 Residual Resistance and ANN Inputs

Table 13 - Showing the input used to generate the pure ANN polar, note the fixed distance between the weather and target boats in the right hand column

TWS	TWA	dist
2	30	0.35
2	35	0.35
2	40	0.35
2	45	0.35
2	50	0.35
2	55	0.35
2	60	0.35
2	65	0.35
2	70	0.35
2	75	0.35
2	80	0.35
2	85	0.35
2	90	0.35
2	95	0.35
2	100	0.35
2	105	0.35
2	110	0.35
2	115	0.35
2	120	0.35
2	125	0.35
2	130	0.35
2	135	0.35
2	140	0.35
2	145	0.35
2	150	0.35
2	155	0.35
2	160	0.35
2	165	0.35
2	170	0.35
2	175	0.35
2	180	0.35

Between Froude numbers of 0.125 & 0.45

Froude No	a0	a1	a2	a3	a4	a5	a6	a7	a8	a9	Rr
0											
0.125	-6.735654	38.36831	-0.00819	0.055234	-1.99724	-38.8608	0.956591	-0.00217	0.272895	-0.01752	
0.15	-0.38287	38.1729	0.007243	0.026644	-5.29533	-39.5503	1.219563	0.000052	0.824568	-0.04784	
0.175	-1.503526	24.40803	0.0122	0.067221	-2.44858	-31.9137	2.216098	0.000074	0.244345	-0.01589	
0.2	11.29218	-14.51947	0.047182	0.085176	-2.67302	-11.4182	5.654065	0.007021	-0.09493	0.006325	
0.225	22.17867	-49.16784	0.085998	0.150725	-2.87868	7.167049	8.600272	0.012981	-0.32709	0.018271	
0.25	25.90867	-74.75668	0.153521	0.188568	-0.88947	24.12137	10.48516	0.025348	-0.85494	0.048449	
0.275	40.97559	-114.2855	0.207226	0.250827	-3.07266	53.0157	13.02177	0.035934	-0.71546	0.039874	
0.3	45.83759	-184.7646	0.357031	0.338343	3.871658	132.2568	10.86054	0.066809	-1.71922	0.095977	
0.325	89.20382	-393.0127	0.617466	0.460472	11.54327	331.1197	8.598136	0.104073	-2.8152	0.15596	
0.35	212.6788	-801.7908	1.087307	0.538938	10.80273	667.6445	12.39815	0.166473	-3.02613	0.165055	
0.375	336.2354	-1085.134	1.644191	0.532702	-1.22417	831.1445	26.18321	0.238795	-2.45047	0.139154	
0.4	566.5476	-1609.632	2.01609	0.265722	-29.2441	1154.091	51.46175	0.288046	-0.17835	0.018446	
0.425	743.4107	-1708.263	2.435809	0.013553	-81.1619	937.4014	115.6006	0.365071	1.838967	-0.06202	
0.45	1200.62	-2751.715	3.208577	0.25492	-132.042	1489.269	196.3406	0.528225	1.379102	0.013577	

Between Froude numbers of 0.475 & 0.7

	c0	c1	c2	c3	c4	c5	Rr
0.475	180.1004	-31.50257	-7.45114	2.195042	2.689623	0.00648	
0.5	243.9994	-44.52551	-11.1546	2.179046	3.857403	0.009676	
0.525	282.9873	-51.51953	-12.9731	2.274505	4.343662	0.011066	
0.55	313.4109	-56.58257	-14.4198	2.326117	4.690432	0.012147	
0.575	337.0038	-59.19029	-16.0698	2.419156	4.766793	0.014147	
0.6	356.4572	-62.85395	-16.8511	2.437056	5.078768	0.01498	
0.625	324.7357	-51.31252	-15.346	2.334146	3.855368	0.013695	
0.65	301.1268	-39.79631	-15.023	2.059657	2.545676	0.013588	
0.675	292.0571	-31.85303	-15.5855	1.847926	1.569917	0.014014	
0.7	284.4641	-25.14558	-16.1542	1.703981	0.817912	0.014575	

Appendix 4 VPP Calculations

In this appendix the methods and techniques used in the author's VPP shall be examined alongside several screen shots of the program. At the beginning of *chapter 5.1* the forces that needed balancing were described in turn. In this section we shall examine the methods used to produce each of these forces in turn beginning with a few other essential equations before moving onto the calculation of the first of these which is R_{total}.

One of the most essential components to determining the characteristics of a yacht is the water plane area (A_w) which is calculated through the usage of Equation (41) below.

$$A_w = B_{wl} \cdot L_{wl}\left[1.313 \cdot C_p + 0.0371\left(\frac{L_{wl}}{\nabla_c^{1/3}}\right) - 0.0857 \cdot C_p\left(\frac{L_{wl}}{\nabla_c^{1/3}}\right)\right] \quad (41)$$

Where

B_{wl} = beam of the yacht at the waterline

L_{wl} = waterline length

C_p = prismatic coefficient

∇_c = volume of displacement of the hull

One of the other important equations that is used in the VPP is the midship coefficient (C_m) which can be summarised by Equation (42) below.

$$C_m = \frac{\nabla_c}{(L_{wl} \cdot B_{wl} \cdot T_c \cdot C_p)} \quad (42)$$

Where T_c is the draft of the hull of the yacht.

The third and final preliminary equation which the midship coefficient feeds into is the calculation of the wetted surface area (S_c). This is a particularly important equation in terms of resistance calculation and can be seen below in Equation (43).

$$S_c = \left[1.97 + 0.171\frac{B_{wl}}{T_c}\right] \cdot \left[\frac{0.65}{C_m}\right]^{1/3} \cdot \left[\nabla_c \cdot L_{wl}\right]^{1/2} \quad (43)$$

Hydrodynamics

Resistance

R_{total} is a combination of multiple different components of resistance which can be summarised in the format of Equation (44) below.

$$R_{total} = R_f + R_r + R_i + R_h \tag{44}$$

Where

R_f = The frictional resistance of the hull and appendages.

R_r = The residual resistance of the hull.

R_i = Induced resistance

R_h = Increased resistance due to heel.

To begin with, the frictional resistance shall be calculated but in order to do so it requires the Reynolds number (Rn) of all the hydrodynamic components including appendages. This is calculated using Equation (45) which can be seen below.

$$Rn = \frac{V \cdot L}{\upsilon} \tag{45}$$

Where

V = the velocity

υ = the kinematic viscosity

L = The average length of the chord for the rudder, keel, bulb and $0.7 \times L_{wl}$ for the hull.

Then in turn the coefficient of friction is calculated for each of the components using Equation (46) below.

$$C_f = \frac{0.075}{(\log(Rn) - 2)^2} \tag{46}$$

If there is a bulb which in most of the Olympic classes there is not the following equation is used to produce the friction coefficient for it.

$$(1 + k) = \left(1 + 1.5\left(\frac{d}{l}\right)^{2/3} + 7\left(\frac{d}{l}\right)^{3}\right) \tag{47}$$

The frictional resistance can now be finally found by multiplying each of the previously calculated coefficients by its respective area. These are then added and the total is multiplied by the stagnation pressure which varies based on water density as seen below.

$$R_f = q \cdot (S_c \cdot C_{fc} + S_k \cdot C_{fk} + S_r \cdot C_{fr} + S_b \cdot C_{fb}) \quad (48)$$

This completes the first of the four segments which make up the total hydrodynamic resistance of the yacht. In the next section the residual resistance shall be examined. The VPP is able to calculate the residual resistance of the yacht at various different Froude numbers. It is able to do this through the use of two large tables produced by Gerritsma et al in 1993 which contains all the coefficients of residual resistance. In the VPP program it is possible to select the correct coefficient through the use of the lookup function in Excel. Again to find values in between the data points the linear interpolation method is used. The first table is for Froude numbers between 0.125 and 0.45. The second covers the range from 0.475 to 0.7. This table can be seen in the previous chapter in Appendix 4. There are two different equations for calculating the residual resistance, one for each table. The equation for the lower table can be seen below in Equation (49) and the higher in Equation (50).

$$R_r = \Delta_c \left[a_0 + a_1 \cdot C_p + a_2 \cdot LCB + a_3 \left(\frac{B_{wl}}{T_c}\right) + a_4 \left(\frac{L_{wl}}{\nabla_c^{1/3}}\right) + a_5 \cdot C_p^2 + a_6 \cdot C_p \left(\frac{L_{wl}}{\nabla_c^{1/3}}\right) + a_7 \cdot \right.$$

$$\left. LCB2 + a8 Lwl \nabla c132 + a9 Lwl \nabla c133 / 1000 \right]$$

(49)

$$R_r = \Delta_c \left[c_0 + c_1 \left(\frac{L_{wl}}{B_{wl}}\right) + c_2 \left(\frac{A_w}{\nabla_c^{2/3}}\right) + c_3 \cdot LCB + c_4 \left(\frac{L_{wl}}{B_{wl}}\right)^2 + c_5 \left(\frac{L_{wl}}{B_{wl}}\right) \left(\frac{A_w}{\nabla_c^{2/3}}\right)^3 \right] / 1000 \quad (50)$$

These two equations complete the section on residuary resistance, the next component of resistance is induced resistance. The calculation of this part is more straightforward than the previous segments, it is however as mentioned in the literature review a simplification of the process. The first step is to calculate the effective draft (T_E) which uses several coefficients which are based on the heel of the yacht. These are shown below first in Equations (51 to 53).

$$A_1 = 4.8080 + 0.0370 \cdot \phi - 4.983 \cdot \phi^3 \quad (51)$$

$$A_2 = -4.179 - 0.809 \cdot \phi + 9.670 \cdot \phi^3 \quad (52)$$

$$A_3 = 0.055 - 0.0339 \cdot \phi - 0.0522 \cdot \phi^3 \quad (53)$$

These then feed into Equation (54) which calculates the effective draft.

$$T_E = T\left[A_1\left(\frac{T_c}{T}\right) + A_2\left(\frac{T_c}{T}\right)^2 + A_3\left(\frac{B_{wl}}{T_c}\right)\right] \quad (54)$$

The final step is to substitute the result from Equation (54) into Equation (55) to calculate the induced resistance of the yacht.

$$R_i = \frac{F_H^2}{\pi \cdot T_E^2 \cdot q} \quad (55)$$

The final segment of the resistance calculation is the resistance due to heel. In the scope of this project most of the Olympic classes will sail at a very small angle of heel, however some classes such as the Star sail at a certain angle of heel constantly upwind to minimise the wetted area. The amount of heel allowed was adjusted on a class by class basis. The method of calculation is relatively simple with the coefficient of heel being calculated first before substituting it into the final equation. This method can be seen below in the two equations respectively.

$$C_H = \frac{6.747\left(\frac{T_c}{T}\right) + 2.517\left(\frac{B_{wl}}{T_c}\right) + 3.710\left(\frac{B_{wl}}{T_c}\right)\cdot\left(\frac{T_c}{T}\right)}{1000} \quad (56)$$

$$R_H = q \cdot S_c \cdot C_H \cdot Fn^2 \cdot \phi \quad (57)$$

Equation (57) concludes the calculation of resistance which is probably one of the more complex parts of the VPP. In the next section the stability of the yacht shall be focussed on with showing the method used for determining the righting moment.

Righting Moment

To calculate the righting moment two equations have to be solved and are called the dynamic increment and the GZ. These two equations (58 and 59) feed into to the righting moment equation; the dynamic increment shall be examined first.

$$D_2 = -0.0406 + 0.0109\frac{B_{wl}}{T_c} - 0.00105\left(\frac{B_{wl}}{T_c}\right)^2 \quad (58)$$

$$D_3 = 0.0636 - 0.0196\frac{B_{wl}}{T_c} \quad (59)$$

$$MN \cdot sin\phi = (D_2 \cdot \phi \cdot Fn + D_3 \cdot \phi^2) \quad (60)$$

Now that the equation for MN has been calculated it feeds into the GZ equation which in turn feeds into the final righting moment calculation along with the crew weight righting moment (M_{rc}). These three equations can be seen below.

$$GZ = (GM + MN) \cdot sin\phi \tag{61}$$

$$M_{rc} = 70 \cdot MVBLCR \cdot cos\phi \cdot CRARM \tag{62}$$

MVBLCR is number of crew that are able to move in the yacht and in this project are hiking or trapezing over the side. CRARM is the distance between the centreline of the yacht and the centre of gravity of the crew.

$$M_{right} = (GZ \cdot \Delta \cdot g) + M_{rc} \tag{63}$$

Side Force

The next and final section of the hydrodynamic section is the side force acting on the yacht. This again uses a look up table which was derived by Gerritsma et al in 1993. This table is present in Excel and linear interpolation is used between the data points and can be seen below. The lookup function is also used for this table, in this case the heel angle is in radians.

Table 14 - Gerritsma side force calculation method

Φ	**b1**	**b2**	**b3**	**b4**	**Lift Slope**
0	2.025	9.551	0.631	-6.575	0.335807
0.17453293	1.989	6.729	0.494	-4.745	0.324726
0.34906585	1.98	0.633	0.194	-0.792	0.308166
0.52359878	1.762	-4.957	-0.087	2.766	0.259373

The columns b1 to b4 are all coefficients which are used in Equation (64) to calculate the lift slope. This can be seen in the last column.

$$F_{side} = \frac{\alpha \cdot q \cdot S_c}{cos\phi}\left[b_1\left(\frac{T^2}{S_c}\right) + b_2\left(\frac{T^2}{S_c}\right)^2 + b_3\left(\frac{T_c}{T}\right) + b_4\left(\frac{T_c}{T}\right)\left(\frac{T^2}{S_c}\right)\right] \tag{64}$$

Where α is leeway

In the next section the methods for calculating the aerodynamic forces that the yacht experiences shall be examined in detail. One part of the calculations which uses the aspect ratios shall be shown in its original form before modification from the ANN, the modified version can be found in the main body of the text.

Aerodynamics

The aerodynamic calculations are again an approximation from a variety of sources and similar to the techniques used by Martin (2001). In this section the three remaining forces shall be calculated which completes the equations that require balancing for the VPP. To begin with the centre of effort and aspect ratios are calculated for the sails which enables coefficients for lift and drag to be derived. This process uses a generic lift and drag coefficient table from Claughton (1999), which is what is modified by the ANN in the main text. After the windage of the hull and rig has been calculated the results are combined to produce F_{drive} and F_{heel}. From these two forces the final force of M_{heel} can be calculated.

Centre of Effort Calculation

Initially the mainsail and jib areas are calculated based on a variety of inputs such as J and BAD. This list of inputs enables the areas of the individual sails to be calculated before finding the CoE of each of the sails. The final stage is to combine the two and produce a CoE for the whole boat. The list of inputs can be seen below.

- BAD = Boom above deck measurement
- E = Foot of the mainsail length measurement
- P = Maximum hoist of the mainsail above the BAD measurement
- I = The maximum hoist of the genoa.
- J = The distance between the bow and the mast
- LPG = The shortest distance between the clew of the jib and the forestay
- EHM = The height of the mast above the deck
- EMDC = The average diameter of the mast section

The CoE formula can be seen below in Equation (65) with the various inputs shown below.

$$CE = \frac{A_m \cdot CE_m + A_j \cdot CE_j}{A_m + A_j} \quad (65)$$

Where

$$A_m = {}^1\!/_2\, PE$$

$$A_j = {}^1\!/_2\, LPG(I^2 + J^2)^{1/2}$$

$$CE_m = 0.39P + BAD$$

$$CE_j = 0.39I$$

Aspect Ratio Calculation

Another important feature that needs calculating is the aspect ratio. For this the method derived by Claughton in 1999 shall be used. This equation can be seen below including the lift and drag from the nominal areas (A_n) calculations that feed into it.

$$A_f = 0.5JI$$

$$A_n = A_f + A_m$$

$$AR = \frac{(rhf(EHM + F_{avg}))^2}{A_n} \quad (66)$$

Where

rhf = Rig height factor which varies between 1.1 and 1 dependent on TWA.

F_{avg} = The average freeboard of the yacht.

Wind Speed Correction

In the next section the TWS shall be corrected for the CoE of the yacht. This technique was first described by Milgram in 1993 in Equation (67) below.

$$V_t(z) = V_t(10)[\ln(z) - \ln(z_o)]/(\ln(10) - \ln(z_0)) \quad (67)$$

Where

$V_t(10)$ = The TWS at ten metres above the water. This is considered to be the maximum velocity of the wind at this height. All of the Olympic classes with have a CoE of considerably less than this.

z_o = The lowest point of the measurement which is considered to be the surface of the water.

Apparent Wind Speed Calculation

The next part is to calculate the effective apparent wind speed (U_a), shown in Equation (68), that is experienced by the yacht. This is in terms to the yacht's course and therefore can also be used to calculate the effective apparent wind angle (β_a) as shown in Equation (69). Heel is also taken into account for this calculation and the method described by Larsson in 1994 shall be used. Figure 74 below shows the velocity triangle that is described by Larsson.

$$U_a = [(V_t(z) sin\beta_t cos\phi)^2 + (V + V_t(z) \cdot cos\beta_t)^2]^{1/2} \quad (68)$$

$$\beta_a = \frac{ar\cos(V + V_t(z) \cdot cos\beta_t)}{U_a} \quad (69)$$

Where

$V_t(z)$ = The TWS at the height of z.

β_t = The TWD with respect to the course of the yacht.

V = The velocity of the yacht.

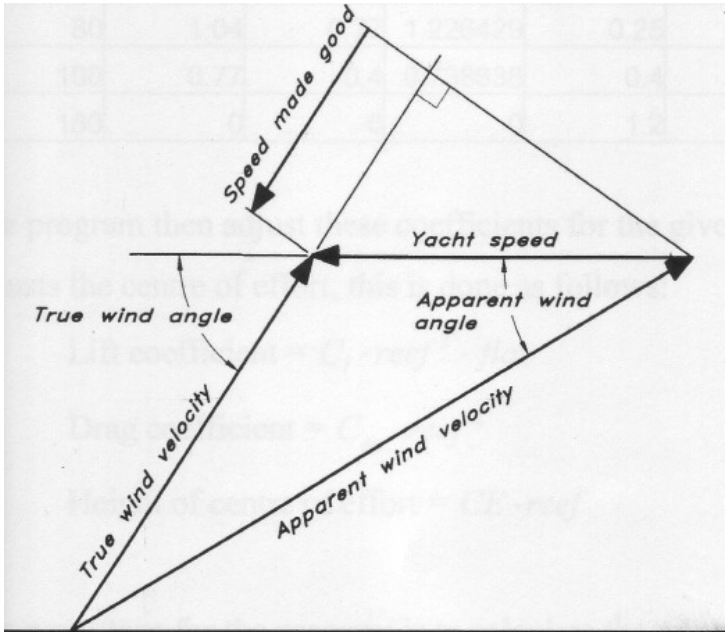

Figure 74 - Showing the different velocities experienced by a yacht (Larsson, 1994)

Lift and Drag Coefficients

With this diagram and the previous two formulae it is now possible to calculate the lift and drag coefficients of the main and the jib using the coefficients described by Claughton. These can be seen in the table below before the modification from the ANN.

Table 15 - Original lift and drag coefficients that were altered

	Lift Coefficients			Drag Coefficients		
AWA	Main	Jib	Combined	Main	Jib	Combined
0	0	0	0	0.04	0.03	0.047553
20	1.6	1.45	2.1511			
27	1.67	1.48	2.211911	0.02	0.02	0.028756
50	1.41	1.42	2.037255	0.08	0.25	0.28432
80	1.04	0.77	1.226429	0.25	0.57	0.678125
100	0.77	0.4	0.738638	0.4	0.72	0.893794
180	0	0	0	1.2	0.9	1.426601

Between the points interpolation is used for the missing TWAs. The coefficients of lift and drag can be calculated using the following two formulae shown in Equations (70 and 71) respectively.

$$C_l = \frac{(C_{lm} \cdot A_m + C_{ij} \cdot A_j)}{A_n} \tag{70}$$

$$C_{dp} = \frac{(C_{dpm} \cdot A_m + C_{djp} \cdot A_j)}{A_n} \quad (71)$$

Flattener and Reef

The VPP also has to make other adjustments for the lift and drag in order to keep the model balanced in stronger winds. It does this through the use of the flatner and the reefing features in solver. When a reef is used, the CoE changes and the VPP is able to recalculate the new position. The three following equations, show how each of the coefficients are calculated and also the change of the CoE.

Lift coefficient = $C_l \cdot reef^2 \cdot flat$

Drag coefficient = $C_{dp} \cdot reef^2$

New CoE = $CE \cdot reef$

The last major segment is the calculation of the drag coefficient which is compromised of several pieces. In the next section the effects of windage on the hull and the rig shall be examined. Below is Equation (72) showing the induced drag coefficient (C_{di}), the AR is the same as was calculated in this chapter.

$$C_{di} = C_l^2 \left(\frac{1}{(\pi \cdot AR)} + 0.005\right) \quad (72)$$

Windage Calculation

Equation (73) below shows the formula as described by Claughton for determining the windage of the rig and the hull.

$$C_{do} = \frac{1.13\left((B \cdot F_{avg} \cdot Q_{rat}) + (EHM \cdot EMDC)\right)}{A_n} \quad (73)$$

Where

B = the beam of the hull

$$Q_{rat} = \frac{U_h^2}{U_a^2}$$

C_{do} is the final part of the equation enabling the complete drag coefficient (C_d) to be calculated. C_{do} is substituted into the equation with the other components and is shown by Equation (74) below.

$$C_d = C_{dp} + C_{di} + C_{do} \tag{74}$$

Lift and Drag Calculation

A complete value of lift and drag with respect to the sails can now be calculated using the following two formulae shown in Equations (75 and 76) respectively.

$$Lift = C_l \, {}^1\!/_2 \, \rho_a \cdot U_a^2 \cdot A_n \tag{75}$$

$$Drag = C_d \, {}^1\!/_2 \, \rho_a \cdot U_a^2 \cdot A_n \tag{76}$$

Where

ρ_a = The density of air which is set at 1.225 kg/m^3

Drive and Heeling Force

It is now possible to calculate the driving and the heeling force that is experienced by the yacht with the two simple equations shown below.

$$F_{drive} = Lsin\beta_\alpha - Dcos\beta_\alpha \tag{77}$$

$$F_{heel} = Lcos\beta_\alpha + Dcos\beta_\alpha \tag{78}$$

As mentioned near the start of the chapter, with the heeling force it is now possible to calculate the heeling moment (M_{heel}). This is shown below in Equation (79) and is the last calculation needed for the VPP. The distance of lateral resistance to the waterline (h) calculation method is also shown below which is required for the final equation.

Moment of Heel

$$M_{heel} = F_{heel} \cdot (CE + F_{avg} + h) \tag{79}$$

$$h = T\left(0.414 - 0.165\left(\frac{T_c}{T}\right)\right) \tag{80}$$

With the M_{heel} value calculated the VPP is now able to balance all of the major forces with the aim of maximising the speed at the given TWA. One of the screenshots from the output from the VPP can be seen on the next page. It is from the Star without the ANN correction. A screenshot showing the Excel spreadsheet that was used with Solver displayed can also be seen on the next page in Figure 75.

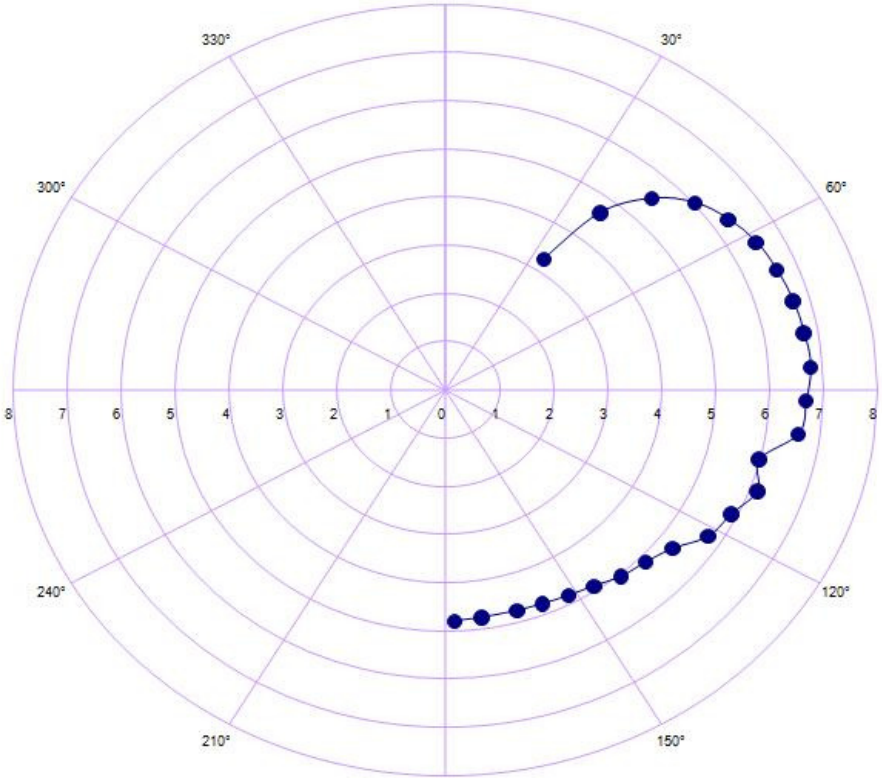

Figure 75 - Star polar in 10 knots of wind

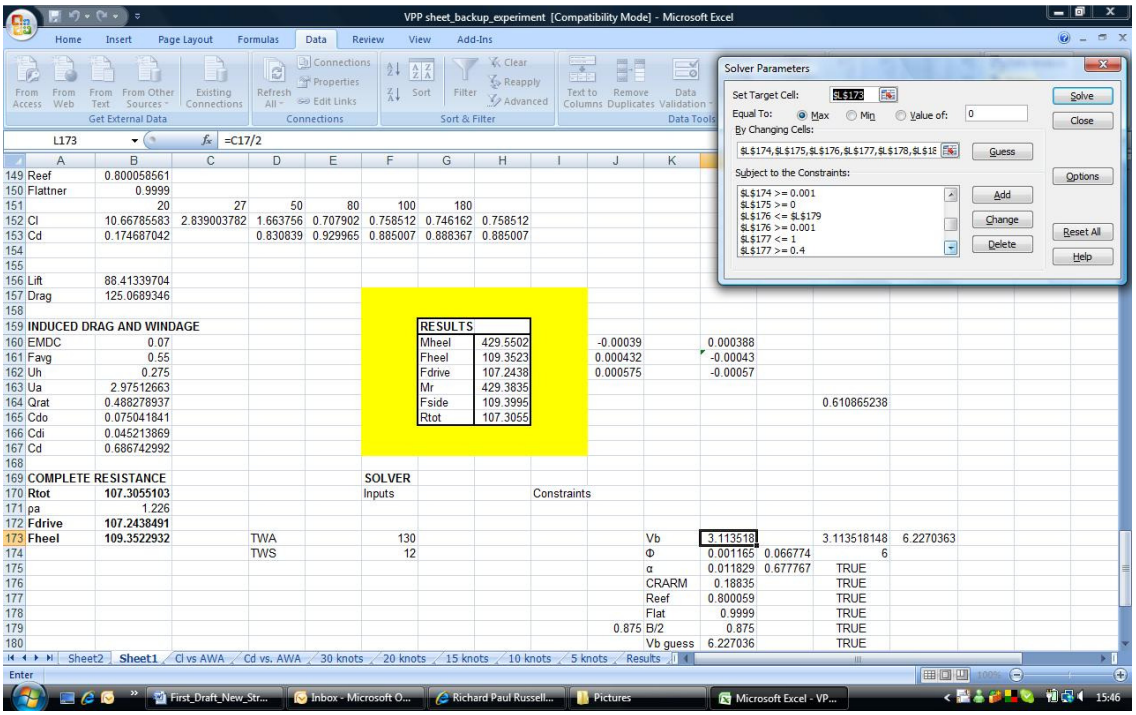

Figure 76 - A screenshot from the VPP program with solver in the top right hand corner

Appendix 5 Image Processing

Images from the initial still picture segmentation process. Figure 77 is the desired output for this process.

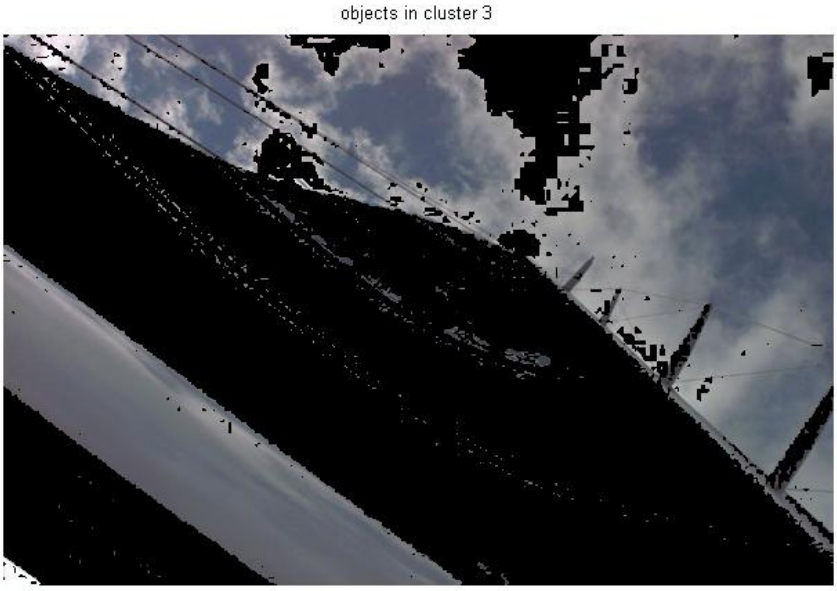

Figure 77 - A segmented image

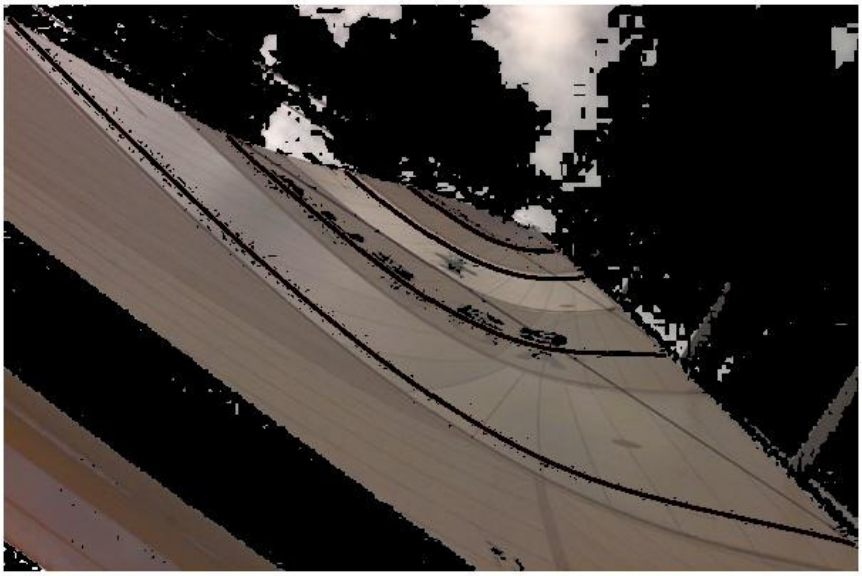

Figure 78 - A segmented image

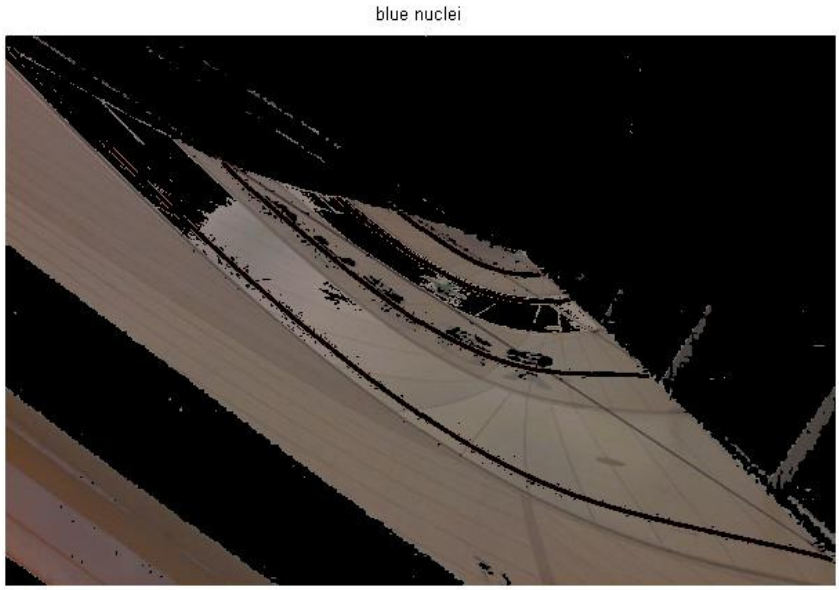

Figure 79 - A Segmented image

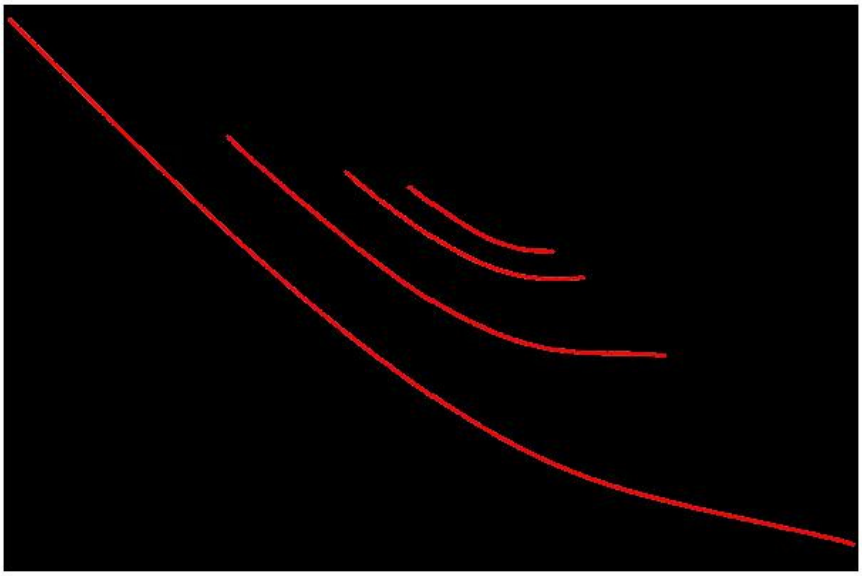

Figure 80 - A segmented image that is used for further analysis

In this section the segmented images from the first demonstration can be seen. Upon viewing these images it is clear that the quality of the image acquisition system was not sufficient. It is so poor that in Figure 81 the analysis of the image is not possible.

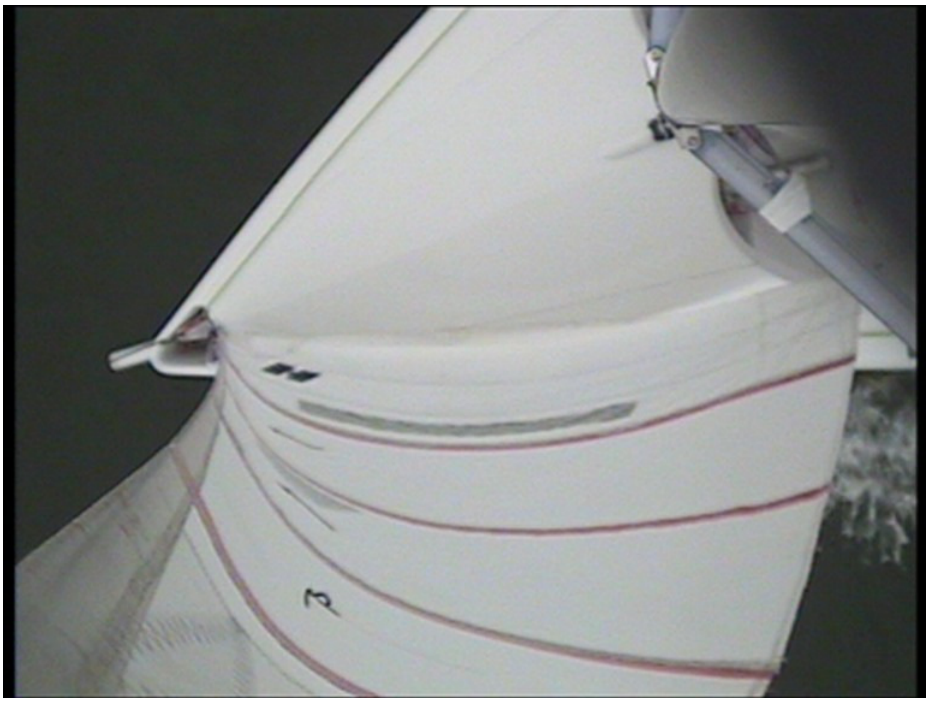

Figure 81 - The raw image captured from the first demonstration. The washed out colours show the poor quality of the captured image with the red stripes considerably faded.

Figure 82 - Cluster image of a segment from the first RS 400 test

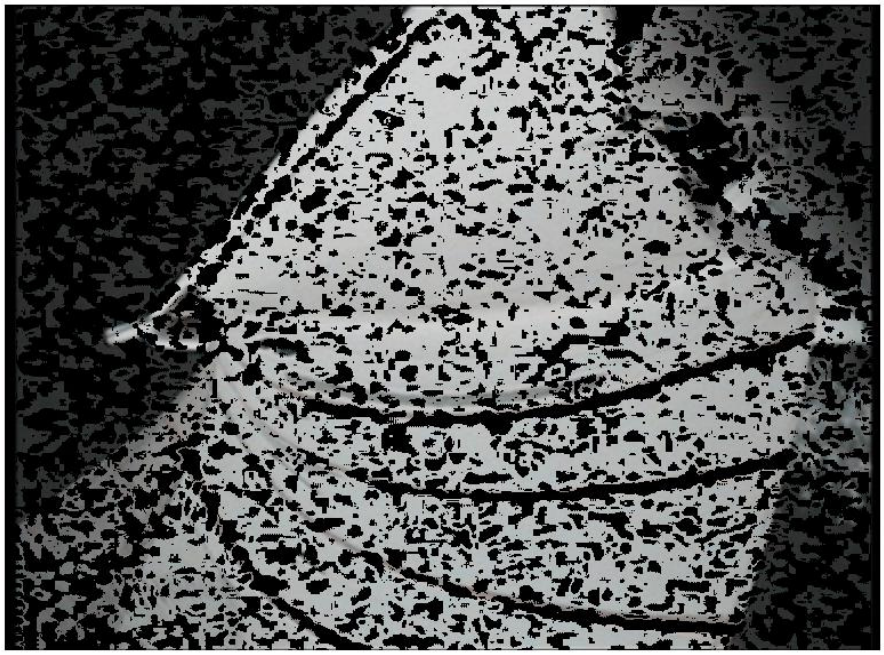

Figure 83 - Another segmented image from the first demonstration

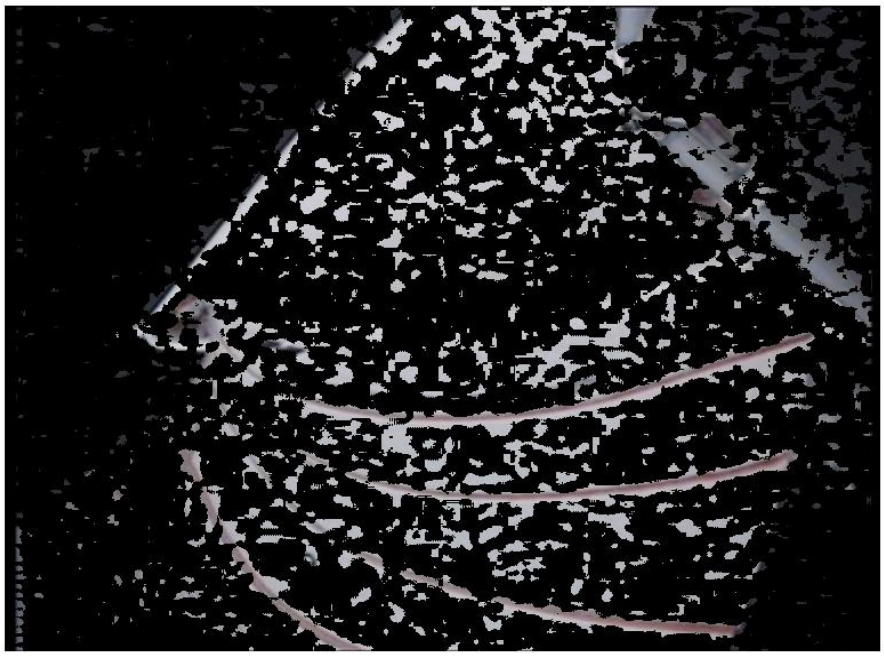

Figure 84 - The segmented image which was meant to show only the stripes

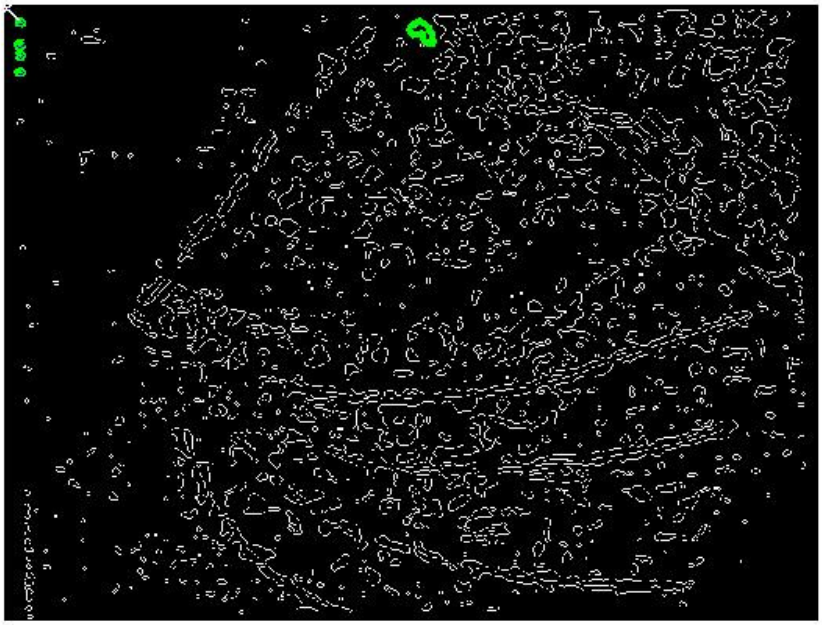

Figure 85 - Failed draft stripe analysis

The next three images are the segmented images from the second test conducted at First Site. This demonstration was deemed to be a success even though the bottom battens were hidden.

Figure 86 - From the second test at First Site

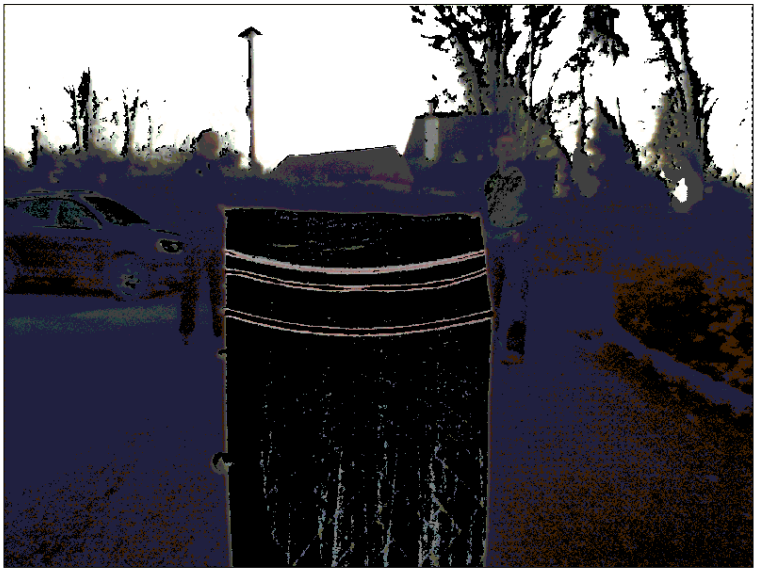

Figure 87 - A segmented image from the second test

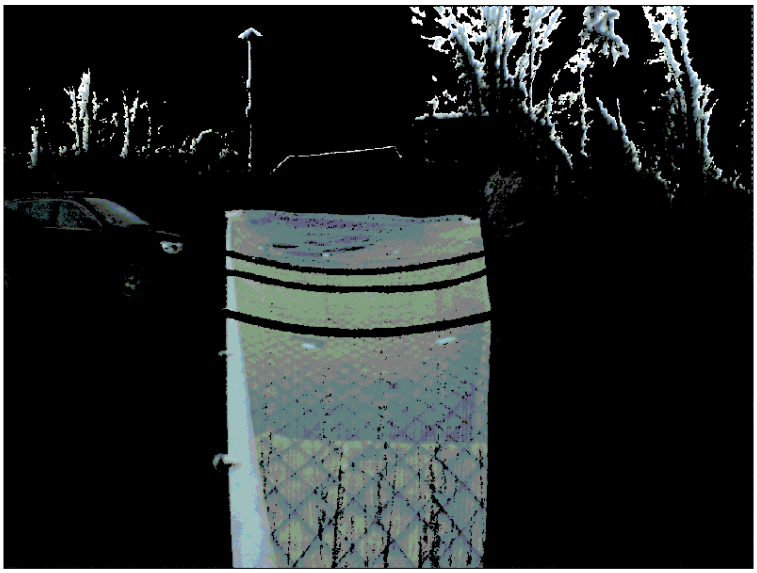

Figure 88 - The third segmented image from the test

The next three images are from the final demonstration using the DogCam hardware and a modified version of the author's software. The first is the original image and the second two are segmented images from the program.

Figure 89 - The raw input image from the camera demonstration with time stamp

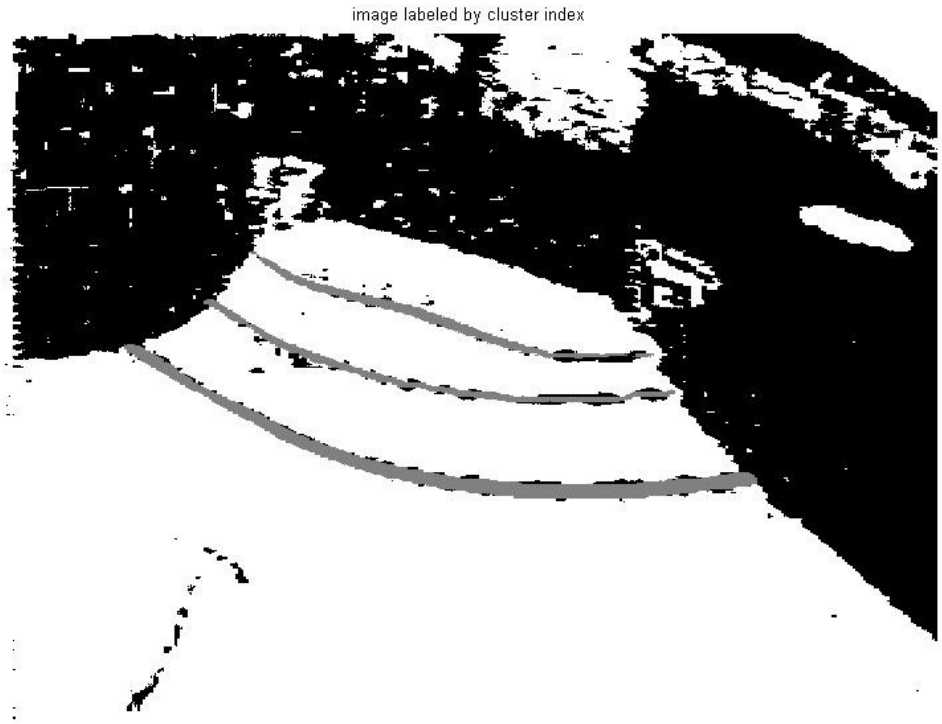

Figure 90 - The first cluster

Figure 91 - The second segmented image

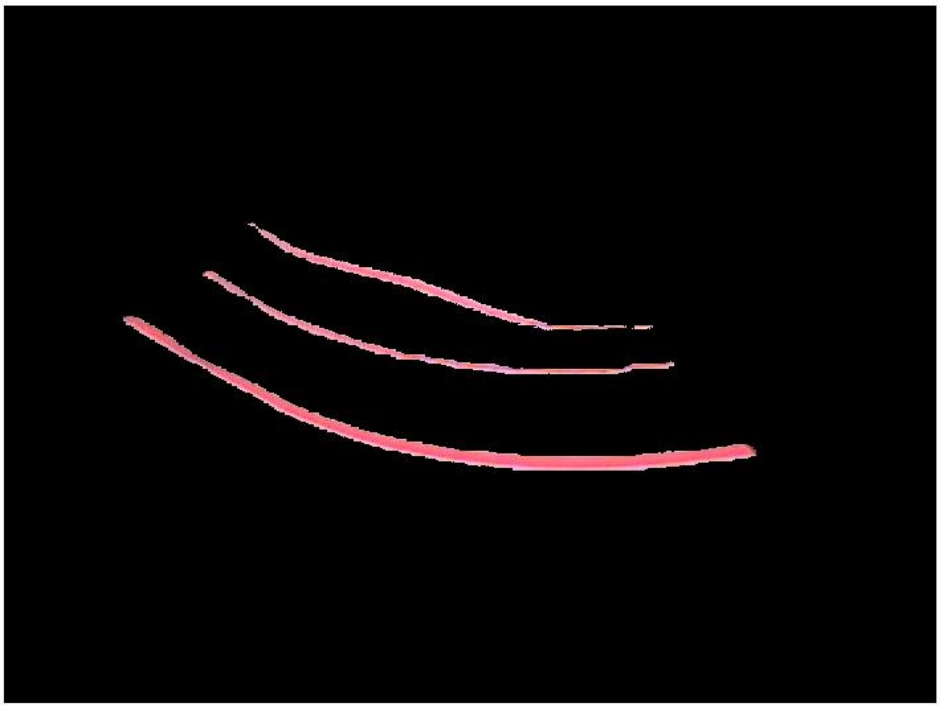

Figure 92 - The draft stripes isolated as one of the outputs

Appendix 6 Additional Polar Diagrams

In this section the remaining polars from the author's VPP shall be shown for different TWS. The TWS for these shall range from 5 to 20 knots missing out the 10 knots previously shown in *chapter five*.

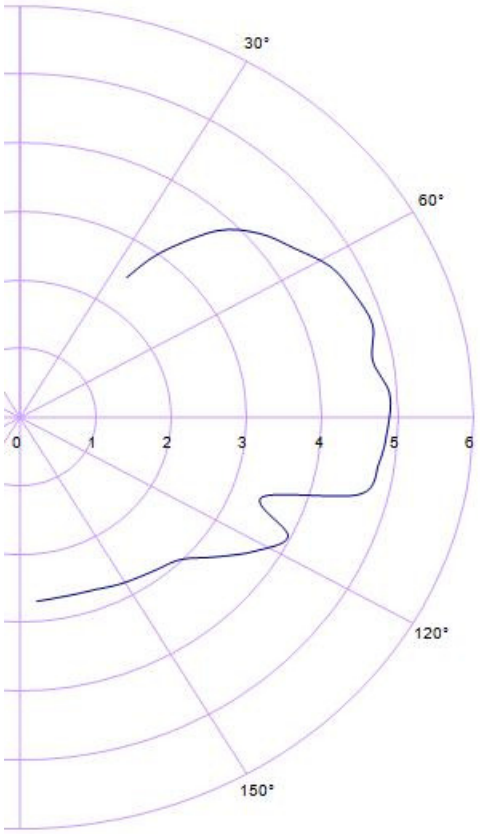

Figure 93 - 5 knots Star Polar

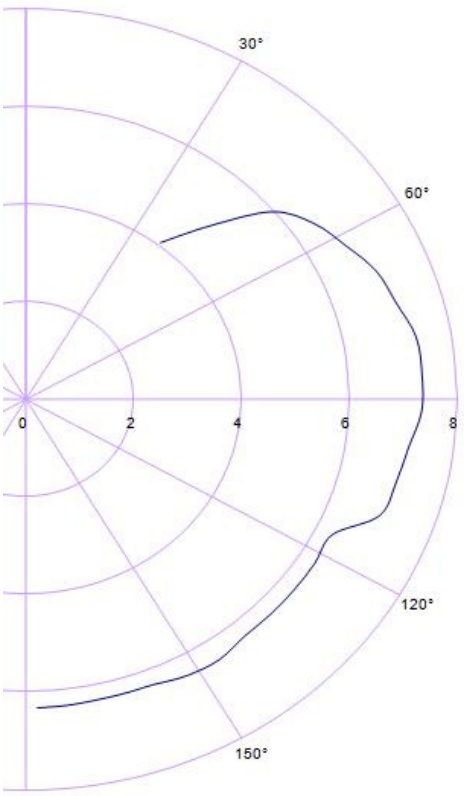

Figure 94 - 15 knots Star Polar

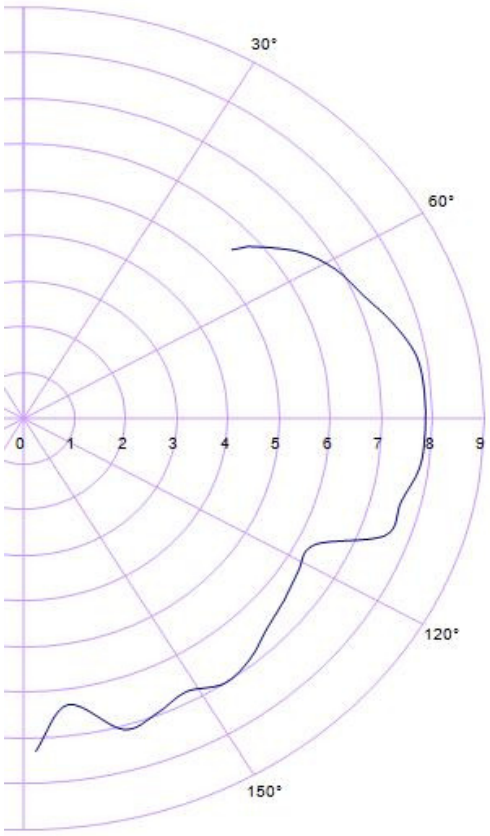

Figure 95 - 20 knots Star Polar

In this section a couple examples of the other polars that were derived and corrected by the VPP and the ANN can be seen. These are from the two other classes with sufficient data which are the Star and the Tornado.

Tornado Polar Diagram

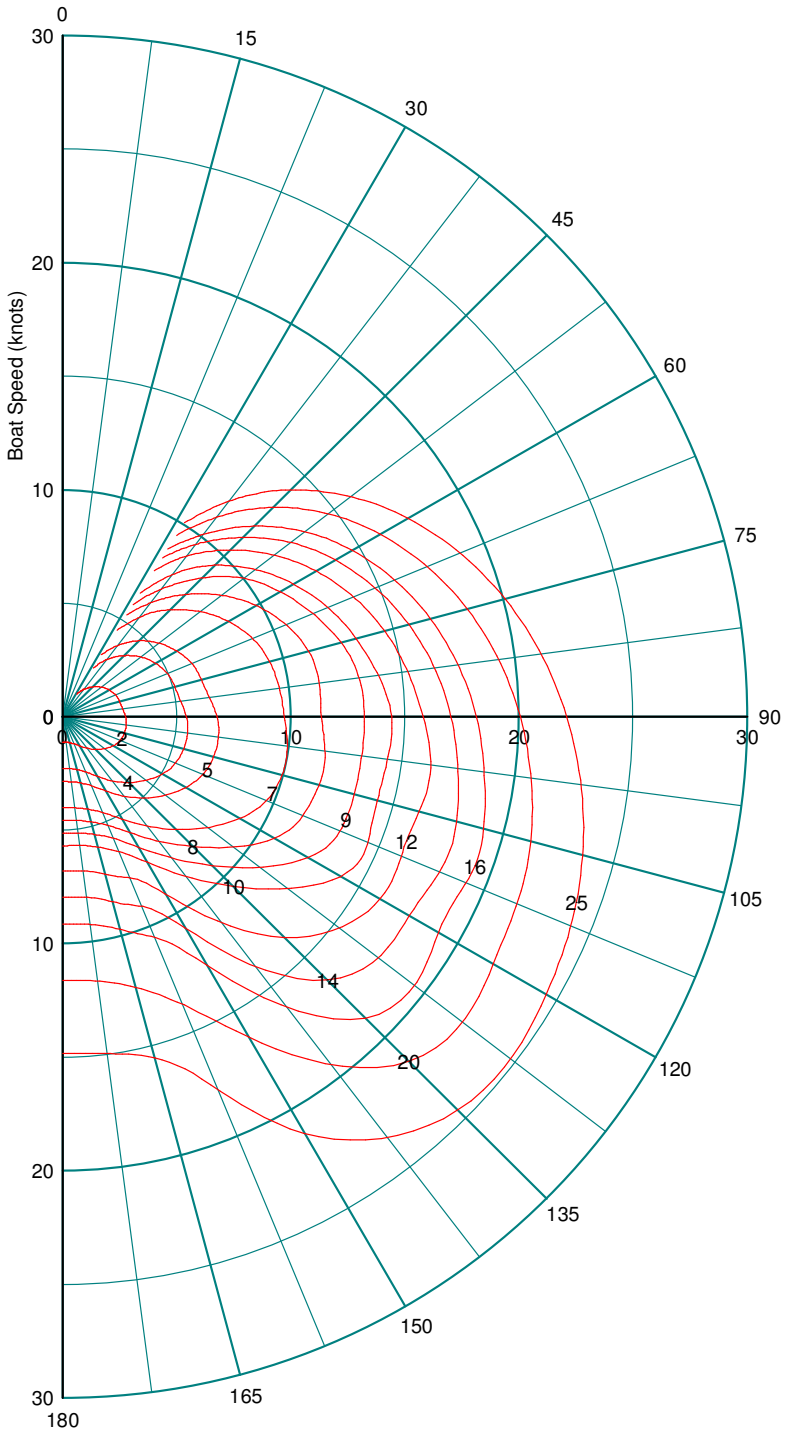

Figure 96 - Tornado Polar Diagram

Star Polar Diagram

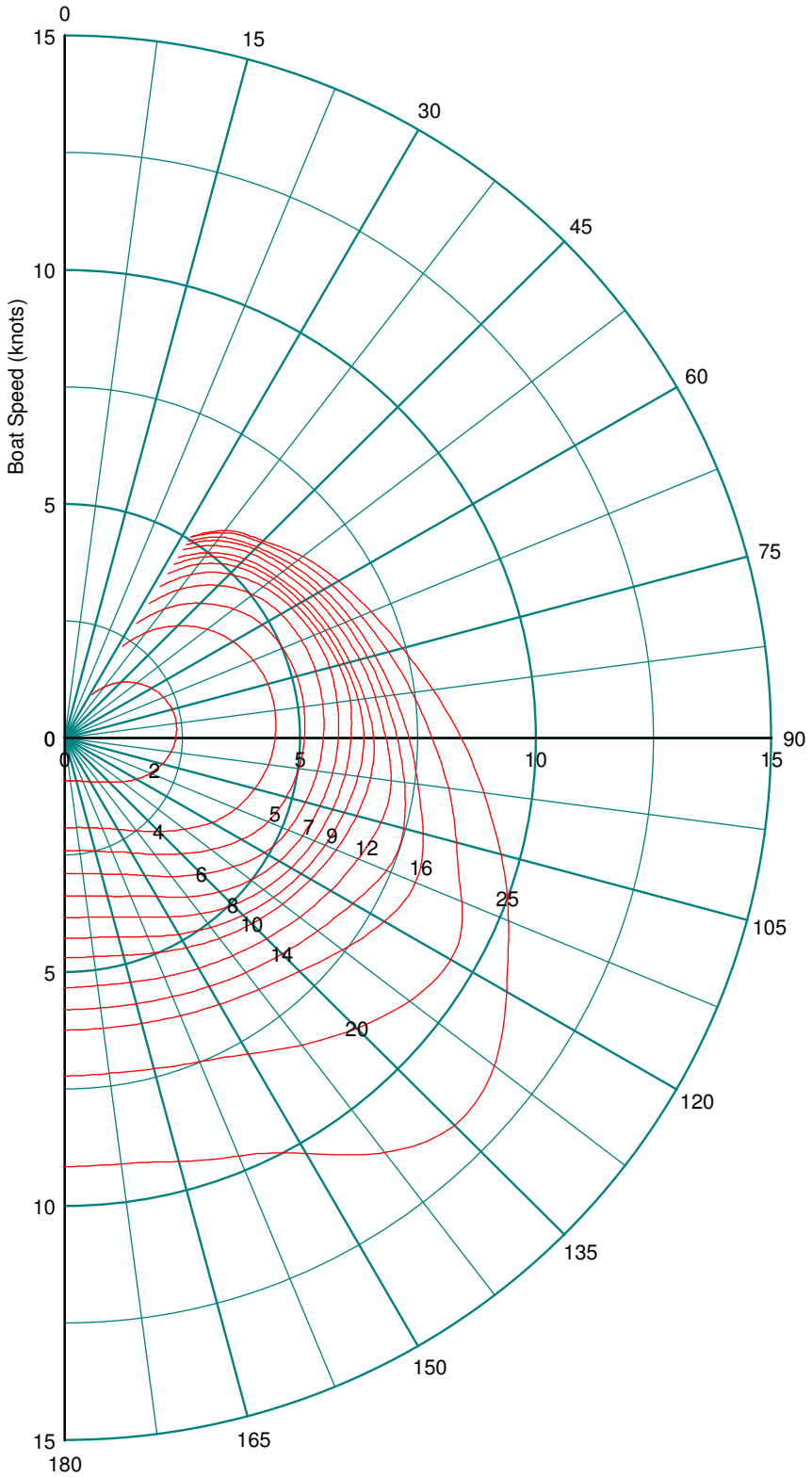

Figure 97 - Star Polar Diagram